Geometry and non-adiabatic response in quantum and classical systems. Lecture notes.

Michael Kolodrubetz[*,†,#], Pankaj Mehta[*], Anatoli Polkovnikov[*]

[*] *Department of Physics, Boston University, Boston, MA 02215*
[†] *Department of Physics, University of California, Berkeley, CA 94720, USA*
[#] *Materials Sciences Division, Lawrence Berkeley National Laboratory, Berkeley, CA 94720, USA*

In these lecture notes, partly based on the course taught at the Karpacz Winter School in March 2014, we discuss the close connections between non-adiabatic response of a system with respect to macroscopic parameters and the geometry of quantum and classical states. We center our discussion around adiabatic gauge potentials, which are the generators of the unitary transformations of the basis states in quantum systems and generators of special canonical transformations in classical systems. In quantum systems, expectation values of these potentials in the eigenstates are the Berry connections and the covariance matrix of these gauge potentials is the geometric tensor, whose antisymmetric part defines the Berry curvature and whose symmetric part is the Fubini-Study metric tensor. In classical systems one simply replaces the eigenstate expectation value by an average over the micro-canonical shell. We express the non-adiabatic response of the physical observables of the system through these gauge potentials. We also demonstrate the close connection of the geometric tensor to the notions of Lorentz force and renormalized mass. We show how one can use this formalism to derive equations of motion for slow macroscopic parameters coupled to fast microscopic degrees of freedom to reproduce and even go beyond macroscopic Hamiltonian dynamics. Finally, we illustrate these ideas with a number of simple examples and highlight a few more complicated ones drawn from recent literature.

Contents

Geometry plays an important role in many aspects of modern physics. In these lecture notes, we will highlight one situation where geometry plays a crucial role, namely the dynamics of closed systems. We will do so by introducing the concept of gauge potentials, which are infinitesimal generators of unitary transformations, specifically $\mathcal{A}_\lambda = i\hbar\partial_\lambda$, where the derivative is understood as acting on a smooth manifold of basis states parameterized by the parameter λ, which can be generally multicomponent. Among gauge potentials a very important role in these notes will be played by adiabatic gauge potentials where by the family of the basis states we will understand a family of eigenstates of some Hamiltonian, which depends on λ: $\mathcal{H}(\lambda)$. These adiabatic gauge potentials are the fundamental objects of both adiabatic perturbation theory and geometry of quantum or classical states.We will see, for instance, that in a moving frame the Hamiltonian picks up an effective Galilean term $\mathcal{H} \to \mathcal{H} - \dot{\lambda}\mathcal{A}_\lambda$, which yields important non-adiabatic corrections to the dynamics. These corrections can be measured through standard linear response techniques or by their back action on λ if it is treated as a dynamical degree of freedom. In classical systems gauge potentials correspond to generators of infinitesimal canonical transformations parameterized by λ. The adiabatic gauge potentials are in turn generators of special canonical transformations $\vec{q}(\lambda)$ and $\vec{p}(\lambda)$, which leave the Hamiltonian conserved for any λ such that

$$\{\mathcal{H}(\lambda, \vec{q}(\lambda), \vec{p}(\lambda)), \mathcal{H}(\lambda + \delta\lambda, \vec{q}(\lambda + \delta\lambda), \vec{p}(\lambda + \delta\lambda))\} = 0,$$

where $\{\dots\}$ stands for the Poisson bracket. Such special canonical transformations in classical systems are analogous to the unitary transformations in quantum systems, which diagonalize the instantaneous Hamiltonian.

We begin the lecture notes in Sec. I by introducing the major concepts in more detail using two simple examples: the quantum spin-1/2 and the simple harmonic oscillator (both quantum and classical). Next, in Sec. II, we introduce the concept of gauge potentials for quantum and classical systems in full generality. Then in Sec. III we introduce the geometric tensor, an object which is known to give the geometric properties of quantum ground state manifolds via the Fubini-Study metric tensor and the Berry curvature tensor. We show how these ideas can be generalized to quantum systems that are far from their ground states as well as to classical systems. In Sec. IV, we connect the dynamical gauge potentials to the geometric tensor by showing how the geometric tensor can be measured via dynamical response. Finally, in Sec. V we show one important consequence of these ideas, namely that the classical parameter λ acquires effective Newtonian dynamics due to excitation of the quantum or classical spin to which it is coupled. To help understand this general concept, in Sec. VI we show explicit examples of this emergent dynamics, ranging from relatively simple (particle in a box) to more complicated (dynamics of the order parameter in a quenched superconductor).

I. INVITATION: QUANTUM SPINS AND CLASSICAL OSCILLATORS OUT OF EQUILIBRIUM

We begin by considering two simple examples where geometry enters into dynamics. The goal of this section is to introduce the main ingredients of the formalism such as gauge potentials, geometric tensor, generalized Coriolis force and mass renormalization. In the following sections we will rigorously introduce these concepts, derive general statements and illustrate them with additional examples. As a first example, consider one of the staple problems in quantum mechanics, a single spin-1/2 particle in a in a time-dependent magnetic field. We will restrict ourselves to considering the case where the field strength is fixed to be h, but the field's direction can vary with time. If we parameterize the magnetic field direction by the spherical angles θ and ϕ, then the Hamiltonian for this problem takes the form

$$\mathcal{H} = -h\left[\cos(\theta)\sigma^z + \sin(\theta)\cos(\phi)\sigma^x + \sin(\theta)\sin(\phi)\sigma^y\right] = -h\begin{pmatrix} \cos\theta & e^{i\phi}\sin\theta \\ e^{-i\phi}\sin\theta & -\cos\theta \end{pmatrix} \tag{1}$$

with ground ($|g\rangle$) and excited ($|e\rangle$) eigenstates

$$|g\rangle = \begin{pmatrix} \cos(\theta/2) \\ e^{i\phi}\sin(\theta/2) \end{pmatrix}\ ,\ |e\rangle = \begin{pmatrix} \sin(\theta/2) \\ -e^{i\phi}\cos(\theta/2) \end{pmatrix}\ . \tag{2}$$

The simple dynamical problem that we want to consider is the case where the field rotates around the z-axis in the lab frame. This problem can be solved exactly by going to the moving (rotating) frame, i.e., by diagonalizing the Hamiltonian by a unitary rotation U to give a diagonal matrix $\tilde{\mathcal{H}} = U^\dagger \mathcal{H} U$, where

$$U(\theta,\phi) = \begin{pmatrix} \cos(\theta/2) & \sin(\theta/2) \\ e^{i\phi}\sin(\theta/2) & -e^{i\phi}\cos(\theta/2) \end{pmatrix} \tag{3}$$

and $\tilde{\mathcal{H}} = -h\sigma^z$. Going to a rotating frame corresponds to the time-dependent unitary transformation on the wave function

$$|\tilde{\psi}\rangle = U^\dagger(\theta,\phi)|\psi\rangle\ . \tag{4}$$

This unitary transformation can be equivalently thought as expanding the wave function in the rotated basis. For rotations around the z axis, only the angle ϕ changes and $|\tilde{\psi}\rangle$ satisfies a new Schrödinger equation given by

$$\begin{aligned} i\hbar\frac{d|\tilde{\psi}\rangle}{dt} &= i\hbar\frac{d(U^\dagger|\psi\rangle)}{dt} = i\hbar\frac{dU^\dagger}{dt}|\psi\rangle + i\hbar U^\dagger\frac{d|\psi\rangle}{dt} = i\hbar\frac{d\phi}{dt}\frac{\partial U^\dagger}{\partial\phi}|\psi\rangle + U^\dagger\mathcal{H}|\psi\rangle \\ &= \frac{d\phi}{dt}\left(i\hbar\frac{\partial U^\dagger}{\partial\phi}U\right)|\psi_m\rangle + U^\dagger\mathcal{H}U|\tilde{\psi}\rangle = \underbrace{\left(\tilde{\mathcal{H}} - \dot{\phi}\tilde{\mathcal{A}}_\phi\right)}_{\tilde{\mathcal{H}}_m}|\tilde{\psi}\rangle\ , \end{aligned} \tag{5}$$

where

$$\tilde{\mathcal{A}}_\phi = -i\hbar\left(\partial_\phi U^\dagger\right)U = -i\hbar\left[\partial_\phi\left(U^\dagger U\right) - U^\dagger\partial_\phi U\right] = i\hbar U^\dagger\partial_\phi U \tag{6}$$

is a very important operator that we will refer to as the adiabatic gauge potential with respect to the parameter ϕ (here in the moving frame) [1]. In writing these equations, we have introduced the notation, which we are going to use later, that the tilde superscript refers to objects in the moving frame basis. In particular, for any operator $\mathcal{O}$ we define $\tilde{\mathcal{O}} = U^\dagger \mathcal{O} U$. By examining Eq. (5), it is clear that the combination $\tilde{\mathcal{H}}_m = \tilde{\mathcal{H}} - \dot{\phi}\tilde{\mathcal{A}}_\phi$ plays the role of the Hamiltonian in the moving frame basis, and we refer to this operator as the moving Hamiltonian. Note that we can remove tilde signs here by doing the inverse unitary transformation to get $\mathcal{H}_m = \mathcal{H} - \dot{\phi}\mathcal{A}_\phi$, which is equivalent to projecting operators back to the original basis. Let's try to understand a bit more about what this gauge potential does in our system by calculating its matrix elements. For instance,

$$\begin{aligned}
\langle e|\mathcal{A}_\phi|g\rangle = \langle\downarrow|\tilde{\mathcal{A}}_\phi|\uparrow\rangle &= \langle\downarrow|i\hbar U^\dagger(\partial_\phi U)|\uparrow\rangle && (7)\\
&= i\hbar\langle\downarrow|U^\dagger\left[\partial_\phi(U|\uparrow\rangle) - U\cancelto{0}{\partial_\phi|\uparrow\rangle}\right] && (8)\\
&= i\hbar\langle e|\partial_\phi g\rangle = \frac{\hbar\sin\theta}{2}\,, && (9)
\end{aligned}$$

where we have used from the definition of U that $U(\theta,\phi)|\uparrow\rangle = |g(\theta,\phi)\rangle$ and similarly for the excited state. From the remaining matrix elements, it becomes clear that we can think of $\mathcal{A}$ as the derivative operator $\mathcal{A}_\phi = i\hbar\hat{\partial}_\phi$. As we will see later, this is a very general property defining the gauge potentials. If instead of rotations we would consider a particle in some potential which depends on $x_0 - x$ and translate x_0 then as we will discuss later the (adiabatic) gauge potential with respect to x_0 will be $\mathcal{A}_{x_0} = i\hbar\partial_{x_0} = -i\hbar\partial_x = p$, which is nothing but the momentum operator.

To see how the gauge potential connects to geometry, we note that its expectation value in the moving frame ground state $|\uparrow\rangle$ is the ground state Berry connection (times Planck's constant) $A_\phi \equiv i\hbar\langle g|\partial_\phi g\rangle = -\hbar\sin^2(\theta/2)$ (Berry, 1984)[2]. The Berry connection is related to both the ground state Berry (a.k.a. geometric) phase φ_B and the Berry curvature $F_{\mu\nu}$: $\hbar F_{\mu\nu} = \partial_\mu A_\nu - \partial_\nu A_\mu$ via

$$\varphi_B = \frac{1}{\hbar}\oint \vec{A}_\lambda \cdot d\vec{\lambda} = \int F_{\mu\nu} d\lambda_\mu \wedge d\lambda_\nu\,, \qquad (10)$$

where for the remainder of this review we use the convention that repeated indices are summed over, unless stated otherwise. More generally, one can think of the gauge potentials as defining a notion of parallel transport of wave functions in parameter space via the covariant derivative

[1] As we explain later the word adiabatic highlights the fact that U in Eq. (6) is a particular unitary operator connecting eigenstates of the Hamiltonian $\mathcal{H}$ at different parameters ϕ. Since in these notes we are mostly dealing with adiabatic gauge potentials we will often omit the word "adiabatic" and simply use gauge potential.

[2] Traditionally the Berry connection A_ϕ is defined without the factor of $\hbar$. However, it is the operator $\mathcal{A}_\phi = i\hbar\partial_\phi$, which has a well defined classical limit. As we are treating classical and quantum systems here on equal footing it is more natural to define A_ϕ as an expectation value of $\mathcal{A}_\phi$ and refer to it as the Berry connection.

$D_\mu = \partial_\mu + i\mathcal{A}_\mu/\hbar$ such that $D_\mu|\psi_n\rangle = 0$ for all energy eigenstates $|\psi_n\rangle$. This is the fundamental geometric definition that will later allow us to define curvature and distances via the covariance matrix of this connection.

Next using this simple example let us discuss the connection of the adiabatic gauge potentials and the dynamical response of the system to slow perturbations. A natural way to analyze this response is to go to the moving frame and then apply the framework of adiabatic perturbation theory (De Grandi and Polkovnikov, 2010; Rigolin et al., 2008). The latter effectively treats the Galilean term $\tilde{\mathcal{H}}_1 = -\dot\phi\tilde{\mathcal{A}}_\phi$ in the moving frame Hamiltonian as a small perturbation around $\tilde{\mathcal{H}}_0 = -h\sigma^z$. If we imagine gradually ramping up the velocity starting from $\dot\phi = 0$ to some constant value then up to the order $\dot\phi^2$ the system will follow the ground state of the moving Hamiltonian $\mathcal{H}_m$. For constant velocity $\dot\phi$ this Hamiltonian is time independent and hence we can use the static perturbation theory to find the non-adiabatic corrections to transition probabilities and various observables in the original lab frame. For example, the transition amplitude to be in the instantaneous excited state $|e\rangle$ in the first order of adiabatic perturbation theory is

$$a_e = \frac{\langle e|\mathcal{H}_1|g\rangle}{E_g^0 - E_e^0} = \dot\phi\frac{\langle\downarrow|\tilde{\mathcal{A}}_\phi|\uparrow\rangle}{2h} = \frac{\hbar\sin\theta}{4h}\dot\phi\ . \tag{11}$$

If we think of the actual time-dependent wave function $|\psi(t)\rangle$ as the ground state of this weakly-perturbed Hamiltonian in the moving frame, then at lowest order in perturbation theory,

$$|\psi(t)\rangle = a_g|g\rangle + a_e|e\rangle, \tag{12}$$

where as always from the normalization condition $|a_g| \approx 1 - |a_e|^2/2$ and the phase of a_g is given by the standard sum of the dynamical and geometric phases.

Let's use this perturbative result to calculate expectation value of the operator $\mathcal{M}_\theta \equiv -\partial_\theta\mathcal{H}$. In thermodynamics the equilibrium expectation value of $\mathcal{M}_\theta$ is known as a generalized force with respect to θ. For example, if the Hamiltonian had a conventional form $\mathcal{H} = p_\theta^2/2m + V(\theta)$, then $\mathcal{M}_\theta = -\partial_\theta V$ and its expectation value is the average angular force (a.k.a. torque) acting on a particle. By analogy we extend the definition of the generalized force to non-equilibrium states and define $M_\theta(t) = \langle\psi(t)|\mathcal{M}_\theta|\psi(t)\rangle$ as a non-equilibrium generalized force. At leading order in the ramp rate $\dot\phi$,

$$M_\theta(t) \equiv \langle\psi(t)|\mathcal{M}_\theta|\psi(t)\rangle = \langle g|\mathcal{M}_\theta|g\rangle + a_e\langle g|\mathcal{M}_\theta|e\rangle + a_e^*\langle e|\mathcal{M}_\theta|g\rangle + O(\dot\phi^2)\ . \tag{13}$$

It is straightforward to check that the matrix elements of $\mathcal{M}_\theta$ are $\langle g|\mathcal{M}_\theta|g\rangle = \langle e|\mathcal{M}_\theta|e\rangle = 0$ and

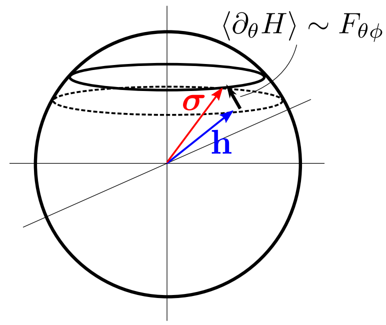

FIG. 1 Ramping the angle ϕ leads to a deflection in $\langle \partial_\theta \mathcal{H} \rangle$ which is proportional to the Berry curvature $F_{\theta\phi}$.

$\langle g|\mathcal{M}_\theta|e\rangle = \langle e|\mathcal{M}_\theta|g\rangle = -h$, so

$$M_\theta(t) \approx 2\hbar \left(\frac{\dot\phi \sin\theta}{4h} \right) (-h) = -\dot\phi \frac{\hbar \sin\theta}{2} = \hbar F_{\theta\phi} \dot\phi \ , \tag{14}$$

where in the last equation we have used the definition of the Berry curvature is $\hbar F_{\theta\phi} = \partial_\theta A_\phi - \partial_\phi A_\theta = -\hbar \sin\theta/2$ for the spin-1/2 ground state. We will see later that this identification of the Berry curvature times the ramp velocity as the leading non-adiabatic correction to the generalized force is a universal result. In turn this means that the Berry curvature underlies the Coriolis or Lorentz-type forces, which are well known from elementary physics.

In addition to the generalized force, we can look at other observables such as the energy. The leading correction to the energy is of order $\dot\phi^2$ and is given by

$$\begin{aligned} \Delta E \ &= \ \langle \psi|\mathcal{H}|\psi\rangle - \langle g|\mathcal{H}|g\rangle = (|a_g|^2 - 1)E_g + |a_e|^2 E_e = -|a_e|^2 E_g + |a_e|^2 E_e \\ &\approx \ 2\hbar h \left(\dot\phi \frac{\sin\theta}{4h} \right)^2 = \hbar \dot\phi^2 \frac{\sin^2\theta}{8h} \ . \end{aligned} \tag{15}$$

An interesting consequence arises if we ask the question “where did this extra energy came from?” For instance, consider a setup as illustrated in Fig. 2 in which the spin-1/2 is placed below a bar magnet that is rotating without friction around an axis inline with the spin. If the magnet has moment of inertia I_0 and the spin is in its ground state, then as we start to rotate the magnet the spin will attempt to follow its rotation. By conservation of energy, the work W done on the magnet in order to accelerate it to the angular velocity $\dot\phi$ will be equal to the total energy change in the system magnet + spin:

$$W = \frac{1}{2} I_0 \dot\phi^2 + \Delta E_{\rm spin}(\dot\phi) = \frac{1}{2} \left(I_0 + \hbar^2 \frac{\sin^2\theta}{4h} \right) \dot\phi^2 \ . \tag{16}$$

Clearly the non-adiabatic excitations of the spin appear as a dressed moment of inertia $\kappa = \hbar^2 \sin^2\theta/4h$ on the magnet, making it appear to have net moment of inertia $I_{\rm eff} = I_0 + \kappa$. The

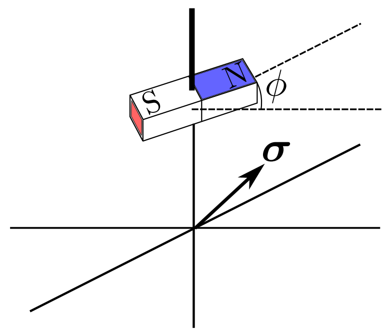

FIG. 2 Possible experimental realization of the rotating magnetic field. The rotation of the bar magnet is dressed by exciting the quantum spin and leads to mass renormalization (see text).

additional positive contribution κ comes from the dressing of the magnet with the spin. Not surprisingly this mass renormalization is stronger if the gap in the system gets smaller. So with this simple example, we have seen that doing perturbation theory in a slowly-moving frame yields important corrections to the dynamics, such as an effective force due to the Berry curvature and a renormalization of the moment of inertia of the macroscopic degree of freedom causing the parameter change.

The second example we will consider in this introduction is a simple harmonic oscillator with an offset in both its position (x_0) and its momentum (p_0). This example is also relatively simple, but importantly has a well-defined classical limit. This system is described by the Hamiltonian:

$$\mathcal{H} = \frac{(\hat{p} - p_0)^2}{2m} + \frac{1}{2} m\omega^2 (\hat{x} - x_0)^2 \ . \tag{17}$$

We use hat-notation for position and momentum operators to distinguish them from the parameters x_0 and p_0. Translations in x_0 are fairly easy to generate by, for example, moving a harmonic trap or spring. It's not as obvious how one gets a time-dependent p_0. One possibility is to consider a pendulum with a charged particle at the end of it in static electric and magnetic fields (see Fig. 3 and Ref. 27). Then the angle of the electric field shifts the equilibrium position of the pendulum (x_0) and the magnetic field prefers a certain angular momentum (p_0).

Exercise I.1. Show that the setup in Fig. 3 gives the Hamiltonian in Eq. (17) with $\hat{x} \to \hat{\phi}$, $\hat{p} \to \hat{p}_\phi$, $x_0 = \alpha QE/(mg + QE)$ and $p_0 = L^2 QB/c$ in the small angle limit $\alpha, \phi \ll 1$.

As with the spin-1/2, we want to go to the moving frame in which we know how to diagonalize $\mathcal{H}$. We can do this with the unitary $U(x_0, p_0) = e^{-i\hat{p}x_0/\hbar} e^{i\hat{x}p_0/\hbar}$, in terms of which

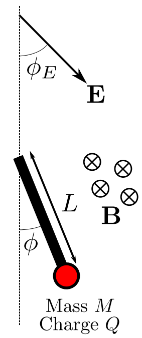

FIG. 3 A charged pendulum in crossed electric and magnetic fields.

$\tilde{\mathcal{H}} = U^\dagger(x_0, p_0)\mathcal{H}(x_0, p_0)U(x_0, p_0) = \mathcal{H}(0,0) = \hbar\omega(\hat{n}+1/2) \equiv \mathcal{H}_0$. The moving Hamiltonian is thus

$$\mathcal{H}_m = \mathcal{H}_0 - \dot{x}_0\tilde{\mathcal{A}}_{x_0} - \dot{p}_0\tilde{\mathcal{A}}_{p_0} \ , \tag{18}$$

where

$$\begin{aligned} \tilde{\mathcal{A}}_{x_0} &= i\hbar U^\dagger \partial_{x_0} U = i\hbar e^{-i\hat{x}p_0/\hbar} e^{i\hat{p}x_0/\hbar} \partial_{x_0} \left(e^{-i\hat{p}x_0/\hbar} e^{i\hat{x}p_0/\hbar} \right) \\ &= i e^{-i\hat{x}p_0/\hbar}(-i\hat{p}) e^{i\hat{x}p_0/\hbar} = \hat{p} + p_0 \\ \tilde{\mathcal{A}}_{p_0} &= i\hbar U^\dagger \partial_{p_0} U = -\hat{x} \ , \end{aligned} \tag{19}$$

which stems from the fact that $\hat{p}$ $(-\hat{x})$ generates translations in position (momentum).

For simplicity, let's consider this system for a fixed value of p_0. Then $\mathcal{H}_m = \mathcal{H}_0 - \dot{x}_0(\hat{p} + p_0)$ and the amplitude to transition from the ground state $|0\rangle$ to the n-th eigenstate $(n \neq 0)$ of the harmonic oscillator is, at first order in $\dot{x}_0$,

$$a_n \approx \frac{\langle n| \left(-\dot{x}_0(\hat{p} + p_0)\right) |0\rangle}{E_0 - E_n} \ . \tag{20}$$

The only non-zero matrix elements of the $\hat{p}$ operator connect the state $|0\rangle$ to the state $|1\rangle$), so $a_{n>1} = 0$ and

$$a_1 \approx \dot{x}_0 \frac{\langle 1|\hat{p}|0\rangle}{\omega} = \frac{\dot{x}_0}{\omega}\langle 1|\frac{i(\hat{a}^\dagger - \hat{a})}{\ell\sqrt{2}}|0\rangle = \frac{i\dot{x}_0}{\omega\ell\sqrt{2}} \ , \tag{21}$$

where $\ell = \sqrt{\hbar/m\omega}$ is the natural length scale of the oscillator, $\hat{a}^\dagger$ and $\hat{a}$ are the standard creation and annihilation operators. Using the non-adiabatic corrections to the wave function we can easily find the leading non-equilibrium correction to the generalized force with respect to p_0, which should be proportional to the Berry curvature as suggested in Eq. (14):

$$\begin{aligned} \Delta F = \langle(-\partial_{p_0}\mathcal{H})\rangle - \langle 0|(-\partial_{p_0}\mathcal{H})|0\rangle &\approx a_1^*\langle 1|(-\partial_{p_0}\mathcal{H})|0\rangle + a_1\langle 0|(-\partial_{p_0}\mathcal{H})|1\rangle \\ &= -\frac{2i\dot{x}_0}{\omega\ell\sqrt{2}}\langle 1|\hat{p}|0\rangle = \dot{x}_0 \cancelto{1}{\left(\frac{\hbar}{m\omega\ell^2}\right)} = \hbar F_{p_0 x_0}\dot{x}_0 \end{aligned} \tag{22}$$

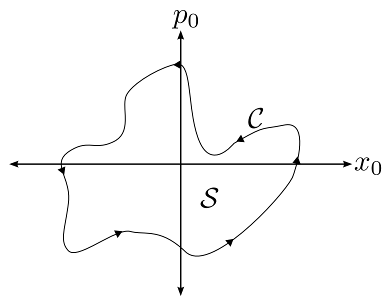

FIG. 4 The Berry phase of the harmonic oscillator is proportional to the area in phase space enclosed by the path $(x_0(t), p_0(t))$.

For consistency one can compute Berry curvature directly from the Berry connection. Indeed , from Eq. (19) it is clear that $A_{x_0} = \langle 0|\mathcal{A}_{x_0}|0\rangle = p_0$ and $A_{p_0} = 0$. Note the apparent asymmetry between the Berry connections is simply a gauge choice.[3] Then $\hbar F_{p_0 x_0} = \partial_{p_0} A_{x_0} - \partial_{x_0} A_{p_0} = 1$. If we consider an arbitrary closed path $(x_0(t), p_0(t))$ as depicted in Fig. 4, the fact that the Berry curvature is $F_{p_0 x_0} = 1/\hbar$ means that we will get a Berry phase of $\varphi_B = \hbar^{-1} \int_C A_\lambda \cdot d\lambda = \int_S dx_0 dp_0 F_{p_0 x_0} = \text{Area}_S/\hbar$, i.e., the Berry phase is just area of the phase space trajectory enclosed by (x_0, p_0) in units of $\hbar$. Similarly, the energy of excitations

$$\Delta E \approx E_1|a_1|^2 + E_0(|a_0|^2 - 1) = (E_1 - E_0)|a_1|^2 = \frac{\dot{x}_0^2}{2}\left(\frac{1}{\omega \ell^2}\right) = \frac{m\dot{x}_0^2}{2}. \tag{23}$$

If the center-of-mass motion of the harmonic oscillator was generated by a trap, we know that by a conservation of energy argument analogous to that for the moment of inertia of the spin-1/2 particle, the trap will feel heavier by an amount equal to the mass of the particle inside this trap. Here we see that this intuitive result comes from the (virtual) excitations of the particle created by the Galilean term.

Exercise I.2. Consider the harmonic oscillator Hamiltonian from the previous section but now initialized in an arbitrary energy eigenstate $|n\rangle$. Show that as x_0 is slowly ramped, the force $-\langle \partial_{p_0} \mathcal{H}\rangle$ and mass renormalization (κ_{x_0}) are the same as those in the ground state: $-\langle \partial_{p_0} \mathcal{H}\rangle = \dot{x}_0 \implies F_{p_0 x_0} = 1$ and $\kappa_{x_0} = m$.

The harmonic oscillator can be also analyzed classically, where we just consider the same Hamiltonian with x and p as canonical phase space variables instead of operators. We can apply much

[3] As with all gauge potentials, while the the expectation value of the gauge potential can depend on gauge choice, physical observables such as the generalized force are independent of it.

of the same machinery to go to a moving frame, solve for corrections to the motion, etc. If the parameters x_0 and p_0 evolve along some generic path $(x_0(t), p_0(t))$, then we can go to the moving frame by performing a (canonical) change of variables to $p' = p - p_0$ and $x' = x - x_0$. We can anticipate that as in the quantum case, the effective Hamiltonian in the moving frame will be

$$\mathcal{H}_m = \mathcal{H}_0 - \mathcal{A}_{p_0}\dot{p}_0 - \mathcal{A}_{x_0}\dot{p}_0 = \mathcal{H}_0 + x'\dot{p}_0 - p'\dot{x}_0 \ , \tag{24}$$

where $\mathcal{H}_0 = p'^2/2m + m\omega^2 x'^2/2$ and we used the classical limit for the gauge potentials introduced in Eq. (19). As we explain in the next section, these gauge potentials in the classical language are simply generators of the canonical transformations to the moving frame, i.e. from x, p to x', p'. The equations of motion in the moving frame are thus

$$\dot{x}' = \frac{\partial \mathcal{H}_m}{\partial p'} = \frac{p'}{m} - \dot{x}_0 \tag{25}$$

$$\dot{p}' = -\frac{\partial \mathcal{H}_m}{\partial x'} = -m\omega^2 x' - \dot{p}_0 \tag{26}$$

Note that these equations can be directly obtained by first writing the lab-frame equations of motion and then shifting the phase space variables $x \to x'$, $p \to p'$. Let us again first consider the setup where p_0 remains constant and only x_0 slowly changes in time. Moreover we assume that we start in a stationary states $x(0) = x_0$ and $p(0) = p_0$. As we know from analytical mechanics in the leading order the adiabatic theorem tells us that the stationary orbit of a classical system with slowly changing parameters maps to another stationary orbit with same adiabatic invariants (Landau and Lifshitz, 1982)[4]. Since for the chosen initial condition the adiabatic invariant is zero the adiabatic theorem simply states that $\dot{x}' \approx 0$ and $\dot{p}' \approx 0$. Then Eq. (25) implies that the particle moves at the same velocity as the potential, i.e., $p' = m\dot{x}_0$, which is not surprising. If instead $x_0 = 0$ and we only ramp p_0, then Eq. (26) yields the slightly less obvious result that the particle is deflected to $x' = -\dot{p}_0/m\omega^2$. For the realization of the harmonic oscillator depicted in Fig. 3, this just reflects the fact that a time-varying magnetic field generates an electric field by the Faraday effect which pushes the charged particle to one side. In our language this Faraday force is nothing but the effective Coriolis force due to the Berry curvature by analogy with the quantum case. For example, for a ramp of p_0,

$$\langle -\partial_{x_0}\mathcal{H}\rangle = m\omega^2 x'\dot{p}_0 = -\dot{p}_0 = \hbar F_{x_0 p_0}\dot{p}_0 \ , \tag{27}$$

[4] We will show later that going to the moving frame first and then using conservation of adiabatic invariants is equivalent to finding leading non-adiabatic corrections in the lab frame.

where in the classical case angular brackets imply averaging over the adiabatically connected stationary distribution. Similarly, the additional energy for a ramp of x_0 is

$$\Delta E = \mathcal{H}(x = x_0, p = m\dot{x}_0) - \mathcal{H}(x = x_0, p = 0) = \frac{1}{2} m\dot{x}_0^2 \ , \tag{28}$$

so as expected the mass of the trap generating the center-of-mass motion of the harmonic oscillator is dressed by a n amount $\kappa_{x_0} = m$.

These examples illustrate how simple dynamical effects can be obtained using gauge potentials and adiabatic perturbation theory. We have seen that by going into a moving frame, one can derive both classically and quantum mechanically the leading corrections to generalized forces and the energy, from which the Coriolis force related to the Berry curvature and the mass renormalization emerge. Both of these systems are quite simple, and these results could have been obtained via a number of other methods. The power of this formalism comes from its generality. In what follows, we revisit the ideas in this section in their full generality, turning back to these two simple examples as useful illustrations throughout.

II. GAUGE POTENTIALS IN CLASSICAL AND QUANTUM HAMILTONIAN SYSTEMS.

Key concept: Gauge potentials are generators of translations in parameter space. They appear as non-adiabatic corrections to the Hamiltonian in a moving frame.

A. Classical Hamiltonian systems.

Classical Hamiltonian systems are defined by specifying the Hamiltonian $\mathcal{H}$ in terms of a set of canonical variables p_j, q_j satisfying the canonical relations

$$\{q_i, p_j\} = \delta_{ij}, \tag{29}$$

where $\{\dots\}$ denotes the Poisson bracket:

$$\{A(\mathbf{p}, \mathbf{q}), B(\mathbf{p}, \mathbf{q})\} = \sum_j \left(\frac{\partial A}{\partial q_j} \frac{\partial B}{\partial p_j} - \frac{\partial B}{\partial q_j} \frac{\partial A}{\partial p_j} \right). \tag{30}$$

This choice of canonical variables is arbitrary, as long as they satisfy Eq. (29). There are therefore many transformations that preserve this Poisson bracket, such as the orthogonal transformation

$$\vec{q} = R(\lambda)\vec{q}_0, \ \vec{p} = R(\lambda)\vec{p}_0 \ , \tag{31}$$

where R is an orthogonal matrix ($R^T = R^{-1}$). A general class of transformations which preserve the Poisson brackets are known as canonical transformations (Landau and Lifshitz, 1982).

In this work, we will mostly be interested in families of canonical transforms that depend continuously on some parameter(s) λ. It is easy to check that continuous canonical transformations can be generate by functions $\mathcal{A}_\lambda$ which we refer to as gauge potentials:

$$\begin{aligned} q_j(\lambda+\delta\lambda) &= q_j(\lambda) - \frac{\partial \mathcal{A}_\lambda(\lambda,\mathbf{p},\mathbf{q})}{\partial p_j}\delta\lambda \implies \frac{\partial q_i}{\partial \lambda} = -\frac{\partial \mathcal{A}_\lambda}{\partial p_i} = \{\mathcal{A}_\lambda, q_i\} \\ p_j(\lambda+\delta\lambda) &= p_j(\lambda) + \frac{\partial \mathcal{A}_\lambda(\lambda,\mathbf{p},\mathbf{q})}{\partial q_j}\delta\lambda \implies \frac{\partial p_j}{\partial \lambda} = \frac{\partial \mathcal{A}_\lambda}{\partial q_j} = \{\mathcal{A}_\lambda, p_j\}, \end{aligned} \tag{32}$$

where λ parameterizes the canonical transformation and the gauge potential is an arbitrary function of q, p, and λ [5]. We can then see that, up to terms of the order of $\delta\lambda^2$, the transformation above preserves the Poisson brackets:

$$\{q_i(\lambda+\delta\lambda), p_j(\lambda+\delta\lambda)\} = \delta_{ij} - \delta\lambda\left(\frac{\partial^2\mathcal{A}_\lambda}{\partial p_j \partial q_i} - \frac{\partial^2\mathcal{A}_\lambda}{\partial p_j \partial q_i}\right) + O(\delta\lambda^2) = \delta_{ij} + O(\delta\lambda^2). \tag{33}$$

Consider a simple example of such a continuous canonical transformation, $q_i(\vec{X}) = q_i(0) - X_i$, in which the position coordinate is shifted by $\vec{X}$ (we use the $\vec{X}$ notation instead of $\vec{\lambda}$ notation for the parameters here to highlight their meaning as the coordinate shift). Let's determine the components if the gauge potential $\mathcal{A}_{X_i}(\vec{q},\vec{p},\vec{X})$ using Eq. (32). First, note that p_i is independent of $\vec{X}$, meaning that $\partial\mathcal{A}_{X_i}/\partial q_j = 0$. Meanwhile, the X-dependence of q gives $\partial q_i/\partial X_j = -\delta_{ij} = -\partial\mathcal{A}_{X_j}/\partial p_i$. These equations are solved by $\mathcal{A}_{X_j} = p_j + C_j$, where C_j are arbitrary constants of integration. The presence of these constants in this solution is the first example we will see of a gauge choice that gives these gauge potentials their name.

For a fixed canonical basis, Hamiltonian dynamics gives a particular canonical transformation parameterized by time

$$\dot{q}_j = -\{\mathcal{H}, q_j\} = \frac{\partial \mathcal{H}}{\partial p_j},\ \dot{p}_j = -\{\mathcal{H}, p_j\} = -\frac{\partial \mathcal{H}}{\partial q_j} \tag{34}$$

Clearly these Hamiltonian equations are equivalent to Eqs. (32) with the convention $\mathcal{A}_t = -\mathcal{H}$. In the same way that Hamiltonians generate motion in time, we see that the gauge potentials $\mathcal{A}_\lambda$ are generators of motion in the parameter space. For instance, we saw that if $\lambda_i = X_i$ corresponds to shifts in position, it is generated by $\mathcal{A}_{X_i} = p_i$.

---

[5] We use the partial derivative notation for $dq/d\lambda$ and $dp/d\lambda$ because later we consider time evolution such that phase space variables will be functions of both λ and t

Exercise II.1. Show that the generator of rotations around z-axis:

$$q_x(\theta)=\cos(\theta)q_{x0}-\sin(\theta)q_{y0},\;\; q_y(\theta)=\cos(\theta)q_{y0}+\sin(\theta)q_{x0},$$

$$p_x(\theta)=\cos(\theta)p_{x0}-\sin(\theta)p_{y0},\;\; p_y(\theta)=\cos(\theta)p_{y0}+\sin(\theta)p_{x0},$$

is the angular momentum operator: $\mathcal{A}_\theta = p_x q_y - p_y q_x$.

Exercise II.2. Another particularly important transformation is dilation, which involves dilating real space by a factor λ, $q(\lambda)=\lambda q_0$, and shrinking momentum space by the same factor, $p(\lambda)=p_0/\lambda$. Show that dilations are canonical transformations, and find the gauge potential $\mathcal{A}_\lambda$ that generates them.

Canonical transformations are conventionally expressed through generating functions (Landau and Lifshitz, 1982), which are usually defined as functions of one old variable (q_0 or p_0) and one new variable ($q(\lambda)$ or $p(\lambda)$). For example, one can use the generating function $G(q_0, q(\lambda), \lambda)$ such that

$$p_0=\frac{\partial G}{\partial q_0},\;\; p(\lambda)=-\frac{\partial G}{\partial q(\lambda)}.$$

Differentiating the second equation with respect to λ at constant $q(\lambda)$ we find

$$\frac{\partial p(\lambda)}{\partial \lambda}=\frac{\partial \mathcal{A}_\lambda}{\partial q(\lambda)}=-\frac{\partial^2 G}{\partial q(\lambda)\partial\lambda}. \tag{35}$$

Clearly this equation can be satisfied if we choose

$$\mathcal{A}_\lambda=-\frac{\partial G}{\partial \lambda}\bigg|_{q_0,q(\lambda)}. \tag{36}$$

Similarly one can check that the gauge potential can be expressed through derivatives of other generating functions expressed through $q_0, p(\lambda)$, $q(\lambda), p_0$ and $p_0, p(\lambda)$. For instance, defining

$$G_1(q_0,p(\lambda),\lambda)=G(q_0,q(\lambda),\lambda)+q(\lambda)p(\lambda)$$

such that $q(\lambda)=\partial G_1/\partial p(\lambda)$ we can check that

$$\mathcal{A}_\lambda=-\frac{\partial G_1}{\partial \lambda}\bigg|_{q_0,p(\lambda)}. \tag{37}$$

Let us illustrate these relations using an example of orthogonal transformations (31). Differentiating these equations with respect to λ we find

$$\begin{aligned}\frac{\partial \vec q}{\partial\lambda}&=\frac{dR}{d\lambda}\vec q_0=\frac{dR}{d\lambda}R^T R\,\vec q_0=\frac{dR}{d\lambda}R^T\vec q=-\frac{\partial\mathcal{A}_\lambda}{\partial\vec p},\\ \frac{\partial \vec p}{\partial\lambda}&=\frac{dR}{d\lambda}\vec p_0=\frac{dR}{d\lambda}R^T R\vec p_0=\frac{dR}{d\lambda}R^T\vec p=\frac{\partial\mathcal{A}_\lambda}{\partial\vec q}\end{aligned} \tag{38}$$

It is straightforward to check that the gauge potential for these orthogonal transformations can be chosen to be

$$\mathcal{A}_\lambda = -\vec{p}^T \frac{dR}{d\lambda} R^T \vec{q} = -p_j \frac{dR_{jk}}{d\lambda} R^T_{ki} q_i \tag{39}$$

One can also check that the generating function for this orthogonal transformation is

$$G_1(\vec{q}_0, \vec{p}(\lambda), \lambda) = \vec{p}^T R \vec{q}_0 \tag{40}$$

such that

$$\frac{\partial G_1}{\partial \vec{q}_0} = \vec{p}^T R = \vec{p}_0, \quad \frac{\partial G_1}{\partial \vec{p}} = R\vec{q}_0 = \vec{q}$$

Then according to Eq. (37)

$$\mathcal{A}_\lambda = -\frac{\partial G_1}{\partial \lambda} = -\vec{p}^T \frac{dR}{d\lambda} \vec{q}_0 = -\vec{p}^T \frac{dR}{d\lambda} R^T \vec{q},$$

which is identical to Eq. (39).

Exercise II.3. Using Eq. (39) find the gauge potential $\mathcal{A}_\lambda$ corresponding to the orthogonal transformation (31) given by the two-dimensional rotation around z-axis:

$$R = \begin{pmatrix} \cos\theta & -\sin\theta \\ \sin\theta & \cos\theta \end{pmatrix}$$

with parameter $\lambda = \theta$ such that

$$\begin{pmatrix} q_x(\theta) \\ q_y(\theta) \end{pmatrix} = R(\theta) \begin{pmatrix} q_{x0} \\ q_{y0} \end{pmatrix}$$

and similarly for p_x and p_y. Show that you recover the result of Exercise II.1

Exercise II.4. Generalize the previous exercise to three dimensional rotations. Namely use that in a three dimensional space they can be decomposed into a product of three elementary rotations parameterized by the Euler angles α, β, γ (Landau and Lifshitz, 1982):

$$R = R_x(\alpha) R_y(\beta) R_z(\gamma), \tag{41}$$

where R_x, R_y, R_z are the rotation matrices

$$R_x(\alpha) = \begin{bmatrix} 1 & 0 & 0 \\ 0 & \cos\alpha & -\sin\alpha \\ 0 & \sin\alpha & \cos\alpha \end{bmatrix}, \; R_y(\beta) = \begin{bmatrix} \cos\beta & 0 & -\sin\beta \\ 0 & 1 & 0 \\ \sin\beta & 0 & \cos\beta \end{bmatrix}, \; R_z(\gamma) = \begin{bmatrix} \cos\gamma & -\sin\gamma & 0 \\ \sin\gamma & \cos\gamma & 0 \\ 0 & 0 & 1 \end{bmatrix}.$$

Choosing the Euler angles as parameters according to Eq. (39) find the components of the gauge potentials $\mathcal{A}_\alpha$, $\mathcal{A}_\beta$, $\mathcal{A}_\gamma$ as the functions of the Euler angles. Show that the gauge potentials corresponding to infinitesimal rotations around x, y and z axes, i.e. $\mathcal{A}_\alpha(\beta=0,\gamma=0)$, $\mathcal{A}_\beta(\alpha=0,\gamma=0)$ and $\mathcal{A}_\gamma(\alpha=0,\beta=0)$ are precisely the x, y and z components of the angular momentum.

As we know well from electromagnetism, when we are dealing with waves it is often convenient to deal with complex canonical variables (wave amplitudes and conjugate momenta). Recalling that normal modes of waves are identical to harmonic oscillators let us show how one can introduce this complex phase space variables for a single normal mode, parameterized by the parameter k (which in a translationally invariant system would be the momentum). Once these variables are introduced we can use them in arbitrary systems linear or not. The Hamiltonian for each mode is

$$\mathcal{H}_k = \frac{p_k^2}{2m} + \frac{m\omega_k^2}{2} q_k^2. \tag{42}$$

Let us define new linear combinations

$$p_k = i\sqrt{\frac{m\omega_k}{2}}(a_k^* - a_k),\ q_k = \sqrt{\frac{1}{2m\omega_k}}(a_k + a_k^*) \tag{43}$$

or equivalently

$$a_k^* = \frac{1}{\sqrt{2}}\left(q_k\sqrt{m\omega_k} - \frac{i}{\sqrt{m\omega_k}}p_k\right),\ a_k = \frac{1}{\sqrt{2}}\left(q_k\sqrt{m\omega_k} + \frac{i}{\sqrt{m\omega_k}}p_k\right). \tag{44}$$

We will refer to a_k^* and a_k as coherent state phase space variables as the eigenstates of the corresponding quantum creation and annihilation operators are precisely coherent states. Next we compute the Poisson brackets of the complex wave amplitudes

$$\{a_k, a_k\} = \{a_k^*, a_k^*\} = 0,\ \{a_k, a_k^*\} = -i. \tag{45}$$

To avoid dealing with the imaginary Poisson brackets it is convenient to introduce new coherent state Poisson brackets

$$\{A, B\}_c = \sum_k \left(\frac{\partial A}{\partial a_k}\frac{\partial B}{\partial a_k^*} - \frac{\partial B}{\partial a_k}\frac{\partial A}{\partial a_k^*}\right)\ , \tag{46}$$

where as usual we treat a and a^* as independent variables. From this definition it is immediately clear that

$$\{a_k, a_q^*\}_c = \delta_{kq}. \tag{47}$$

Comparing this relation with Eq. (45) we see that standard and coherent state Poisson brackets differ by the factor of i:

$$\{\dots\} = -i\{\dots\}_c. \tag{48}$$

In terms of these coherent states, infinitesimal canonical transformations preserving the coherent state Poisson brackets can be defined by the gauge potentials:

$$i\frac{\partial a_k}{\partial \lambda} = -\frac{\partial \mathcal{A}_\lambda}{\partial a_k^*}, \quad i\frac{\partial a_k^*}{\partial \lambda} = \frac{\partial \mathcal{A}_\lambda}{\partial a_k}. \tag{49}$$

We can write the Hamiltonian equations of motion for the new coherent variables. For any function of time and phase space variables $A(q,p,t)$ (or equivalently $A(a,a^*,t)$) we have

$$\frac{dA}{dt} = \frac{\partial A}{\partial t} + \frac{\partial A}{\partial q}\dot{q} + \frac{\partial A}{\partial p}\dot{p} = \frac{\partial A}{\partial t} + \{A, \mathcal{H}\} = \frac{\partial A}{\partial t} - i\{A, \mathcal{H}\}_c. \tag{50}$$

Let us apply now this equation to coherent state variables a_k and a_k^*. Using that they do not explicitly depend on time (such dependence would amount to going to a moving frame, which we will discuss later) we find

$$i\frac{da_k}{dt} = \{a_k, \mathcal{H}\}_c = \frac{\partial \mathcal{H}}{\partial a_k^*},\ i\frac{da_k^*}{dt} = \{a_k^*, \mathcal{H}\}_c = -\frac{\partial \mathcal{H}}{\partial a_k} \tag{51}$$

These are also known as the Gross-Pitaevskii equations. Note that deriving these equations we did not assume any specific form of the Hamiltonian, so they equally apply to linear and nonlinear Hamiltonians.

Exercise II.5. Check that any unitary transformation $\tilde{a}_k = U_{k,k'} a'_k$, where U is a unitary matrix, preserves the coherent state Poisson bracket, i.e. $\{\tilde{a}_k, \tilde{a}_q^*\}_c = \delta_{k,q}$.

Exercise II.6. Verify that the Bogoliubov transformation

$$\gamma_k = \cosh(\theta_k) a_k + \sinh(\theta_k) a_{-k}^*,\ \gamma_k^* = \cosh(\theta_k) a_k^* + \sinh(\theta_k) a_{-k}, \tag{52}$$

with $\theta_k = \theta_{-k}$ also preserves the coherent state Poisson bracket, i.e.

$$\{\gamma_k, \gamma_{-k}\}_c = \{\gamma_k, \gamma_{-k}^*\}_c = 0,\ \{\gamma_k, \gamma_k^*\}_c = \{\gamma_{-k}, \gamma_{-k}^*\}_c = 1. \tag{53}$$

Assume that θ_k are known functions of some parameter λ, e.g. the interaction strength. Find the gauge potential $\mathcal{A}_\lambda = \sum_k \mathcal{A}_{\lambda,k}$, which generates such transformations.

B. Quantum Hamiltonian systems.

The analogues of canonical transformations in classical mechanics are unitary transformations in quantum mechanics. In classical systems these transformations reflect the freedom of choosing canonical variables while in quantum systems they reflect the freedom of choosing basis states.

The wave function [6] representing some state can be always expanded in some basis:

$$|\psi\rangle = \sum_n \psi_n |n\rangle_0, \tag{54}$$

where $|n\rangle_0$ is some fixed, parameter independent basis. One can always make a unitary transformation to some other basis $|m(\lambda)\rangle = \sum_n U_{nm}(\lambda)|n\rangle_0$ or equivalently $|n\rangle_0 = \sum_m U_{nm}(\lambda)^*|m(\lambda)\rangle$. Then $|\psi\rangle$ can be rewritten as

$$|\psi\rangle = \sum_{mn} \psi_n U^*_{nm}|m(\lambda)\rangle = \sum_m \tilde{\psi}_m(\lambda)|m(\lambda)\rangle, \tag{55}$$

where $\tilde{\psi}_m(\lambda) = \langle m(\lambda)|\psi\rangle = \sum_n U^*_{nm}\psi_n$, which is equivalent to the vector notation

$$\tilde{\psi} = U^\dagger(\lambda)\psi.$$

We can introduce gauge potentials by analogy with the classical systems as generators of continuous unitary transformations, namely

$$i\hbar\partial_\lambda|\tilde{\psi}(\lambda)\rangle = i\hbar\partial_\lambda\left(U^\dagger|\psi\rangle\right) = i\hbar\left(\partial_\lambda U^\dagger\right)\left(U|\tilde{\psi}\rangle\right) = -\tilde{\mathcal{A}}_\lambda|\tilde{\psi}\rangle \ , \tag{56}$$

where we used the fact that $|\psi\rangle$ is independent of λ. We use the tilde notation in the gauge potentials to highlight that they act on the rotated wave function $|\tilde{\psi}\rangle$.

$$\tilde{\mathcal{A}}_\lambda = -i\hbar\partial_\lambda U^\dagger U = i\hbar U^\dagger\partial_\lambda U = (\tilde{\mathcal{A}}_\lambda)^\dagger. \tag{57}$$

The second equality follows from the fact that

$$\partial_\lambda(UU^\dagger) = \partial_\lambda \mathbb{1} = 0 \implies U\partial_\lambda U^\dagger = -\partial_\lambda U\, U^\dagger \ . \tag{58}$$

As in the classical case, the gauge potential generates motion in parameter space. From Eq. (57) it follows that $\tilde{\mathcal{A}}_\lambda$ is a Hermitian operator, which can be formally defined through its matrix elements:

$$_0\langle n|\tilde{\mathcal{A}}_\lambda|m\rangle_0 = i\hbar\, _0\langle n|U^\dagger\partial_\lambda U|m\rangle_0 = i\hbar\langle n(\lambda)|\partial_\lambda|m(\lambda)\rangle \ , \tag{59}$$

[6] This discussion also directly extends to density matrices.

so we can think of the gauge potential in the lab frame, $\mathcal{A}_\lambda = U\tilde{\mathcal{A}}_\lambda U^\dagger$, as just $i\hbar$ times the derivative operator ∂_λ:

$$\mathcal{A}_\lambda = i\hbar\partial_\lambda, \tag{60}$$

which immediately follows from the fact that $\langle n(\lambda)|\mathcal{A}_\lambda|m(\lambda\rangle =_0 \langle n|\tilde{\mathcal{A}}_\lambda|m\rangle_0$.

Exercise II.7. Verify that the gauge potential corresponding to the translations: $\tilde{\psi}(x) = \psi(\lambda + x)$ is the momentum operator. Similarly verify that the gauge potential for rotations is the angular momentum operator.

Exercise II.8. It is often useful to think in terms of the action of $\tilde{\mathcal{A}}_\lambda$ on operators instead of wave functions. Consider the case where our basis-changing unitary takes a λ-dependent operator $\tilde{\mathcal{O}}(\lambda)$ to a λ-independent operator $\mathcal{O} = U\tilde{\mathcal{O}}U^\dagger = \text{const}(\lambda)$.

- Show that $\tilde{\mathcal{A}}_\lambda = i\hbar U^\dagger\partial_\lambda U$ differentiates the operator $\tilde{\mathcal{O}}$: $[\tilde{\mathcal{A}}_\lambda, \tilde{\mathcal{O}}(\lambda)] = -i\hbar\partial_\lambda\tilde{\mathcal{O}}$.
- In the previous problem, shifting the position is equivalent to defining the new operator $X' = \lambda + X$. Show that $\tilde{\mathcal{A}}_\lambda = P$ satisfies the correct commutation relations, with $\tilde{\mathcal{O}} = X'$ and $\mathcal{O} = X$.
- What is the momentum operator P' in this new basis? Show that it also satisfies the appropriate commutation relations with $\tilde{\mathcal{A}}_\lambda = P$.

Exercise II.9. Consider the quantum version of the Bogoliubov transformations discussed in the previous section (Eq. (52)). Show that the quantum and classical gauge potentials coincide if we identify complex amplitudes a_k and a_k^* with the annihilation and creation operators respectively. Note that you can do this one of two ways:

- <u>The easy way –</u> Consider a unitary operator U that rotates the θ-dependent number operator $\gamma_k^\dagger\gamma_k$ to the original basis $a_k^\dagger a_k$. Show that $\tilde{\mathcal{A}}_\theta$ satisfies the appropriate commutation relation with γ_k, using the results of the previous exercise.
- <u>The hard way –</u> Verify by direct computation on the θ-dependent number eigenstates $|n_k, n_{-k}\rangle \propto \left(\gamma_k^\dagger\right)^{n_k}\left(\gamma_{-k}^\dagger\right)^{n-k}|\Omega_\gamma\rangle$, where $|\Omega_\gamma\rangle$ is the γ vacuum, that the matrix elements satisfy $\langle m_k, m_{-k}|\tilde{\mathcal{A}}_\theta|n_k, n_{-k}\rangle = i\hbar\langle m_k, m_{-k}|\partial_\theta|n_k, n_{-k}\rangle$.

C. Adiabatic Gauge Potentials

Up to now gauge potentials we introduced were generators of arbitrary continuous canonical (classical) or unitary (quantum) transformations. In these notes we will be particularly interested in a special class of such gauge potentials, which we call adiabatic. It is easier to introduce them using the language of quantum mechanics first and then extend their definition to classical systems.

Imagine that we are dealing with a family of Hamiltonians parameterized by some continuous parameter λ: $\mathcal{H}(\lambda)$. We will assume that the Hamiltonians are non-singular and differentiable. At each value of λ, the the Hamiltonian are diagonalized by a set of eigenstates $|m(\lambda)\rangle$, which we call the adiabatic basis. When the parameters λ are varied adiabatically (infinitely slow), these states are related by the adiabatic theorem. In these notes, we assume no degeneracies ensuring that the basis states are unique up to a phase factor. [7] These basis states $|m(\lambda)\rangle$ are related by a particular adiabatic unitary transformation and we call the associated gauge potentials adiabatic gauge potentials. Such potentials satisfy several properties, which we are going to use later.

First let us note that the diagonal elements of the adiabatic gauge potentials in the basis of $\mathcal{H}(\lambda)$ are, by definition, the Berry connections

$$A_\lambda^{(n)} = \langle n(\lambda)|\mathcal{A}_\lambda|n(\lambda)\rangle = i\hbar\langle n(\lambda)|\partial_\lambda|n(\lambda)\rangle.$$

Recall that up to the sign the gauge potential with respect to time translations is the Hamiltonian itself, and its expectation value is negative the energy. Another important property of these gauge potentials can be found by differentiating the following identity

$$\langle m|\mathcal{H}(\lambda)|n\rangle = 0 \text{ for } n \neq m$$

with respect to λ:

$$\begin{aligned} 0 &= \langle \partial_\lambda m|\mathcal{H}|n\rangle + \langle m|\partial_\lambda \mathcal{H}|n\rangle + \langle m|\mathcal{H}|\partial_\lambda n\rangle & (61) \\ &= E_n\langle \partial_\lambda m|n\rangle + E_m\langle m|\partial_\lambda n\rangle + \langle m|\partial_\lambda \mathcal{H}|n\rangle = (E_m - E_n)\ \underbrace{\langle m|\partial_\lambda n\rangle}_{-i/\hbar\langle m|\mathcal{A}_\lambda|n\rangle}\ + \langle m|\partial_\lambda \mathcal{H}|n\rangle \\ \Longrightarrow \quad \langle m|\mathcal{A}_\lambda|n\rangle &= i\hbar\frac{\langle m|\partial_\lambda \mathcal{H}|n\rangle}{E_n - E_m}\ . & (62) \end{aligned}$$

This relation can be also written in the matrix form

$$i\hbar\partial_\lambda \mathcal{H} = [\mathcal{A}_\lambda, \mathcal{H}] - i\hbar M_\lambda, \tag{63}$$

---

[7] More generally one can define an adiabatic basis as a family of adiabatically connected eigenstates, i.e. eigenstates related to a particular initial basis by adiabatic (infinitesimally slow) evolution of the parameter λ. For example, if two levels cross they will exchange order energetically but the adiabatic connection will be non-singular.

where

$$M_\lambda = -\sum_n \frac{\partial E^{(n)}(\lambda)}{\partial \lambda} |n(\lambda)\rangle\langle n(\lambda)| \tag{64}$$

is an operator that is diagonal in the instantaneous energy eigenbasis, whose values are the generalized forces corresponding to different eigenstates of the Hamiltonian.

As is clear from Eq. (62) the adiabatic gauge potentials maybe ill defined if the energy spectrum is dense and there are non-zero matrix elements of the generalized force operator, $-\partial_\lambda \mathcal{H}$, between nearby eigenstates. This is known as the problem of small denominators. If these divergences happen at isolated points like e.g. phase transitions then they can be easily dealt with as we discuss in Sec. III. But in generic chaotic systems the situation is more subtle and requires careful regularization. Because this is beyond the scope of our lecture notes we will focus on quantum systems with discrete level spacing or on, usually integrable, systems where there is a finite (not exponentially small) energy spacing between energy levels connected by $\partial_\lambda \mathcal{H}$.

Because energy eigenstates are not well-defined in classical systems, we cannot directly extend the expression Eq. (62) to define the classical adiabatic gauge potential. However, we can instead use the matrix relation Eq. (63) recalling that in the classical limit the commutator between two operators corresponds to the Poisson bracket between corresponding functions: $[\dots] \to i\hbar\{\dots\}$. Then classical adiabatic gauge potentials must satisfy

$$-\partial_\lambda \mathcal{H} = M_\lambda - \{\mathcal{A}_\lambda, \mathcal{H}\}, \tag{65}$$

where M_λ is the classical generalized force, which is formally defined as the average of $-\partial_\lambda \mathcal{H}$ over time. This can be seen by recalling that time-averaging is the classical analogue of the quantum average over stationary eigenstates. In the non-chaotic systems that we are focusing on, this time average is equivalent to the average over the stationary orbit containing phase space points $\vec{p}, \vec{q}$. Note that because M_λ is an averaged object it depends only on conserved quantities like energy. An example of how the adiabatic gauge potential is obtained in this way can be found in Sec. III.D.

A different way of defining the adiabatic gauge potential in classical system is to note that the corresponding quantum transformation keeps the Hamiltonian $\tilde{\mathcal{H}}(\lambda)$ in the diagonal form, which means that these Hamiltonians commute with each other at different values of λ. In classical language these corresponds to the canonical transformation such that the Hamiltonians $\mathcal{H}(\lambda, \vec{q}(\lambda), \vec{p}(\lambda))$ have vanishing Poisson brackets at different values of λ if we ignore λ-dependence of $\vec{q}$ and $\vec{p}$. For example if we take the Hamiltonian

$$\mathcal{H} = \frac{p_0^2}{2m} + V(q_0 - \lambda) \tag{66}$$

Then clearly the canonical transformation $q = q_0 + \lambda$ and $p = p_0$ keeps the Hamiltonian independent of λ:

$$\mathcal{H} = \frac{p^2}{2m} + V(q)$$

and thus in this case the corresponding gauge potential is the adiabatic gauge potential. If we take a slightly more complicated example

$$\mathcal{H} = \frac{p_0^2}{2m} + \frac{\lambda^2}{2} q_0^2 \tag{67}$$

and perform the canonical (dilation) transformation to new variables $q = q_0/\sqrt{\lambda}$, $p = p_0\sqrt{\lambda}$ then the resulting family of Hamiltonians reads

$$\mathcal{H} = \lambda \left(\frac{p^2}{2m} + \frac{1}{2} q^2 \right). \tag{68}$$

These Hamiltonians are not identical but differ by an overall scale factor. As a result the Poisson bracket between them at different values of λ vanishes.[8] Therefore the gauge potential corresponding to this particular canonical transformation is the adiabatic gauge potential.

D. Hamiltonian dynamics in the moving frame. Galilean transformation.

Gauge potentials are closely integrated into Hamiltonian dynamics. We will see that they naturally appear not only in gauge theories like electromagnetism, but also in other problems where we attempt a time-dependent change of basis. We will come to issues of gauge invariance later, but for now we simply note that the equations of motion should be invariant under these gauge transformations. Indeed we can describe the same system using an arbitrary set of canonical variables in the classical language or an arbitrary basis in the quantum language.

1. Classical Systems.

Let us first consider the classical equations of motion of some system described by a Hamiltonian that possibly depends on time for the canonical variables $q_i(\lambda, t)$ and $p_i(\lambda, t)$, where as before the index i runs over both the particles and spatial components of the coordinates and momenta. If

[8] In computing this Poisson bracket, q and p are treated as independent variables, rather than functions of λ. Then $\{H(q,p,\lambda), H(q,p,\lambda+d\lambda)\} \approx d\lambda\{H(q,p,\lambda), \partial_\lambda H(q,p,\lambda)\} = d\lambda\{H, \{A_\lambda, H\} - M_\lambda\} = 0$, since $\{H, \{A_\lambda, H\} = \{A_\lambda, \{H,H\} = 0$ and M_λ commutes with H because it is a time-averaged quantity that therefore is a function of only the energy and other conserved quantities.

$\lambda = \lambda_0$ is time independent then we are dealing with normal Hamiltonian dynamics

$$\left[\frac{dq_i}{dt}\right]_l = \{q_i, \mathcal{H}\},\ \left[\frac{dp_i}{dt}\right]_l = \{p_i, \mathcal{H}\}, \tag{69}$$

where the subindex l implies that the derivative is taken in the lab frame at $\lambda = \lambda_0$. Now let us consider the moving frame, where λ also depends on time, i.e. not only do the variables q_i and p_i evolve in time but also their very definition changes with time. Then using Eq. (32) we find

$$\begin{aligned}\left[\frac{dq_i}{dt}\right]_m &= \left[\frac{dq_i}{dt}\right]_l + \dot\lambda\frac{\partial q_i}{\partial\lambda} = \{q_i, \mathcal{H}\} - \dot\lambda\{q_i, \mathcal{A}_\lambda\} = \{q_i, \mathcal{H}_m\}\\ \left[\frac{dp_i}{dt}\right]_m &= \left[\frac{dp_i}{dt}\right]_l + \dot\lambda\frac{\partial p_i}{\partial\lambda} = \{p_i, \mathcal{H}\} - \dot\lambda\{p_i, \mathcal{A}_\lambda\} = \{p_i, \mathcal{H}_m\},\end{aligned} \tag{70}$$

where the subindex m at time derivative highlights that it is taken in the moving frame and we defined the effective moving frame Hamiltonian by generalizing the Galilean transformation

$$\mathcal{H}_m = \mathcal{H} - \dot\lambda\mathcal{A}_\lambda\ . \tag{71}$$

We thus see that the equations of motion in the moving frame preserve their Hamiltonian nature. If λ stands for an x-coordinate of the reference frame, then as we discussed earlier $\mathcal{A}_\lambda = p_x$ and the expression above reduces to the standard Galilean transformation. If λ stands for the angle of the reference frame with respect to the lab frame, then $\mathcal{A}_\lambda$ is the angular momentum and we recover the Hamiltonian in the rotating frame. If λ is the dilation parameter then

$$\mathcal{H}_m = \mathcal{H} - \frac{\dot\lambda}{\lambda}\sum_j q_j p_j\ , \tag{72}$$

using the form of the gauge potential derived in Exercise (II.2).

It is instructive to re-derive the equations of motion in a moving frame using a slightly different, but equivalent approach. Consider the equations of motion in terms of the lab frame coordinates q_0 and p_0:

$$\frac{dq_0}{dt} = \{q_0, \mathcal{H}\},\ \frac{dp_0}{dt} = \{p_0, \mathcal{H}\} \tag{73}$$

Now let us go to the moving frame, i.e., let us find the analogous equations of motion in terms of canonical variables $q(q_0, p_0, \lambda, t)$ and $p(q_0, p_0, \lambda, t)$. Then by the chain rule,

$$\frac{dq}{dt} = \frac{\partial q}{\partial t} + \dot\lambda\frac{\partial q}{\partial\lambda} + \dot q_0\frac{\partial q}{\partial q_0} + \dot p_0\frac{\partial q}{\partial p_0} = \frac{\partial q}{\partial t} + \dot\lambda\{A_\lambda, q\} - \{\mathcal{H}, q\}\ , \tag{74}$$

and similarly for p (and for each component of multi-dimensional $\mathbf{q}$). For the majority of the cases we consider, the basis choice will not depend explicitly on time (only implicitly through λ), so that $\partial_t q = \partial_t p = 0$. Then we see that the equations of motion in the moving frame reduce to Eqs. (70).

Exercise II.10. Find the gauge potential $\mathcal{A}_p$ corresponding to the translations of the momentum $p = p_0 + \partial_q g(q, \lambda)$, $q = q_0$, where $g(q, \lambda)$ is an arbitrary function of the coordinate q and the parameter λ, which in turn can depend on time. Show that the moving frame Hamiltonian with the Galilean term amounts to the standard gauge transformation in electromagnetism, where the vector potential (which adds to the momentum) is transformed according to $\Lambda \to \Lambda + \nabla_q f$ and the scalar potential (which adds to the energy) transforms as $V \to V - \partial_t f$. Find the relation between the gauge potential $\mathcal{A}_p$ and the function f. We use the notation Λ for the electromagnetic vector potential to avoid confusion with the parameter-dependent gauge potential $\mathcal{A}$.

It is interesting to note that the Galilean transformation can be understood from the extended variational principle, where the equations of motion can be obtained by extremizing the action in the extended parameter space-time

$$S = \int [p_i \, dq_i - \mathcal{H} dt + \mathcal{A}_\lambda d\lambda] \tag{75}$$

with respect to all possible trajectories $p_i(\lambda, t)$, $q(\lambda, t)$ satisfying the initial conditions. The derivation is a straightforward generalization of the standard variational procedure found in most textbooks, c.f. Ref. (Landau and Lifshitz, 1982). Extremizing the action at constant time t clearly gives back the canonical transformations (32). Extremizing this action at constant λ with respect to time reproduces the Hamiltonian equations of motion in the lab frame. If we extremize the action along some space time trajectory $\lambda(t)$ such that $d\lambda = \dot{\lambda} dt$ we will clearly reproduce the Hamiltonian equations of motion with the Galilean term (71).

While we are focusing in these notes on conventional canonical transformations, it is easy to use this variational formalism to consider more general transformation where we treat time on equal footing with the other parameters. In particular, we can consider a transformation that maps (t, λ) to new coordinates (τ, μ). When the parameters represent translations in the physical coordinates themselves, this class of transformations are space-time transformation that mix time and space degrees of freedom (e.g., Lorenz transformations in special relativity). For these extended class of transformations, both λ and t can be viewed as functions of μ and τ. By noting that $d\lambda = \frac{\partial \lambda}{\partial \mu} d\mu + \frac{\partial \lambda}{\partial \tau} d\tau$ and $dt = \frac{\partial t}{\partial \mu} d\mu + \frac{\partial t}{\partial \tau} d\tau$, we can rewrite the action Eq. (75) as

$$S = \int \left[p_i \, dq_i - d\tau \left(\mathcal{H} \frac{\partial t}{\partial \tau} - \mathcal{A}_\lambda \frac{\partial \lambda}{\partial \tau} \right) + d\mu \left(\mathcal{A}_\lambda \frac{\partial \lambda}{\partial \mu} - \mathcal{H} \frac{\partial t}{\partial \mu} \right) \right] \tag{76}$$

It is clear that in this generalized moving frame defined by (τ, μ) the Hamiltonian and the gauge potential are given by

$$\mathcal{H}_\tau = \mathcal{H}\frac{\partial t}{\partial \tau} - \mathcal{A}_\lambda \frac{\partial \lambda}{\partial \tau}, \quad \mathcal{A}_\mu = \mathcal{A}_\lambda \frac{\partial \lambda}{\partial \mu} - \mathcal{H}\frac{\partial t}{\partial \mu}.$$

and the corresponding equations of motion are given by (compare to Eq. 70)

$$\frac{\partial q_i}{\partial \tau} = \{q_i, \mathcal{H}_\tau\} - \frac{d\mu}{d\tau}\{q_i, \mathcal{A}_\mu\}, \quad \frac{\partial p_i}{\partial \tau} = \{p_i, \mathcal{H}_\tau\} - \frac{d\mu}{d\tau}\{p_i, \mathcal{A}_\mu\} \tag{77}$$

For the choice, $t = \cosh(\theta)\tau - \sinh(\theta)\mu$ and $\mu = \cosh(\theta)\lambda - \sinh(\theta)\tau$, with θ being a constant, the expression above reproduce Lorentz transformations.

Gauge transformations give us a lot of freedom to choose the moving frame that gives the simplest equations of motion by utilizing symmetries of the Hamiltonian; they allow us to map superficially different problems on each other and so on. In Appendix A we illustrate this idea by analyzing the dynamics of a harmonic one-dimensional system with a time-dependent mass. We also show how using these ideas we can identify a class of interacting models with time-dependent parameters, which effectively behave as time-independent in an appropriately chosen moving frame.

So far our discussion of equations of motion focused on arbitrary gauge transformations. In these notes we, however, are particularly interested in adiabatic gauge transformations. Dynamics in such special adiabatic moving frames is ideally suited for developing adiabatic perturbation theory (discussed in detail in Sec. V). For now, let us show that the adiabatic gauge potentials are responsible for non-adiabatic corrections to the energy change of the system:

$$E(t) = \int dq_i \, dp_i \, \mathcal{H}(q_i, p_i, \lambda)\rho(q_i, p_i, t), \tag{78}$$

where $\rho(q_i, p_i, t)$ is the time dependent density matrix. There is a word of caution needed in understanding this integral as it is usually the subject of confusion. The Hamiltonian and the integration variables here go over all phase space and in this sense they are time independent, while the density matrix evolves according to the Hamiltonian dynamics. Thus, if we choose our integration variables q and p to denote lab-frame coordinates, we get

$$\begin{aligned} \frac{d\mathcal{H}(q_i, p_i, \lambda)}{dt} &= \frac{\partial \mathcal{H}}{\partial \lambda}\dot{\lambda} = \dot{\lambda}\left(\{\mathcal{A}_\lambda, \mathcal{H}\} - M_\lambda\right) \\ \frac{d\rho(q_i, p_i, t)}{dt} &= \{\rho, H\} \end{aligned}$$

where we have rewritten $\partial_\lambda H$ using Eq. (65). Putting this back into Eq, (78) and employing the cyclicity of the integral

$$\int dqdp \, A(q,p)\{B(q,p), C(q,p)\} = \int dqdp \, B(q,p)\{C(q,p), A(q,p)\}$$

for any A, B, and C, we find

$$\begin{aligned}\frac{dE}{dt} &= \int dq_i dp_i \left[\dot{\lambda}\left(\{\mathcal{A}_\lambda, \mathcal{H}\} - M_\lambda\right)\rho + H\{\rho, H\}\right] \\ &= -\dot{\lambda}\int dq_i dp_i\, \rho M_\lambda + \dot{\lambda}\int dq_i dp_i\, \mathcal{A}_\lambda\{\mathcal{H}, \rho\} + \int dq_i dp_i \rho \cancelto{0}{\{H, H\}}.\end{aligned} \tag{79}$$

The first term here gives the standard adiabatic work averaged over the distribution function, as M_λ is the generalized force. The second term gives the non-adiabatic corrections. In particular, it vanishes it vanishes to the leading order in $\dot{\lambda}$ if the initial density matrix is stationary, since then $\{\rho_0, \mathcal{H}\} = 0$. So the leading non-adiabatic contribution in the last term in Eq. (79) due to the adiabatic gauge potential is of order $\dot{\lambda}^2$.

2. Quantum Systems.

Very similar analysis goes through for the quantum systems. Interestingly the derivations for quantum systems are even simpler than for classical ones. Consider the Schrödinger equation

$$i\hbar d_t|\psi\rangle = \mathcal{H}|\psi\rangle \tag{80}$$

after the transformation to the moving frame: $|\psi\rangle = U(\lambda)|\tilde{\psi}\rangle$:

$$i\hbar\dot{\lambda}(\partial_\lambda U)|\tilde{\psi}\rangle + i\hbar U\partial_t|\tilde{\psi}\rangle = \mathcal{H}U|\tilde{\psi}\rangle \tag{81}$$

Multiplying both sides of this equation by $U^\dagger$ and moving the first term in the L.H.S. of this equation to the right we find

$$i\hbar d_t|\tilde{\psi}\rangle = \left[U^\dagger \mathcal{H} U - \dot{\lambda}\tilde{\mathcal{A}}_\lambda\right]|\tilde{\psi}\rangle = \left[\tilde{\mathcal{H}} - \dot{\lambda}\tilde{\mathcal{A}}_\lambda\right]|\tilde{\psi}\rangle = \tilde{\mathcal{H}}_m|\tilde{\psi}\rangle\ . \tag{82}$$

Here $\tilde{\mathcal{H}} = U^\dagger\mathcal{H}U$ is the original Hamiltonian written in the moving basis while $-\dot{\lambda}\tilde{\mathcal{A}}_\lambda$ is the Galilean term. The moving Hamiltonian $\mathcal{H}_m = \mathcal{H} - \dot{\lambda}\mathcal{A}_\lambda$ thus retains the same form as in classical systems.

In the adiabatic moving frame it is easy to get the analogue of Eq. (79) by differentiating energy with respect to time and using (82):

$$\frac{dE}{dt} = \frac{d}{dt}\langle\tilde{\psi}|\tilde{\mathcal{H}}|\tilde{\psi}\rangle = \dot{\lambda}\langle\tilde{\psi}|\partial_\lambda\tilde{\mathcal{H}}|\tilde{\psi}\rangle - \frac{i}{\hbar}\dot{\lambda}\langle\tilde{\psi}|[\tilde{\mathcal{A}}_\lambda, \tilde{\mathcal{H}}|\tilde{\psi}\rangle = -\dot{\lambda}M_\lambda - -\frac{i}{\hbar}\dot{\lambda}\langle\psi|[\mathcal{A}_\lambda, \mathcal{H}|\psi\rangle. \tag{83}$$

Because the Hamiltonian $\tilde{\mathcal{H}}$ is diagonal in the instantaneous basis the expectation value $\langle\tilde{\psi}|\partial_\lambda\tilde{\mathcal{H}}|\tilde{\psi}\rangle$ is nothing but negative the generalized force defined in Eq. (64). We also note that expectation value of any operator is invariant under choice of basis so we can remove tilde sign in all final expressions. Let us point out that the the second term vanishes at leading order in $\dot{\lambda}$ if the initial state is an energy eigenstate. Then up to higher orders in $\dot{\lambda}$, $|\psi\rangle$ remains the eigenstate of the instantaneous Hamiltonian and the expectation value of the commutator $[\mathcal{A}_\lambda, \mathcal{H}]$ vanishes. It is easy to see that these considerations apply to mixed states as well.

From Eq. (82) we see that one gets a generalized Galilean correction to the Hamiltonian which is proportional to the gauge potential $\mathcal{A}_\lambda$. Later in these lectures, we will see many ways in which this term manifests in the dynamics of closed systems. We will do so after discussing in more detail the geometric properties that are encoded in the $\mathcal{A}_\lambda$ operator.

E. Galilean transformation and shortcuts to adiabaticity.

We will conclude this section by a brief discussion of another interesting application of the generalized gauge transformation which has been termed shortcuts to adiabaticity. We will refer interested readers to a recent paper (Deffner et al., 2014) and references therein for more details while presenting here only the basic idea originally suggested by M. Demirplak and S. A. Rice in 2003.

In the previous section we discussed that the Galilean term is the one causing transitions between energy levels of the original Hamiltonian $\mathcal{H}$. In order to eliminate these transitions it suffices to simply add a counter-adiabatic (or counter Galilean) term $\dot{\lambda}\mathcal{A}_\lambda$ to the driving protocol such that the system evolves under the Hamiltonian

$$\mathcal{H}(\lambda) + \dot{\lambda}\mathcal{A}_\lambda(\lambda) \tag{84}$$

Then if we go to the moving frame of the instantaneous Hamiltonian $\mathcal{H}$ (we will stick to the quantum language here as we already explained equivalence with the classical language) then the moving Hamiltonian will be

$$\tilde{\mathcal{H}}_m = \tilde{\mathcal{H}} - \dot{\lambda}\tilde{\mathcal{A}}_\lambda + \dot{\lambda}\tilde{\mathcal{A}}_\lambda = \tilde{\mathcal{H}} \tag{85}$$

By definition $\tilde{\mathcal{H}}$ is the diagonalized version of $\mathcal{H}$. Thus, if the system is initially prepared in a stationary distribution, say the ground state, it will always remain in such a stationary distribution no matter how fast the protocol is. An important but not yet well understood question, especially in many-particle systems, is in which situations $\mathcal{A}_\lambda$ is a physically-realistic operator. Even when this is not the case, one can attempt to construct local operators which approximate $\mathcal{A}_\lambda$ to a sufficient degree that non-adiabatic effects are reduced, if not to zero, then to a very small value. These questions are beyond the scope of these notes. Instead we will illustrate the idea with a few simple examples.

Particle in a moving box. We will start from the simplest and most intuitive example of a particle of mass m confined to some potential $V(q-X)$ which depends on the parameter X, say the minimum of this potential. We want to move this potential from some initial point X_0 to final point X_1 without exciting the particle inside. From exercise II.7 we know that the gauge potential corresponding to translations is the momentum operator: $\tilde{\mathcal{A}}_X = \mathcal{A}_X = \hat{p}$. Thus the counter-adiabatic term should be $\dot{X}\hat{p}$ such that the desired time-dependent Hamiltonian is

$$\mathcal{H} = \frac{\hat{p}^2}{2m} + V(q - X(t)) + \dot{X}(t)\hat{p}. \tag{86}$$

To bring this Hamiltonian to a more familiar form one can make another gauge transformation corresponding to the momentum shift $\hat{p} \to \hat{p} + m\dot{X}$ (see exercise II.10) resulting in a moving Hamiltonian

$$\mathcal{H} = \frac{\hat{p}^2}{2m} + V(q - X) - m\ddot{X}q - \frac{m\dot{X}^2}{2}. \tag{87}$$

The last term here, which comes from completing the square can be omitted as it does not depend on q and p, while the third term is nothing but an effective gravitational field, which compensates the acceleration of the system. In the classical language this term ensures that in the accelerating frame there are no additional forces acting on the particle due to the acceleration.

Potential squeezing. Let us now consider a slightly more complex example of a particle in a squeezing potential. Now we will analyze the problem classically using the language of canonical transformations. An example of such a squeezing would be a particle confined to a box of size L with the length changing in time. Another example would be squeezing a particle in a harmonic potential. To ensure the symmetry of the system under dilations (such that the relevant adiabatic gauge potential takes a simple form) we will assume that the potential is scale invariant, i.e. $V(q\lambda) = \lambda^n V(q_0)$, where n is an arbitrary power (for a specific example of a particle in a Morse potential with $n = 2$ see Ref. (Deffner et al., 2014) and Ref. [33] by C. Jarzynski therein). Our goal now is to evolve the system adiabatically by going from the initial potential $V(q)$ to the final potential $V(\xi q_0) = \xi^n V(q_0)$, where ξ is a given scale factor. To solve this problem let us first consider a general dilation transformation on the system $q = \lambda q_0$ and $p = p_0/\lambda$. The Hamiltonian

$$\mathcal{H} = \frac{p_0^2}{2m} + \xi^n V(q_0)$$

in these new transformed variables reads

$$\mathcal{H} = \frac{p^2\lambda^2}{2m} + \frac{\xi^n}{\lambda^n}V(q) = \lambda^2\left(\frac{p^2}{2m} + \frac{\xi^n}{\lambda^{2+n}}V(q)\right). \tag{88}$$

We thus see that if we choose

$$\lambda = \xi^{\frac{n}{n+2}}$$

then up to an overall scale factor (which can be absorbed into the time dilation) the Hamiltonian in new variables is equivalent to $\mathcal{H} = p^2/(2m) + V(q)$. Thus changing the factor ξ as a function of time is equivalent to changing the scale factor λ according to the relation above. The gauge potential corresponding to dilations (see exercise II.2) is $\mathcal{A}_\lambda = -qp/\lambda = -q_0 p_0/\lambda$ thus with the counter-adiabatic term the Hamiltonian which does not excite the system is

$$\mathcal{H} = \lambda^2 \left(\frac{p^2}{2m} + V(q) \right) - \frac{\dot{\lambda}}{\lambda} qp = \frac{p_0^2}{2m} + \xi^n V(q_0) - \frac{n}{n+2} \frac{\dot{\xi}}{\xi} q_0 p_0, \tag{89}$$

where we used that $\dot{\lambda}/\lambda = \frac{n}{n+2} \dot{\xi}/\xi$ and we re-expressed the Hamiltonian in terms of original lab variables. As in the previous example it is convenient to shift the momentum variable $p' = p_0 - m \frac{n}{n+2} \frac{\dot{\xi}}{\xi} q_0$ resulting in an equivalent Hamiltonian

$$\begin{aligned} \mathcal{H} = \frac{p'^2}{2m} + \xi^n V(q_0) + \frac{m}{2} \left[\frac{n}{n+2} \frac{d^2 \log \xi}{dt^2} - \left(\frac{n}{n+2} \frac{d \log \xi}{dt} \right)^2 \right] q_0^2 \\ = \frac{p'^2}{2m} + \lambda^{n+2} V(q_0) + \frac{m}{2} \left[\frac{d^2 \log \lambda}{dt^2} - \left(\frac{d \log \lambda}{dt} \right)^2 \right] q_0^2. \end{aligned} \tag{90}$$

So the counter-adiabatic term amounts to adding a harmonic potential proportional to the second derivative of the logarithm of the scale factor.

Exercise II.11. Show that Eq. (89) applies to quantum systems if we identify q_0 with the position operator q, p_0 with the momentum operator $\hat{p}$ and $q_0 p_0 \to (\hat{q}\hat{p} + \hat{p}\hat{q})/2$.

Exercise II.12. Write down explicitly the Hamiltonian equations of motion corresponding to the Hamiltonian (90). Check that under substitutions $dt = d\tau/\lambda^2$, $q = \tilde{q}/\lambda$ and $p' = \tilde{p}\lambda$ the equations of motion become independent of λ for any time dependence $\lambda(t)$:

$$\frac{d\tilde{p}}{d\tau} = -\partial_{\tilde{q}} V(\tilde{q}), \quad \frac{d\tilde{q}}{d\tau} = \frac{\tilde{p}}{m}. \tag{91}$$

From this conclude that the evolution of the system is strictly adiabatic, which e.g. manifests in exact conservation of the adiabatic invariants, zero heat generation and complete reversibility for any cyclic function $\lambda(t)$.

Exercise II.13. Consider a quantum particle in a one dimensional harmonic potential $V(q) = kq^2/2$ with a time dependent k. By appropriately choosing λ check explicitly that the time dependent

Schrödinger equation corresponding to the Hamiltonian (90) results in adiabatic dynamics. One can for example, check that the particle in the ground state always remains in the ground state and then generalize this result to excited states.

Exercise II.14. Repeat the previous exercise for a particle in an infinite square well potential of length L with L being an arbitrary function of time. Note that the infinite square well confined between $-L/2$ and $L/2$ can be approximated by the potential $V(q) = (2q/L)^n$ for an even integer n in the limit $n \to \infty$.

III. GEOMETRY OF IN STATE SPACE. THE FUBINI-STUDY METRIC AND THE BERRY CURVATURE.

Key concept: The geometry of the wave function in parameter space can be characterized by the geometric tensor, which is the covariance matrix of the gauge potentials. Its symmetric and antisymmetric parts define the Fubini-Study metric and the Berry curvature respectively. One can generalize these to classical systems using their representation as two-time correlation functions.

A. Geometry of the quantum ground state manifold

Up till now, we have treated quantum and classical systems on an equal footing. In this section we will mostly focus on the geometric properties of the ground state manifold in quantum systems. For this reason, with the exception of Sec. III.D, we restrict our discussion to the quantum case. We will return to classical systems later in the notes when we discuss non-adiabatic dynamical response.

The first notion of the quantum geometric tensor appeared in 1980 in Ref. 37. Formally the geometric tensor is defined on any manifold of states smoothly varying with some parameter $\boldsymbol{\lambda}$: $|\psi_0(\boldsymbol{\lambda})\rangle$.[9] For now we will be primarily interested in the family of ground states of some Hamiltonian. We will assume that the ground state is either non-degenerate or, in the case of degeneracy, ground states are not connected by the matrix elements of generalized force operators $\mathcal{M}_\alpha \equiv \mathcal{M}_{\lambda_\alpha} = -\partial \mathcal{H}/\partial \lambda_\alpha$. The geometric tensor naturally appears when one defines the "distance" ds between nearby states $|\psi_0(\boldsymbol{\lambda})\rangle$ and $|\psi_0(\boldsymbol{\lambda} + d\boldsymbol{\lambda})\rangle$:

$$ds^2 \equiv 1 - f^2 = 1 - |\langle \psi_0(\boldsymbol{\lambda})|\psi_0(\boldsymbol{\lambda} + d\boldsymbol{\lambda})\rangle|^2, \tag{92}$$

[9] From now on we will assume that the parameters can be multi-component.

where $f = |\langle\psi_0(\boldsymbol{\lambda})|\psi_0(\boldsymbol{\lambda} + d\boldsymbol{\lambda})\rangle|$ is the so called fidelity of the ground state. Note that $1 - f^2$ is always positive. Therefore, the Taylor expansion about $d\boldsymbol{\lambda} = 0$ does not contain any first order terms in $d\boldsymbol{\lambda}$, and starts with a quadratic term:

$$ds^2 = d\lambda_\alpha \chi_{\alpha\beta} d\lambda_\beta + O(|d\boldsymbol{\lambda}|^3), \tag{93}$$

where $\chi_{\alpha\beta}$ is as object known as the geometric tensor. To find this tensor explicitly let us note that $1 - f^2$ is nothing but the probability to excite the system during a quantum quench where the parameter suddenly changes from $\boldsymbol{\lambda}$ to $\boldsymbol{\lambda} + d\boldsymbol{\lambda}$. Indeed f^2 is simply the probability to remain in the ground state after this quench. The amplitude of going to the excited state $|\psi_n\rangle$ is

$$a_n = \langle\psi_n(\boldsymbol{\lambda} + d\boldsymbol{\lambda})|\psi_0(\boldsymbol{\lambda})\rangle \approx d\lambda_\alpha \langle n|\overleftarrow{\partial}_\alpha|0\rangle = -d\lambda_\alpha \langle n|\partial_\alpha|0\rangle, \tag{94}$$

where the arrow over the derivative indicates that it acts on the left (derivatives without arrows implicitly act to the right). To shorten the notations, we introduce $\partial_\alpha \equiv \partial_{\lambda_\alpha}$ and $|n\rangle \equiv |\psi_n(\boldsymbol{\lambda})\rangle$. Recall that (see Eq. (59))

$$i\langle n|\partial_\alpha|m\rangle = \langle n|\mathcal{A}_\alpha|m\rangle^{10}, \tag{95}$$

Thus we see that the amplitude of going to the excited state at leading order in $d\boldsymbol{\lambda}$ is proportional to the matrix element of the gauge potential

$$a_n = -d\lambda_\alpha \langle n|\partial_\alpha|0\rangle = i\langle n|\mathcal{A}_\alpha|0\rangle d\lambda_\alpha\ . \tag{96}$$

Therefore the probability of transitioning to any excited state is given by taking a sum over $n \neq 0$:

$$ds^2 = \sum_{n\neq 0} |a_n^2| = \sum_{n\neq 0} d\lambda_\alpha d\lambda_\beta \langle 0|\mathcal{A}_\alpha|n\rangle\langle n|\mathcal{A}_\beta|0\rangle + O(|d\boldsymbol{\lambda}|^3) = d\lambda_\alpha d\lambda_\beta \langle 0|\mathcal{A}_\alpha\mathcal{A}_\beta|0\rangle_c + O(|d\boldsymbol{\lambda}|^3), \tag{97}$$

where the subscript c implies that we are taking the connected correlation function (a.k.a. the covariance):

$$\langle 0|\mathcal{A}_\alpha\mathcal{A}_\beta|0\rangle_c \equiv \langle 0|\mathcal{A}_\alpha\mathcal{A}_\beta|0\rangle - \langle 0|\mathcal{A}_\alpha|0\rangle\langle 0|\mathcal{A}_\beta|0\rangle. \tag{98}$$

This covariance precisely determines the geometric tensor introduced by Provost and Vallee (Provost and Vallee, 1980)

$$\chi_{\alpha\beta} = \langle 0|\mathcal{A}_\alpha\mathcal{A}_\beta|0\rangle_c. \tag{99}$$

[10] As this section largely focuses on quantum systems, we set $\hbar = 1$.

In terms of many-body wave functions the geometric tensor can be expressed through the overlap of derivatives:

$$\chi_{\alpha\beta} = \langle 0|\overleftarrow{\partial}_\alpha \partial_\beta|0\rangle_c = \langle \partial_\alpha \psi_0|\partial_\beta \psi_0\rangle_c = \langle \partial_\alpha \psi_0|\partial_\beta \psi_0\rangle - \langle \partial_\alpha \psi_0|\psi_0\rangle\langle \psi_0|\partial_\beta \psi_0\rangle. \tag{100}$$

When $\hbar$ is not set to unity the two definitions of the geometric tensor (99) and (100) differ by a factor of $\hbar^2$ as $\mathcal{A}_\alpha = i\hbar\partial_\alpha$. We will stick to Eq. (100) as the fundamental one because in this way it is always related to the distance between wave functions. The last term in this expression is necessary to enforce invariance of the geometric tensor under arbitrary global phase transformations of the wave function $\psi_0(\boldsymbol{\lambda}) \to \exp[i\phi(\boldsymbol{\lambda})]\psi_0(\boldsymbol{\lambda})$, which should not affect the notion of the distance between different ground states.

Exercise III.1. Consider the global phase transformation $\psi_n(\boldsymbol{\lambda}) \to \exp[i\phi_n(\boldsymbol{\lambda})]\psi_n(\boldsymbol{\lambda})$ where $\phi_n(\boldsymbol{\lambda})$ are smooth functions defined over the entire parameter manifold for each eigenstate ψ_n. What is the effect of this transformation on the gauge potential $\mathcal{A}$? Show that the ground state geometric tensor $\chi_{\alpha\beta}$ is invariant under this gauge transformation.

Note that in general the geometric tensor is not symmetric. Indeed because the operators $\mathcal{A}_\alpha$ are Hermitian one can show that χ is also Hermitian:

$$\chi_{\alpha\beta} = \chi^*_{\beta\alpha}. \tag{101}$$

Only the symmetric part of $\chi_{\alpha\beta}$ determines the distance between the states; in the quadratic form

$$ds^2 = d\lambda_\alpha \chi_{\alpha\beta} d\lambda_\beta$$

one can always symmetrize the indexes α and β so that the antisymmetric part drops out. Nevertheless, both the symmetric and the anti-symmetric parts of the geometric tensor are very important. The symmetric part,

$$g_{\alpha\beta} = \frac{\chi_{\alpha\beta} + \chi_{\beta\alpha}}{2} = \frac{1}{2}\langle 0|(\mathcal{A}_\alpha \mathcal{A}_\beta + \mathcal{A}_\beta \mathcal{A}_\alpha)|0\rangle_c = \Re\langle 0|\mathcal{A}_\alpha \mathcal{A}_\beta|0\rangle_c \tag{102}$$

is called the Fubini-Study metric tensor.[11] The antisymmetric part of the geometric tensor defines

[11] Sometimes in the literature one understands the Fubini-Study metric to mean the complete metric in the projective Hilbert space where the number of parameters λ_α coincides with the dimension of the Hilbert space. Throughout this article, we mean by Fubini-Study the metric in parameter space defined by distances between wave functions, which can be thought of as the projection (or pullback) of the full Hilbert space metric onto the manifold of ground states.

the Berry curvature

$$F_{\alpha\beta} = i(\chi_{\alpha\beta} - \chi_{\beta\alpha}) = -2\Im\chi_{\alpha\beta} = i\langle 0|[\mathcal{A}_\alpha, \mathcal{A}_\beta]|0\rangle \ , \tag{103}$$

which we introduced earlier. The Berry curvature plays a crucial role in most known quantum geometric and topological phenomena.

Let us note that the Berry curvature can be expressed through the derivatives of the Berry connections:

$$F_{\alpha\beta} = \partial_\alpha A_\beta - \partial_\beta A_\alpha, \tag{104}$$

where the Berry connection,

$$A_\alpha = \langle 0|\mathcal{A}_\alpha|0\rangle = i\langle 0|\partial_\alpha|0\rangle \ , \tag{105}$$

is just the ground state expectation of the gauge potential. One can easily check this through direct differentiation:

$$\partial_\alpha A_\beta - \partial_\beta A_\alpha = i\langle 0|\overleftarrow{\partial}_\alpha \partial_\beta|0\rangle - i\langle 0|\overleftarrow{\partial}_\beta \partial_\alpha|0\rangle + i\langle 0|\partial^2_{\alpha\beta}|0\rangle - i\langle 0|\partial^2_{\beta\alpha}|0\rangle = i(\chi_{\alpha\beta} - \chi_{\beta\alpha}) \ . \tag{106}$$

It is well known that the Berry connection is directly related to the phase of the ground state wave function. Indeed if the wave function in e.g. coordinate representation, can be written as

$$\psi_0 = |\psi_0(\mathbf{r}, \boldsymbol{\lambda})| \exp[i\phi(\boldsymbol{\lambda})] \tag{107}$$

we find that

$$A_\alpha = -\int d\mathbf{r} |\psi_0|^2 \partial_\alpha \phi = -\partial_\alpha \phi \tag{108}$$

Therefore the integral of A_α over a closed path $\mathcal{C}$ represents the total phase (Berry phase) accumulated by the wave function during the adiabatic evolution

$$\varphi_B = \oint_{\mathcal{C}} \partial_\alpha \phi d\lambda_\alpha = -\oint_{\mathcal{C}} A_\alpha d\lambda_\alpha \ . \tag{109}$$

By Stokes' theorem, the same phase can be represented as the integral of the Berry curvature over the surface enclosed by the contour $\mathcal{C}$:

$$\varphi_B = \int_S F_{\alpha\beta} d\lambda_\alpha \wedge d\lambda_\beta, \tag{110}$$

where the wedge product implies that the integral is directed.

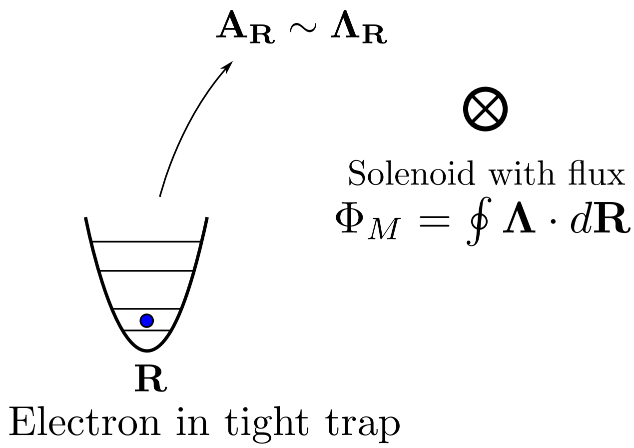

FIG. 5 Illustration of Aharonov-Bohm geometry being considered.

To get an intuition about the Berry curvature and the metric tensor let us consider two simple examples. First, following the original paper by Berry, let us consider the Aharonov-Bohm geometry (Fig. 5), namely a particle confined in a deep potential in the presence of a solenoid. The Hamiltonian for this system is

$$\mathcal{H} = \frac{(\mathbf{p} - e\mathbf{\Lambda}(\mathbf{r}))^2}{2m} + V(\mathbf{r} - \mathbf{R}), \tag{111}$$

where $\mathbf{\Lambda}$ is the electromagnetic vector potential (we use $\mathbf{\Lambda}$ to avoid the confusion with the Berry connection) and $V(\mathbf{r} - \mathbf{R})$ is a confining potential near some point $\mathbf{R}$ outside the solenoid, where there is no magnetic field. For example, one can choose $V(r) = m\omega^2 r^2/2$, which is simply the potential of a two-dimensional harmonic oscillator. Far from the solenoid, there is no magnetic field hence $\mathbf{\nabla} \times \mathbf{\Lambda} = 0$, which implies that the vector potential can be written as a gradient of the magnetic potential (cf. Jackson (Jackson, 1999))

$$\mathbf{\Lambda} = \mathbf{\nabla}\Phi \Rightarrow \Phi(\mathbf{r}, \mathbf{R}) = \int_{\mathbf{R}}^{\mathbf{r}} \mathbf{\Lambda} \cdot d\mathbf{r}\ .$$

Note that because the vector potential is curl-free the integral does not depend on the path so the path can be as straight line. In principle, the lower limit of integration is arbitrary and does not have to be tied to $\mathbf{R}$. With this choice, however, it is guaranteed that whenever $\mathbf{r}$ is close to $\mathbf{R}$ the path does not cross the solenoid, where the curl-free condition for the vector potential is broken and the magnetic potential is not defined. One can easily check by explicitly plugging in the following functional form into the Schrödinger's equation that the vector potential can be locally eliminated by a gauge transformation:

$$\psi_0(\mathbf{r}) = \tilde{\psi}_0(\mathbf{r} - \mathbf{R}) \exp\left[ie\Phi(\mathbf{r}, \mathbf{R})\right]. \tag{112}$$

Electromagnetism	**Quantum geometry**
Vector potential $\mathbf{A}(\mathbf{x})$	Berry connection $\mathbf{A}(\boldsymbol{\lambda}) = i\langle\psi_0(\boldsymbol{\lambda})\vert\nabla_\lambda\psi_0(\boldsymbol{\lambda})\rangle$
Magnetic field/EM tensor $F_{ab}(\mathbf{x}) = \partial_{x_a}A_b(\mathbf{x}) - \partial_{x_b}A_a(\mathbf{x}) = \sum_c \epsilon_{abc}B_c$	Berry curvature $F_{\mu\nu}(\boldsymbol{\lambda}) = \partial_{\lambda_\mu}A_\nu(\boldsymbol{\lambda}) - \partial_{x_\nu}A_\mu(\boldsymbol{\lambda})$
Aharonov-Bohm phase $\varphi_{AB} = \oint \mathbf{A}(\mathbf{x})\cdot d\mathbf{x}$	Berry phase $\varphi_B = \oint \mathbf{A}(\boldsymbol{\lambda})\cdot d\boldsymbol{\lambda}$

TABLE I Comparison between electromagnetism and ground state (Berry) geometry in quantum mechanics. ϵ_{abc} is the Levi-Civita symbol.

Then the Hamiltonian for $\tilde{\psi}$ becomes independent of the vector potential and thus the wave function $\tilde{\psi}_0$, which is the ground state in the absence of the vector potential, can be chosen to be real. In this case the Berry connection with respect to the position of the trap $\mathbf{R}$ is, as we just discussed, the derivative of the phase with respect to $\mathbf{R}$:

$$\mathbf{A}_{\mathbf{R}} = -e\partial_{\mathbf{R}}\Phi = e\partial_{\mathbf{r}}\Phi = e\boldsymbol{\Lambda}(\mathbf{r}) \tag{113}$$

More accurately one needs to average the vector potential over the wave function $\tilde{\psi}(\mathbf{r}-\mathbf{R})$ but assuming that it is localized near $\mathbf{R}$ the averaging simply reduces to $\boldsymbol{\Lambda}(\mathbf{R})$. Then, the Berry phase for a cyclic path $\mathbf{R}(t)$ is $\varphi_B = \oint \mathbf{A}\cdot d\mathbf{R} = 2\pi\Phi_M/\Phi_0$ if the path surrounds the solenoid, and zero if it does not, where $\Phi_0 = 2\pi\hbar/e$ is the flux quantum of the electron. This follows directly from $\Phi_M = \oint \boldsymbol{\Lambda}(\mathbf{R})\cdot d\mathbf{R}$ and the definition of the flux quantum with reinserted Planck's constant.

From the above arguments we see that, up to fundamental constants, the Berry connection plays the role of the vector potential, hence the Berry phase assumes the role of the Aharonov-Bohm phase and the Berry curvature (curl of the Berry connection) plays the role of the magnetic field. We summarize this analogy in Table I. Note that the Berry curvature is more generally written as the arbitrary-dimensional curl, $F_{\alpha\beta} = \partial_\alpha A_\beta - \partial_\beta A_\alpha$, which is equivalent to representing the magnetic field as the off-diagonal components of the electromagnetic field-strength tensor. This analogy is very useful when we think about general parameter space and, as we will see later, this analogy is not coincidental. For example, we will see that like the magnetic field, the Berry curvature is the source of a Lorentz force.

Unlike the Berry phase/curvature, in this example the metric tensor depends on details of the trapping potential $V(r)$. This is readily seen by considering that the particle is bound within some radius $\ell \ll R$ (for instance $\ell \sim 1/\sqrt{m\omega}$ for the harmonic oscillator). If we move the trap away from the solenoid by an amount ΔR such that $R \gg \Delta R \gg \ell$ the phase independent wave function $\tilde{\psi}_0(\mathbf{r}-\mathbf{R})$ will rapidly change such that $\tilde{\psi}_0(\mathbf{r}-\mathbf{R})$ and $\tilde{\psi}_0(\mathbf{r}-\mathbf{R}-\mathbf{\Delta R})$ will become almost orthogonal, while the phase ϕ will stay almost constant. So the metric tensor only slightly depends on the flux through the solenoid and instead strongly depends on how the ground state of V changes with the position $\mathbf{R}$. For the isotropic harmonic oscillator, one easily sees that the metric tensor is isotropic:

$$g_{R_xR_x} = g_{R_yR_y} = \langle \mathcal{A}_x\mathcal{A}_x\rangle_c = \langle p_x^2\rangle_c = \langle p_x^2\rangle = \frac{m\omega}{2}. \tag{114}$$

Going along a path, cyclic or not, one can define an invariant dimensionless length

$$L_g = \oint ds = \int dt\sqrt{g_{\alpha\beta}\dot{R}_\alpha\dot{R}_\beta} = L\sqrt{\frac{m\omega}{2}}\ , \tag{115}$$

where $L = \int |\dot{\mathbf{R}}|dt$ is the length of the path in real space. Loosely speaking this length measures the number of orthogonal ground states traversed along the path.

Let us now analyze the geometry of another simple system, which we already encountered earlier: the quantum spin-1/2 in a magnetic field. As before, we choose parameters to be the angles θ and ϕ of the magnetic field. As a reminder, ground and excited states are (see Eq. (2))

$$|g\rangle = \begin{pmatrix} \cos(\theta/2) \\ e^{i\phi}\sin(\theta/2) \end{pmatrix}\ ,\ |e\rangle = \begin{pmatrix} \sin(\theta/2) \\ -e^{i\phi}\cos(\theta/2) \end{pmatrix}\ . \tag{116}$$

Direct evaluation of the geometric tensor for the ground state gives

$$\chi_{\theta\theta} = \langle\partial_\theta g|\partial_\theta g\rangle - \langle\partial_\theta g|g\rangle\langle g|\partial_\theta g\rangle = \frac{1}{4},\ \chi_{\phi\phi} = \frac{1}{4}\sin^2(\theta),\ \chi_{\theta\phi} = \frac{i}{4}\sin(\theta)\ .s \tag{117}$$

These expressions can also be obtained by calculating the covariance matrix of the gauge potentials,

$$\mathcal{A}_\theta = i\partial_\theta = -\frac{1}{2}\tau_y,\ \mathcal{A}_\phi = i\partial_\phi = \frac{1}{2}\big(\sigma_z - 1\big) = \frac{1}{2}\big(\tau_z\cos\theta + \tau_x\sin\theta - 1\big)\ , \tag{118}$$

which are generators of rotations in the θ and ϕ directions. Here the Pauli matrices τ are rotated to act in the basis of instantaneous eigenstates, e.g. $\langle e|\tau_x|g\rangle$=1. In this instantaneous basis the Hamiltonian is $\mathcal{H} = -h\tau_z$ (see Fig. 6). The equations above generalize to particles with arbitrary spin where instead of spin one-half operators like $\tau_y/2$, one uses the angular momentum operator S_y.

From the expression for the geometric tensor we see that the nonzero metric tensor components are

$$g_{\theta\theta} = \frac{1}{4},\ g_{\phi\phi} = \frac{1}{4}\sin^2\theta, \tag{119}$$

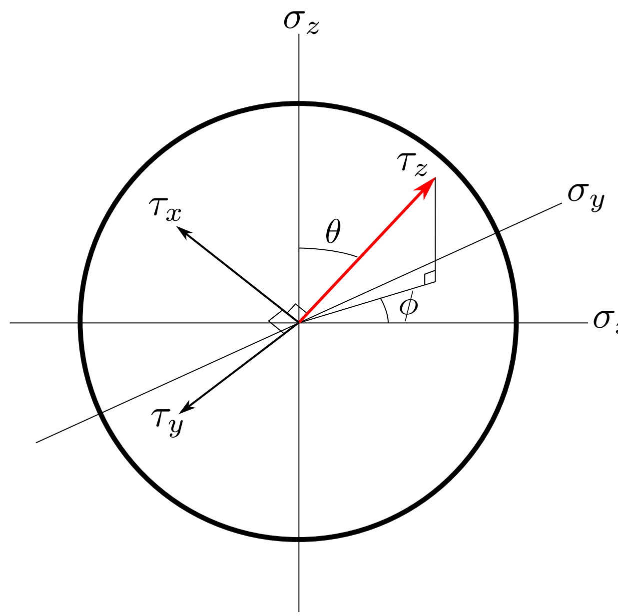

FIG. 6 Comparison of instantaneous eigenbasis (τ) with the original one (σ). Rotations in the θ (ϕ) direction correspond to rotations about the $-y'$ (z) axes, which are generated by $-\tau_y/2$ and $\sigma_z/2$ respectively.

and the Berry curvature is

$$F_{\theta\phi} = \partial_\theta A_\phi - \partial_\phi A_\theta = \frac{1}{2}\partial_\theta \cos(\theta) = -\frac{1}{2}\sin(\theta) = -F_{\phi\theta} \ . \tag{120}$$

Note that the Fubini-Study metric for this model is equivalent to the metric of a sphere of radius $r = 1/2$. It is interesting to note that for the excited state the metric tensor is the same while the Berry curvature has an opposite sign.

Exercise III.2. Calculate the covariance matrix of the spin-1/2 gauge potentials (Eq. (118)) and show that it gives the correct values for the geometric tensor.

Exercise III.3. Find the geometric tensor of the shifted harmonic oscillator (Eq. (17)) using the gauge potentials $\mathcal{A}_{x_0} = \hat{p} + p_0$ and $\mathcal{A}_{p_0} = -x$ (Eq. (19)).

The notion of distance between wave functions is very simple and intuitive but not directly measurable. As we discuss next the geometric tensor can be related to a standard Kubo susceptibility. Specifically it can be expressed through the non-equal time correlation functions of physical operators in both real and imaginary times. We start by taking the geometric tensor in the so-called Kallen-Lehmann representation (Kallen, 1952; Lehmann, 1954),

$$\chi_{\alpha\beta} = \sum_{n\neq 0} \langle 0|\mathcal{A}_\alpha|n\rangle\langle n|\mathcal{A}_\beta|0\rangle = \sum_{n\neq 0} \frac{\langle 0|\partial_\alpha \mathcal{H}|n\rangle\langle n|\partial_\beta \mathcal{H}|0\rangle}{(E_n - E_0)^2} \ , \tag{121}$$

where the second equality follows from Eq. (62) and we assumed that the ground state is not degenerate. Let us use the following standard trick to connecting the Kallen-Lehmann representation of some observable to its non-equal time correlation functions:

$$\frac{1}{(E_n - E_0)^2} = \int_{-\infty}^{\infty} d\omega \frac{1}{\omega^2}\delta(E_n - E_0 - \omega) = \int_{-\infty}^{\infty} \frac{d\omega}{\omega^2} \int_{-\infty}^{\infty} \frac{dt}{2\pi} \mathrm{e}^{-i(E_n - E_0 - \omega)t}. \tag{122}$$

We can always add $\exp[-\epsilon|t|]$ to this integral to ensure convergence. Next we note that

$$\langle 0|\mathrm{e}^{iE_0 t}\partial_\alpha \mathcal{H}\mathrm{e}^{-iE_n t}|n\rangle = \langle 0|\partial_\alpha \mathcal{H}(t)|n\rangle \tag{123}$$

is the matrix element of the operator $\partial_\alpha \mathcal{H}$ in the Heisenberg representation. Plugging this into Eq. (121) we find

$$\chi_{\alpha\beta} = \int_{-\infty}^{\infty} \frac{d\omega}{2\pi} \frac{S_{\alpha\beta}(\omega)}{\omega^2} = \int_0^{\infty} \frac{d\omega}{2\pi} \frac{S_{\alpha\beta}(\omega) + S_{\alpha\beta}(-\omega)}{\omega^2}, \tag{124}$$

where

$$S_{\alpha\beta}(\omega) = \int_{-\infty}^{\infty} dt \mathrm{e}^{i\omega t} \langle 0|\partial_\alpha \mathcal{H}(t) \partial_\beta \mathcal{H}(0)|0\rangle_c. \tag{125}$$

This object $S_{\alpha\beta}(\omega)$ is just the Fourier transform of the observables' fluctuations, and it is intricately related to standard Kubo linear response susceptibilities $\epsilon_{\alpha\beta}$ through the fluctuation-dissipation relation, which for the zero temperature, i.e. for the ground state reads (Jensen and Mackintosh, 1991) (see also Appendix B):

$$S_{\alpha\beta}(\omega) = \begin{cases} 2\epsilon''_{\alpha\beta}(\omega) & \omega > 0 \\ 0 & \omega < 0 \end{cases} \tag{126}$$

In particular this relation implies that

$$g_{\alpha\beta} = \int_0^{\infty} \frac{d\omega}{2\pi} \frac{\epsilon''_{\alpha\beta}(\omega) + \epsilon''_{\beta\alpha}(\omega)}{\omega^2}. \tag{127}$$

Thus the metric tensor can be directly measured from the symmetric part of $\epsilon''_{\alpha\beta}(\omega)$, which defines fluctuations (noise) and the energy absorption (Jensen and Mackintosh, 1991). As we will discuss in detail in Sec. IV.A the Berry curvature $F_{\beta\alpha}$ defines the Coriolis (or the Lorentz) force in the parameter space. So it can be measured directly through the linear response of the generalized force M_β to the ramp rate of the parameter λ_α. We note that a similar formula was derived independently in Ref. (Hauke et al., 2015).

B. Topology of the ground state manifold

The geometric properties derived above give a local description of the wave functions living on the parameter manifold. From these local geometric properties, one can derive robust global properties of the manifold, i.e., its topology. In this section, we will discuss two types of topology that can be defined on the geometric tensor: the Chern number, which describes how the wave function wraps a closed parameter manifold via integrating the Berry curvature, and the Euler characteristic describing the topological shape of the Riemannian manifold encoded in the metric tensor.

As the Chern number has been extensively discussed in literature in many different contexts we will mention it rather briefly and will concentrate more on the Euler characteristic, which has been discussed much less with respect to physical systems. We will also focus exclusively on two-dimensional manifolds, since the geometry and topology of higher-dimensional manifolds is much more complex and is often understood through various two-dimensional cuts. Please note that this section closely follows Ref. 29, and we refer interested readers there for more details.

1. Basic definitions of the Euler characteristic and the first Chern number.

The Euler characteristic of a (possibly open) manifold $\mathcal{M}$ is an integer equal to the integrated Gaussian curvature over the manifold with an additional boundary term:

$$\xi(\mathcal{M}) = \frac{1}{2\pi}\left[\int_{\mathcal{M}} K dS + \oint_{\partial\mathcal{M}} k_g dl\right], \tag{128}$$

A standard notation for the Euler characteristic is χ, but because we used this symbol for the geometric tensor, we will use ξ instead. The two terms on the left side of Eq. (128) are the bulk and boundary contributions to the Euler characteristic of the manifold. We refer to the first term,

$$\xi_{\text{bulk}}(\mathcal{M}) = \frac{1}{2\pi}\int_{\mathcal{M}} K dS \ , \tag{129}$$

and the second term,

$$\xi_{\text{boundary}}(\mathcal{M}) = \frac{1}{2\pi}\oint_{\partial\mathcal{M}} k_g dl \ , \tag{130}$$

as the bulk and boundary Euler integrals, respectively. These terms, along with their constituents – the Gaussian curvature (K), the geodesic curvature (k_g), the area element (dS), and the line element (dl) – are geometric invariants, meaning that they remain unmodified under any change of variables. More explicitly, if the metric is written in first fundamental form as

$$ds^2 = Ed\lambda_1^2 + 2Fd\lambda_1 d\lambda_2 + Gd\lambda_2^2 \ , \tag{131}$$

then these invariants are given by

$$\begin{aligned} K &= \frac{1}{\sqrt{g}}\left[\frac{\partial}{\partial\lambda_2}\left(\frac{\sqrt{g}\,\Gamma_{11}^2}{E}\right) - \frac{\partial}{\partial\lambda_1}\left(\frac{\sqrt{g}\,\Gamma_{12}^2}{E}\right)\right] \\ k_g &= \sqrt{g}G^{-3/2}\Gamma_{22}^1 \\ dS &= \sqrt{g}d\lambda_1 d\lambda_2 \\ dl &= \sqrt{G}d\lambda_2\ , \end{aligned} \tag{132}$$

where k_g and dl are given for a curve of constant λ_1. The metric determinant g and Christoffel symbols Γ_{ij}^k are

$$g = EG - F^2 \tag{133}$$

$$\Gamma_{ij}^k = \frac{1}{2}g^{km}\left(\partial_j g_{im} + \partial_i g_{jm} - \partial_m g_{ij}\right)\ , \tag{134}$$

where g^{ij} is the inverse of the metric tensor g_{ij}. As we see, the explicit expressions for the Euler characteristic are quite cumbersome but they are known and unique functions of the metric tensor. A simple intuitive understanding of the Gaussian curvature of a two-parameter manifold comes from embedding the manifold in three dimensions. Then

$$K = \frac{1}{R_1 R_2},$$

where R_1 and R_2 are the principal radii of curvature, i.e., the minimal and the maximal radii of the circles touching the surface (see Fig. 7). The geodesic curvature is the curvature of the boundary projected to the tangent plane, and is zero for a geodesic as the projection of the latter is locally a straight line. Thus, for example, the geodesic curvature of a great circle on a sphere is zero. For manifolds without boundaries like a torus or a sphere, the Euler characteristic simply counts the number of holes in the manifold. Thus for a sphere the Euler characteristic is $\xi = 2$ for a torus $\xi = 0$ and each additional hole gives an extra contribution of -2.

Another important topological invariant is the (first) Chern number, which is defined through the Berry curvature. To understand where it comes from, let us consider a closed manifold as shown in Fig. 8 and choose an arbitrary closed contour on that sphere like the dashed line. Let us compute the Berry phase (flux) along this contour by two ways:

$$\varphi_B^{\text{top}} = \int_{S_{\text{top}}} F_{\alpha\beta}\, d\lambda_\alpha \wedge d\lambda_\beta, \quad \varphi_B^{\text{bottom}} = -\int_{S_{\text{bottom}}} F_{\alpha\beta}\, d\lambda_\alpha \wedge d\lambda_\beta, \tag{135}$$

where the minus sign in the second term appears because the top and bottom surfaces of the sphere bounded by the curve have opposite orientations with respect to this curve. Recall that φ_B

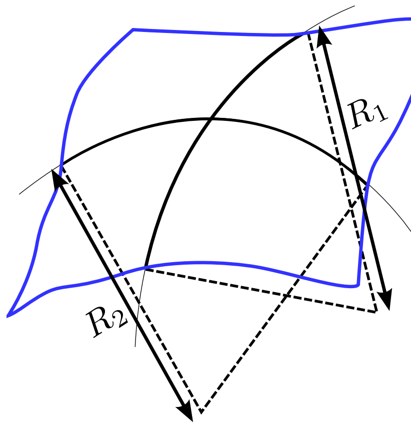

FIG. 7 Illustration of the principle radii R_1 and R_2 of a two dimensional manifold embedded in three dimensions.

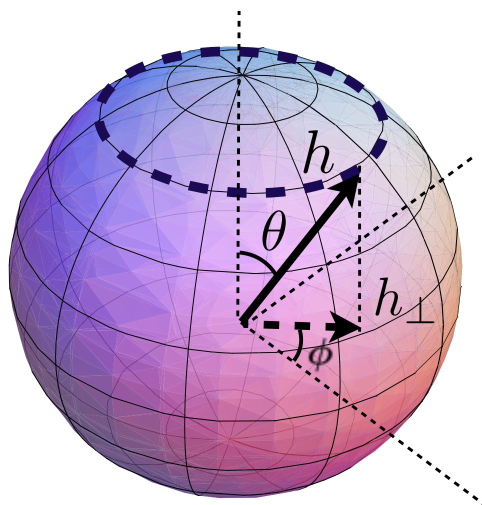

FIG. 8 Schematic representation of the spin in an external magnetic field, where the angles of the magnetic field θ and ϕ are the parameters.

represents the physical phase acquired by the wave function during the (adiabatic) motion in the parameter space. Since the wave function is unique the two phases should be identical up to an overall constant $2\pi n$. Thus we find that

$$2\pi n = \varphi_B^{\text{top}} - \varphi_B^{\text{bottom}} = \oint_S F_{\alpha\beta}\, d\lambda_\alpha \wedge d\lambda_\beta \tag{136}$$

The integer n is precisely the Chern number C_1 so we get

$$C_1 = \frac{1}{2\pi} \oint_S F_{\alpha\beta}\, d\lambda_\alpha \wedge d\lambda_\beta\ . \tag{137}$$

Some intuition for the meaning of the Chern number can be obtained by returning to our electromagnetic analogy. We've seen that the Chern number is proportional to the Berry flux through a closed manifold S in parameter space, which by Gauss's law for magnetism suggests that $C_1 \propto q_m$, the effective magnetic charge enclosed by the manifold. Indeed, it is known that if magnetic monopoles exist, they must be quantized (Dirac, 1931), which directly gives quantization of the Chern number. Berry showed that isolated degeneracies could act as sources of Berry curvature, and it is precisely the flux from these degeneracies that give rise to this topological invariant.

2. Topology of a spin in a magnetic field

As our first example of these types of topology, let's pick up on the spin-1/2 in a magnetic field from the previous section. As before, the two-dimensional parameter space corresponds to the angles (θ, ϕ) of the magnetic field with fixed magnitude, whose geometric tensor is given in Eq. (117). The diagonal real components of the geometric tensor $\chi_{\theta\theta} = g_{\theta\theta} = 1/4$ and $\chi_{\phi\phi} = g_{\phi\phi} = 1/4\sin^2(\theta)$ define a Riemannian metric which coincides with that of the sphere of the radius $1/2$ and constant Gaussian curvature $K = 4$. The imaginary off-diagonal component of χ gives the Berry curvature: $F_{\phi\theta} = 1/2\sin(\theta)$. Thus we see that the Euler invariant and Chern number are:

$$\xi = \frac{1}{2\pi}\int K dS = \frac{1}{2\pi}4\int \sqrt{g}\, d\theta d\phi = 2 \tag{138}$$

$$C_1 = \frac{1}{2\pi}\int F_{\phi\theta}\, d\phi \wedge d\theta = 1. \tag{139}$$

The Euler characteristic implies that the metric topology of the spin-1/2 ground state in a rotating field is that of a sphere and the Chern number of one tells us that the wave function (i.e., the Bloch vector) "wraps" once if we adiabatically change the magnetic field over a full spherical angle. We can think of this Chern number as sourced by the degeneracy at magnetic field equal to zero, which our magnetic field sphere clearly encloses.

The example above can be generalized to an arbitrary spin S in a magnetic field. The result is very simple: the spin-1/2 metric tensor is simply multiplied by $2S$:

$$\chi_{\theta\theta} = \frac{S}{2}, \quad \chi_{\phi\phi} = \frac{S}{2}\sin^2(\theta), \quad \chi_{\theta\phi} = \frac{iS}{2}\sin(\theta). \tag{140}$$

The metric of the ground state manifold now coincides with that of the sphere of radius $\sqrt{S/2}$. The Euler characteristic, however, does not depend on the radius and thus we see that $\xi = 2$ for any spin. Conversely, the Chern number is proportional to S: $C_1 = 2S$.

Exercise III.4. Prove Eq. (140). It may be useful to remember that S_i is the generator of rotations about the $i = x, y, z$ axis.

Exercise III.5. The Chern number naturally appears in a band theory, where it is used to define various topological invariants and leads to numerous interesting physical effects such as topologically-quantized charge pumps (Thouless, 1994), the quantum Hall effect (Thouless et al., 1982) and quantized spin-Hall effect in topological insulators (Moore and Balents, 2007; Qi and Zhang, 2010). The Chern number for a (non-degenerate) band α is defined in a standard way: $C_1 = \int_{BZ} dk_x dk_y F^{\alpha}_{k_x,k_y}$, where $F^{\alpha}_{k_x k_y} = \partial_{k_x} A^{\alpha}_{k_y} - \partial_{k_y} A^{\alpha}_{k_x}$ is the band Berry curvature and $A^{\alpha}_{k_j} = i\langle u_\alpha(\mathbf{k})|\partial_{k_j} u_\alpha(\mathbf{k})\rangle$ is the band Berry connection. Here $|u_\alpha(\mathbf{k})\rangle$ are the Bloch wave functions corresponding to the band α.

The simplest band model with a nontrivial topological structure is two-dimensional with two atoms/orbitals per unit cell and complex hopping amplitudes such that the Hamiltonian reads

$$\mathcal{H} = \sum_{k_x,k_y} \left(a^\dagger_{\mathbf{k}}, b^\dagger_{\mathbf{k}}\right) \begin{pmatrix} h^z_{\mathbf{k}} & h^x_{\mathbf{k}} - i h^y_{\mathbf{k}} \\ h^x_{\mathbf{k}} - i h^y_{\mathbf{k}} & -h^z_{\mathbf{k}} \end{pmatrix} \begin{pmatrix} a_{\mathbf{k}} \\ b_{\mathbf{k}} \end{pmatrix} + M \sum_{k_x,k_y} \left(a^\dagger_{\mathbf{k}}, b^\dagger_{\mathbf{k}}\right) \begin{pmatrix} 1 & 0 \\ 0 & -1 \end{pmatrix} \begin{pmatrix} a_{\mathbf{k}} \\ b_{\mathbf{k}} \end{pmatrix} \tag{141}$$

where $a^\dagger_{\mathbf{k}}, b^\dagger_{\mathbf{k}}, a_{\mathbf{k}}, b_{\mathbf{k}}$ are the momentum space fermion creation and annihilation operators corresponding to the two sublattices, $h^i_{\mathbf{k}}$, $i = x, y, z$ are smooth functions of $\mathbf{k}$ satisfying periodicity conditions $h^i_{\mathbf{k}+\mathbf{G}} = h^i_{\mathbf{k}}$, where $\mathbf{G}$ is the reciprocal lattice vector, and M is the symmetry breaking field between two sublattices. For example for a Haldane model on a square lattice with a π-flux per plaquette and equal nearest neighbor and next nearest neighbor hopping t we have (Neupert et al., 2011):

$$\begin{aligned} h^z_{\mathbf{k}} &= 2t(\cos k_x - \cos k_y), \\ h^x_{\mathbf{k}} &= t\left(\cos(\pi/4) + \cos(k_y - k_x - \pi/4) + \cos(k_y + \pi/4) + \cos(k_x - \pi/4)\right), \\ h^y_{\mathbf{k}} &= t\left(-\sin(\pi/4) + \sin(k_y - k_x - \pi/4) + \sin(k_y + \pi/4) - \sin(k_x - \pi/4)\right). \end{aligned}$$

- Show that this problem can be mapped to the spin one half in an effective $\mathbf{k}$-dependent magnetic field of magnitude

  $$h_{\mathbf{k}} = \sqrt{(2t(\cos k_x - \cos k_y) + M)^2 + 4t^2(1 + \cos k_x \cos k_y)}$$

  and angles $\theta_{\mathbf{k}}$ and $\phi_{\mathbf{k}}$ defined according to

  $$\tan(\theta_{\mathbf{k}}) = \frac{\sqrt{(h^x_{\mathbf{k}})^2 + (h^y_{\mathbf{k}})^2}}{h^z_{\mathbf{k}} + M} = \frac{2t\sqrt{1 + \cos k_x \cos k_y}}{2t(\cos k_x - \cos k_y) + M}, \ \tan\phi_{\mathbf{k}} = \frac{h^y_{\mathbf{k}}}{h^x_{\mathbf{k}}}.$$

- Identify the momenta corresponding to the north and south poles of the sphere. Argue that for $M = 0$, region A labeled in Fig. 9 maps to the top of the sphere and region B maps to the bottom of the sphere. By arguing that the Chern number is invariant under parameterization from this mapping conclude that the Chern number of the lower band (corresponding to the ground state manifold) with respect to k_x and k_y is equal to one and the Chern number of the higher band (corresponding to the excited state manifold) is equal to negative one.

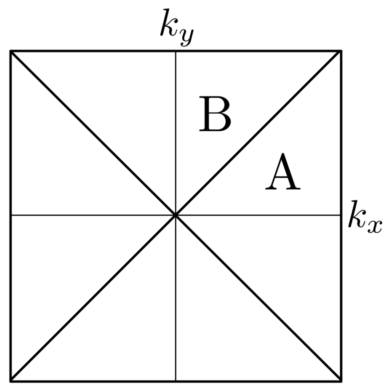

FIG. 9 First Brillouin zone illustrating the regions A and B that map to the two hemispheres.

- Argue that both Chern numbers do not change with M as long as $M < 4t$ and that for $M > 4t$ the band Chern numbers become zero.

We will not explore the Chern number further in this section, though we will return to it in the context of dynamical response in Sec. IV.A. More recently, a few works have explored the ground state metric topology of assorted systems. We will now detail one such system, namely the metric of the quantum XY chain, closely following Ref. 29.

3. Metric geometry and topology of the quantum XY chain

Let us now analyze the geometric invariants for a particular model - the quantum XY chain. This model is sufficiently simple so that all calculations can be done analytically, yet it has a very rich phase diagram with two different phase transitions and multicritical points.

The quantum XY chain is described by the Hamiltonian

$$\mathcal{H} = -\sum_j \left[J_x \sigma_j^x \sigma_{j+1}^x + J_y \sigma_j^y \sigma_{j+1}^y + h\sigma_j^z\right] , \tag{142}$$

where $J_{x,y}$ are exchange couplings, h is a transverse field, the spins are represented as Pauli matrices $\sigma^{x,y,z}$ and the index $j = 1 \ldots L$ runs over the length of the spin chain assuming periodic boundary conditions. It is convenient to re-parameterize the model in terms of new couplings J and γ as

$$J_x = J\left(\frac{1+\gamma}{2}\right), \ J_y = J\left(\frac{1-\gamma}{2}\right) , \tag{143}$$

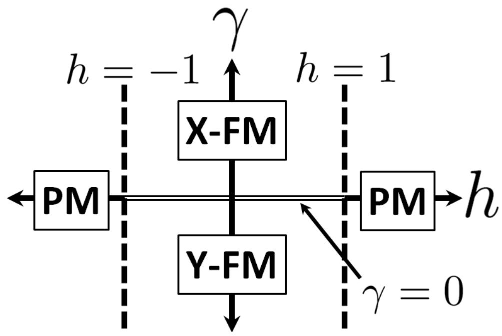

FIG. 10 Ground state phase diagram of the XY Hamiltonian (Eq. (142)) for $\phi = 0$. The rotation parameter ϕ modifies the Ising ferromagnetic directions, otherwise maintaining all features of the phase diagram. As a function of transverse field h and anisotropy γ, the ground state undergoes continuous Ising-like phase transitions between paramagnet and ferromagnet at $h = \pm 1$ and anisotropic transitions between ferromagnets aligned along X and Y directions (X/Y-FM) at $\gamma = 0$.

where J is the energy scale of the exchange interaction and γ is its anisotropy. We add an additional tuning parameter ϕ, corresponding to simultaneous rotation of all the spins about the z-axis by angle $\phi/2$. While rotating the angle ϕ has no effect on the spectrum of $\mathcal{H}$, it does modify the eigenstate wave functions. To fix the overall energy scale, we set $J = 1$.

Since the Hamiltonian is invariant under the mapping $\gamma \to -\gamma$, $\phi \to \phi + \pi$, we generally restrict ourselves to $\gamma \geq 0$. The phase diagram for this model is shown in Fig. 10 (see Ref. (Damle and Sachdev, 1996) for details). There is a phase transition between paramagnet and Ising ferromagnet at $|h| = 1$ and $\gamma \neq 0$. There is an additional critical line at the isotropic point ($\gamma = 0$) for $|h| < 1$. The two transitions meet at multi-critical points when $\gamma = 0$ and $|h| = 1$. Another notable line is $\gamma = 1$, which corresponds to the transverse-field Ising (TFI) chain. Finally let us note that there are two other special lines $\gamma = 0$ and $|h| > 1$ where the ground state is fully polarized along the magnetic field and thus h-independent. These lines are characterized by vanishing susceptibilities including vanishing metric along the h-direction. One can show that such state is fully protected by the rotational symmetry of the model and can be terminated only at the critical (gapless) point (Kolodrubetz et al., 2013). The phase diagram is invariant under changes of the rotation angle ϕ.

We now follow a standard set of tricks to solve such a Hamiltonian (Sachdev, 1999). Rewriting the spin Hamiltonian in terms of free fermions via a Jordan-Wigner transformation, $\mathcal{H}$ can be mapped to an effective non-interacting spin one-half model with

$$\mathcal{H} = \sum_k \mathcal{H}_k; \quad \mathcal{H}_k = -\begin{pmatrix} h - \cos(k) & \gamma \sin(k) \mathrm{e}^{-i\phi} \\ \gamma \sin(k) \mathrm{e}^{i\phi} & -[h - \cos(k)] \end{pmatrix}.$$

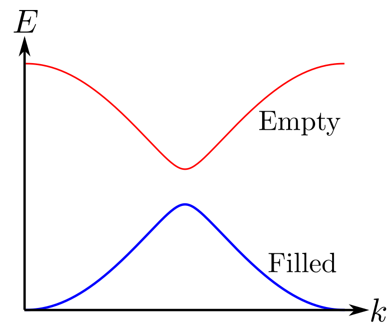

FIG. 11 Illustration of the effective band structure of the XY chain that results after a Jordan-Wigner transformation. In the ground state, the lower band is filled and the upper band is empty. Each mode k can be excited by kicking the fermion into the upper band (see Eq. (144)).

The details of this transformation can be found elsewhere[12]; for our purposes, it is important to note that it has allowed us to reduce the interacting spin model in Eq. (142) to a non-interacting fermionic two-band model which is at half-filling (see Fig. 11). Then calculating the geometric tensor corresponds to asking how the mode wave functions $|g_k\rangle$ and $|e_k\rangle$ – the ground and excited bands respectively – change with parameters.

The ground state of $\mathcal{H}_k$ is a Bloch vector with azimuthal angle ϕ and polar angle

$$\theta_k = \tan^{-1}\left[\frac{\gamma\sin(k)}{h-\cos(k)}\right] . \tag{144}$$

Because the Hamiltonian effectively describes an independent set of two-level systems we can immediately extend the results from the previous section to find the expression for different metric tensor components. In particular, differentiating the ground state in each momentum sector with respect to h we find

$$\partial_h|g_k\rangle = \frac{\partial_h\theta_k}{2}\begin{pmatrix} -\sin\left(\frac{\theta_k}{2}\right) \\ \cos\left(\frac{\theta_k}{2}\right)e^{i\phi}\end{pmatrix} = -\frac{\partial_h\theta_k}{2}|e_k\rangle. \tag{145}$$

The same derivation applies to the anisotropy γ, since changing either γ or h only modifies θ_k and not ϕ. Thus we find

$$\mathcal{A}_\lambda = -\frac{1}{2}\sum_k (\partial_\lambda\theta_k)\tau_k^y, \tag{146}$$

where $\lambda = \{h,\gamma\}$ and $\tau_k^{x,y,z}$ are Pauli matrices that act in the instantaneous ground/excited state basis (the basis in which $H_k = -\sqrt{(h-\cos k)^2+\gamma^2\sin^2 k}\ \tau_k^z$). Similarly, for the parameter ϕ, we

[12] We note that the sign convention for ϕ, i.e., which direction the spins are rotated around the z axis, differs from Ref. (Kolodrubetz et al., 2013). This, and other differences in gauge choice, are done to match the conventions of earlier spin-1/2 examples in this review. The choices have no effect on the final measurable quantities such as the metric tensor.

find that

$$\mathcal{A}_\phi = \frac{1}{2}\sum_k \left[\cos(\theta_k)\tau_k^z + \sin(\theta_k)\tau_k^x - 1\right]. \tag{147}$$

Using that

$$g_{\mu\nu} = \frac{1}{2}\langle g|(\mathcal{A}_\mu\mathcal{A}_\nu + \mathcal{A}_\nu\mathcal{A}_\mu)|g\rangle_c \tag{148}$$

we find

$$g_{hh} = \frac{1}{4}\sum_k \left(\frac{\partial\theta_k}{\partial h}\right)^2,\ g_{\gamma\gamma} = \frac{1}{4}\sum_k \left(\frac{\partial\theta_k}{\partial \gamma}\right)^2,\ g_{h\gamma} = \frac{1}{4}\sum_k \frac{\partial\theta_k}{\partial h}\frac{\partial\theta_k}{\partial \gamma},\ g_{\phi\phi} = \frac{1}{4}\sum_k \sin^2(\theta_k), \tag{149}$$

The remaining two components of the metric tensor, $g_{h\phi}$ and $g_{\gamma\phi}$, are equal to zero.

The expressions for the metric tensor can be analytically evaluated in the thermodynamic limit, where the summation becomes integration over momentum space. It is convenient to divide all components of the metric tensor by the system size and deal with intensive quantities $g_{\mu\nu} \to g_{\mu\nu}/L$. Then one calculates these integrals to find that

$$\begin{aligned}
g_{\phi\phi} &= \frac{1}{8}\begin{cases} \frac{|\gamma|}{|\gamma|+1}, & |h|<1 \\ \frac{\gamma^2}{1-\gamma^2}\left(\frac{|h|}{\sqrt{h^2-1+\gamma^2}}-1\right), & |h|>1 \end{cases} \\
g_{hh} &= \frac{1}{16}\begin{cases} \frac{1}{|\gamma|(1-h^2)}, & |h|<1 \\ \frac{|h|\gamma^2}{(h^2-1)(h^2-1+\gamma^2)^{3/2}}, & |h|>1 \end{cases} \\
g_{\gamma\gamma} &= \frac{1}{16}\begin{cases} \frac{1}{|\gamma|(1+|\gamma|)^2}, & |h|<1 \\ \left(\begin{array}{c} \frac{2}{(1-\gamma^2)^2}\left[\frac{|h|}{\sqrt{h^2-1+\gamma^2}}-1\right]- \\ \frac{|h|\gamma^2}{(1-\gamma^2)(h^2-1+\gamma^2)^{3/2}} \end{array}\right), & |h|>1 \end{cases} \\
g_{h\gamma} &= \frac{1}{16}\begin{cases} 0, & |h|<1 \\ \frac{-|h|\gamma}{h(h^2-1+\gamma^2)^{3/2}}, & |h|>1 \end{cases}
\end{aligned} \tag{150}$$

Using the metric tensor we can visualize the ground state manifold by building an equivalent (i.e., isometric) surface and plotting its shape. It is convenient to focus on a two-dimensional manifold by fixing one of the parameters. We then represent the two-dimensional manifold as an equivalent three-dimensional surface. To start, let's fix the anisotropy parameter γ and consider the $h-\phi$ manifold. Since the metric tensor has cylindrical symmetry, so does the equivalent surface. Parameterizing our shape in cylindrical coordinates and requiring that

$$dz^2 + dr^2 + r^2 d\phi^2 = g_{hh}dh^2 + g_{\phi\phi}d\phi^2\ , \tag{151}$$

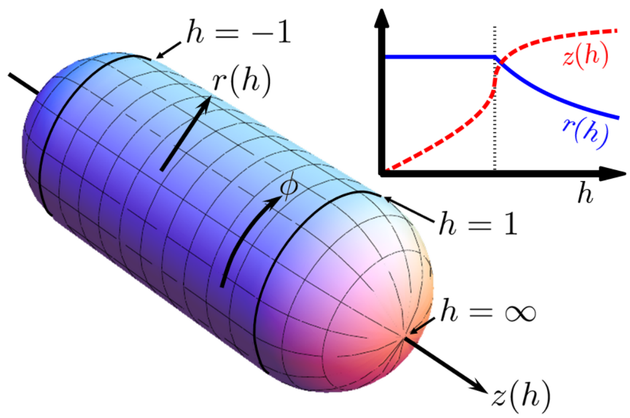

FIG. 12 Equivalent graphical representation of the phase diagram of the transverse field Ising model ($\gamma = 1$) in the $h - \phi$ plane. The ordered ferromagnetic phase maps to a cylinder of constant radius. The disordered paramagnetic phases $h > 1$ and $h < -1$ map to the two hemispherical caps. The inset shows how the cylindrical coordinates z and r depend on the transverse field h.

we see that

$$r(h) = \sqrt{g_{\phi\phi}},\ z(h) = \int_0^h dh_1 \sqrt{g_{hh}(h_1) - \left(\frac{dr(h_1)}{dh_1}\right)^2}. \tag{152}$$

Using Eq. (150), we explicitly find the shape representing the XY chain. In the Ising limit ($\gamma = 1$), we get

$$r(h) = \frac{1}{4}\ ,\ z(h) = \frac{\arcsin(h)}{4} \text{ for } |h| < 1\ ; r(h) = \frac{1}{4|h|}\ ,\ z(h) = \frac{\pi}{8}\frac{|h|}{h} + \frac{\sqrt{h^2-1}}{4h} \text{ for } |h| > 1\ .$$

The phase diagram is thus represented by a cylinder of radius 1/4 corresponding to the ferromagnetic phase capped by the two hemispheres representing the paramagnetic phase, as shown in Fig. 12. It is easy to check that the shape of each phase does not depend on the anisotropy parameter γ, which simply changes the aspect ratio and radius of the cylinder. Because of the relation $r(h) = \sqrt{g_{\phi\phi}}$ this radius vanishes as the anisotropy parameter γ goes to zero. By an elementary integration of the Gaussian curvature, the phases have bulk Euler integral 0 for the ferromagnetic cylinder and 1 for each paramagnetic hemisphere. These numbers add up to 2 as required, since the full phase diagram is topologically equivalent to a sphere. From Fig. 12, it is also clear that the phase boundaries at $h = \pm 1$ are geodesics, meaning that the geodesic curvature (and thus the boundary contribution ξ_{boundary}) is zero for a contour along the phase boundary. One can show that this boundary integral protects the value of the bulk integral and vice versa.

In the Ising limit ($\gamma = 1$), the shape shown in Fig. 12, can also be easily seen from directly computing the curvature K using Eq. (132). Within the ferromagnetic phase, the curvature is zero – no surprise, given that the metric is flat by inspection. The only shape with zero curvature and

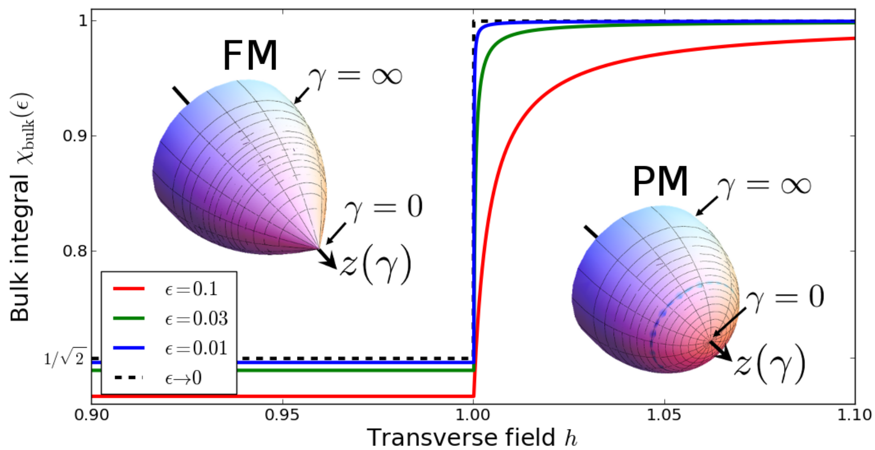

FIG. 13 (insets) Equivalent graphical representation of the phase diagram of the XY model in the $\gamma-\phi$ plane, where $\gamma \in [0, \infty)$ and $\phi \in [0, 2\pi]$. The right inset shows the paramagnetic disordered phase and the left inset represents the ferromagnetic phase. It is clear that in the latter case there is a conical singularity developing at $\gamma = 0$ which represents the anisotropic phase transition. The plots show bulk Euler integral $\xi_{\mathrm{bulk}}(\epsilon)$ as defined in Eq. (153), demonstrating the jump in ξ_{bulk} at the phase transition between the paramagnet and ferromagnet in the limit $\epsilon \to 0^+$.

cylindrical symmetry is a cylinder. Similarly, within the paramagnet, the curvature is a constant $K = 16$, like that of a sphere. Therefore, to get cylindrical symmetry, the phase diagram is clearly seen to be a cylinder capped by two hemispheres.

We can also reconstruct an equivalent shape in the $\gamma - \phi$ plane. In this case we expect to see a qualitative difference for $|h| > 1$ and $|h| < 1$ because in the latter case there is an anisotropic phase transition at the isotropic point $\gamma = 0$, while in the former case there is none. These two shapes are shown in Fig. 13. The anisotropic phase transition is manifest in the conical singularity that develops at $\gamma = 0$.[13]

The singularity at $\gamma = 0$ yields a non-trivial bulk Euler integral for the anisotropic phase transition. To see this, consider the bulk integral

$$\xi_{\mathrm{bulk}}(\epsilon) = \lim_{L\to\infty} \int_0^{2\pi} d\phi \int_\epsilon^\infty d\gamma \, \sqrt{g(\gamma, \phi)} K(\gamma, \phi) \; . \tag{153}$$

In the limit $\epsilon \to 0^+$, this integral has a discontinuity as a function of h at the phase transition, as seen in Fig. 13. Thus, $\xi_{\mathrm{bulk}} \equiv \xi_{\mathrm{bulk}}(\epsilon = 0^+)$ can be used as a geometric characteristic of the anisotropic phase transition. Direct calculation shows that $\xi_{\mathrm{bulk}} = 1/\sqrt{2}$ in the ferromagnetic

[13] We note a potential point of confusion, namely that a naive application of Eq. (132) would seem to indicate that the curvature is a constant $K = 4$ in the ferromagnetic phase for $\gamma > 0$, in which case the singularity at $\gamma = 0$ is not apparent. However, a more careful derivation shows that the curvature is indeed singular at $\gamma = 0$: $K = 4 - 8(1-\gamma)\frac{\partial^2}{\partial^2\gamma}|\gamma| = 4 - 16\delta(\gamma)$, where $\delta(\gamma)$ is the Dirac delta function.

phase and $\xi_{\rm bulk} = 1$ in the paramagnetic phase. This non-integer geometric invariant is due to the existence of a conical singularity.

A careful analysis shows that in both cases the bulk Euler characteristics are protected by the universality of the transition, i.e., if one adds extra terms to the Hamiltonian which do not qualitatively affect the phase diagram, then the bulk Euler characteristic does not change. The details of the proof are available in Ref. 29, but the basic idea is very simple. The sum of the bulk and the boundary Euler characteristics is protected by the geometry of the parameter manifold. As long as the boundary of the manifold coincides with the phase boundary, all components of the metric tensor become universal (Campos Venuti and Zanardi, 2007). Therefore it is not surprising that the geodesic curvature also becomes universal and thus the boundary Euler characteristic is protected. As a result the bulk Euler characteristic is protected too. It is interesting that, unlike critical exponents, the bulk Euler characteristic truly characterizes the phase transition and does not depend on the parameterization. One can also analyze the Euler characteristic and the Gaussian curvature in the $h-\gamma$ plane (Kolodrubetz et al., 2013; Zanardi et al., 2007b). One finds additional non-integrable curvature singularities near the anisotropic phase transition and near the multi-critical point. This curvature singularity implies that the Euler characteristic of different phases becomes ill defined and can no longer be used for their characterization.

C. Extension to steady state density matrices

Having explored (global) topological properties of the ground state manifold, it is natural to ask how these ideas can be generalized to classical and/or finite temperature systems. To make the classical limit explicit we will reintroduce the Planck's constant $\hbar$ to all expressions. Previously we derived the geometric tensor for the ground state manifold, but clearly the arguments flow through trivially for arbitrary excited states $|\psi_m\rangle \equiv |m\rangle$:

$$\chi^m_{\alpha\beta} = \frac{\langle m|\mathcal{A}_\alpha \mathcal{A}_\beta|m\rangle - \langle m|\mathcal{A}_\alpha|m\rangle\langle m|\mathcal{A}_\beta|m\rangle}{\hbar^2} = \sum_{n\neq m} \frac{\langle m|\partial_\alpha \mathcal{H}|n\rangle\langle n|\partial_\beta \mathcal{H}|m\rangle}{(E_n - E_m)^2} \ . \tag{154}$$

While this may be relevant to microscopic or mesoscopic systems, it is generally very difficult to prepare excited energy eigenstates. We are therefore interested in exciting systems into some steady state density matrix. To ensure that it is stationary, we consider a density matrix of the form $\rho = \sum_n \rho_n |n\rangle\langle n|$. Then as before, we can define the geometric tensor as the covariance matrix of the gauge potentials: $\chi_{\alpha\beta} = \langle \mathcal{A}_\alpha \mathcal{A}_\beta\rangle_c/\hbar^2$.

There remains a slightly subtle question that we must answer: what is the meaning of $\langle \cdots \rangle_c$ for a density matrix? Two natural solutions present themselves. The first option, $\langle AB\rangle_c = \langle AB\rangle - \langle A\rangle\langle B\rangle = \mathrm{Tr}\,[\rho AB] - \mathrm{Tr}\,[\rho A]\,\mathrm{Tr}\,[\rho B]$ which we call the coherent connection, is the type of connected correlation function that appears in the theory of phase transitions, where it will often be singular near the transition. The second option,

$$\langle AB\rangle_c = \sum_n \rho_n \langle n|AB|n\rangle_c = \sum_n \rho_n \left(\langle n|AB|n\rangle - \langle n|A|n\rangle\langle n|B|n\rangle\right) \tag{155}$$

at first seems much less natural, as it does not take the form of a simple operator expectation value. However, it will turn out that this second "incoherent" definition is the one which appears in the dynamical response in isolated systems and can be related to noise and dissipation (cf. Appendix B). It is worth noting that the difference between the two ways of defining the connected correlation function is in their handling of the diagonal elements of the density matrix. Therefore, the anti-symmetric Berry curvature, which only depends on the off-diagonal part, does not care which definition we use. For the symmetric part of the correlation function, however, there is a difference between the two options.[14] Let us also point that the geometric tensor defined in this way does not correspond to a natural Bures distance between density matrices (see e.g. Eq. (3) in Ref. (Zanardi et al., 2007a)) so the relation of χ defined in this way with quantum information geometry becomes less clear. Nevertheless we will stick to this definition as it will naturally emerges in dynamical response and leave discussion of the relationship between these two natural metrics for future work.

The natural extension of the geometric tensor to mixed stationary states is thus

$$\chi_{\alpha\beta}(\rho) = \sum_n \rho_n \chi^n_{\alpha\beta}\ . \tag{156}$$

As this is simply a sum over all eigenstates, it is trivial to write it as a response function by plugging in the expression for $\chi^n_{\alpha\beta}$ from Eqs. (124) and (125) (with $|0\rangle \to |n\rangle$). For a finite temperature density matrix, it is similarly straightforward to see that this is connected to the dissipative part of linear response, which is shown in more detail in Appendix B.

In exercise III.3, we derived the metric tensor of the harmonic oscillator with respect to shifts in the position or momentum coordinate. In the exercises below, we will see how this generalizes to finite temperature states. Let us analyze explicitly the metric of the harmonic oscillator with

[14] We note that if A and B are local operators describing some physical observables and $|n\rangle$ are eigenstates of an ergodic many-body Hamiltonian then the difference between the two definitions is small, vanishing in the thermodynamic limit. However, since we are not making any assumptions about taking the thermodynamic limit and generally are working with non-ergodic systems, we must be careful with choosing the right definition.

Hamiltonian $\mathcal{H} = p^2/2m + kx^2/2$ with respect to changing a slightly less trivial parameter: the spring constant k. If the mass is held fixed, then the generalized force with respect to changes of k is $\partial_k \mathcal{H} = x^2/2$. Then the metric tensor for an arbitrary harmonic oscillator state $|n\rangle$ is

$$\begin{aligned} g^n_{kk} &= \sum_{m\neq n} \frac{\left|\langle m|\,(x^2/2)\,|n\rangle\right|^2}{(E_n - E_m)^2} = \frac{\ell^4}{4} \sum_{m\neq n} \frac{\left|\langle m|\,(a+a^\dagger)^2\,|n\rangle\right|^2}{(E_n - E_m)^2} \\ &= \frac{\ell^4}{16\hbar^2\Omega^2} \left(\left|\langle n-2|\, a^2\,|n\rangle\right|^2 + \left|\langle n+2|\,(a^\dagger)^2\,|n\rangle\right|^2 \right) = \frac{\ell^4}{8\hbar^2\Omega^2}\left(n^2+n+1\right) \ , \end{aligned} \tag{157}$$

where $\Omega = \sqrt{k/m}$ is the oscillator frequency and $\ell = \sqrt{\hbar/2m\Omega}$ are the natural frequency and length scales of the oscillator. Then for an arbitrary stationary state, the metric tensor is clearly

$$g^\rho_{kk} = \frac{\ell^4}{8\hbar^2\hbar^2\Omega^2}\left(\langle n^2\rangle + \langle n\rangle + 1\right) = \frac{1}{32\hbar^2 m^2\Omega^4}\left(\langle n^2\rangle + \langle n\rangle + 1\right).$$

For the Gibbs ensemble, $\rho_n = e^{-\hbar\beta\Omega(n+1/2)}/Z$, one finds that $\langle n\rangle = 1/(e^{\hbar\beta\Omega} - 1)$ and $\langle n^2\rangle = (e^{\hbar\beta\Omega} + 1)/(e^{\hbar\beta\Omega} - 1)^2$. In the high temperature or classical limit, $\beta\hbar\Omega \ll 1$, this reduces to

$$\hbar^2 g^{T\gg\hbar\Omega}_{kk} \to \frac{\hbar^2}{32m^2\Omega^4}\frac{2}{\hbar^2\beta^2\Omega^2} = \frac{(k_B T)^2}{16m^2\Omega^6}. \ , \tag{158}$$

We see that in the classical (high-temperature) limit it is the product $\hbar^2 g_{kk} = \langle \mathcal{A}_k^2\rangle_c$ which is well defined.

We can also arrive to the result above by calculating the variance of the gauge potential. Note that the eigenstates of the Harmonic oscillator are

$$\psi_n(x) = \frac{1}{\sqrt{\ell}}\phi_n(x/\ell),$$

where ϕ_n is the dimensionless eigenfunction of the oscillator expressed through the Hermite polynomials (Landau and Lifshitz, 1981). Differentiating this wave-function with respect to k we find:

$$\partial_k\psi_n(x) = -\frac{1}{2\ell}\frac{d\ell}{dk}\psi_n(x) - \frac{x}{\ell}\frac{d\ell}{dk}\partial_x\psi_n(x) = -\frac{d\ell}{dk}\frac{1+2x\partial_x}{2\ell}\psi_n(x). \tag{159}$$

Therefore

$$\mathcal{A}_k = i\hbar\partial_k = \frac{d\ell}{dk}\frac{x\hat{p}+\hat{p}x}{2\ell} = -\frac{1}{4}\frac{\ell}{k}\mathcal{D}, \tag{160}$$

where

$$\mathcal{D} = \frac{x\hat{p}+\hat{p}x}{2\ell} \tag{161}$$

is nothing but the quantum dilation operator (c.f. Exercise II.2). This is not surprising as rescaling of the spring constant amounts to dilations. In the second quantized notation

$$\frac{x\hat{p}+\hat{p}x}{2} = \frac{i}{2}\left[(a^\dagger + a)(a^\dagger - a) + (a^\dagger - a)(a^\dagger + a)\right] = i(a^\dagger a^\dagger - aa)$$

Using this expression and substituting it into the definition of the metric tensor:

$$\hbar^2 g_{kk} = \langle \mathcal{A}_k^2 \rangle_c$$

we can reproduce the expression for the metric tensor (157). In particular, in the classical limit, using the equipartition theorem we recover Eq. (158):

$$\langle \mathcal{A}_k^2 \rangle_c = \frac{1}{16k^2} \langle x^2 p^2 \rangle_c = \frac{1}{16k^2} \frac{4m}{k} \left\langle \frac{kx^2}{2} \right\rangle \left\langle \frac{p^2}{2m} \right\rangle = \frac{m(k_b T)^2}{16k^3} = \frac{(k_b T)^2}{16 m \Omega^6}$$

Exercise III.6. Verify that the variance of the gauge potential $\mathcal{A}_k$ in Eq. (160) reproduces the metric tensor (158).

Exercise III.7. Repeat Exercise (III.3) for the thermal state at temperature T. Check that at the zero temperature you reproduce the ground state geometric tensor. Find the asymptotic expression for the geometric tensor in the classical limit $T \gg \hbar\omega$.

D. Geometric tensor in the classical limit

Having defined the thermal geometric tensor for a quantum system, we expect to be able to define a classical (i.e., $\hbar \to 0$) limit of the metric tensor that matches Eq. (158). In the classical problem we have the stationary state $\rho(p,q) \propto e^{-\beta \mathcal{H}(p,q)}$. Unfortunately, the definition of "matrix elements" of the operator $\partial_k \mathcal{H}$ is less clear, so we must resort to the dynamical definition of the geometric tensor given in Eqs. (64), (124) , (125), and (156). The sum over eigenstates, $\sum_n \rho_n$, is replaced by and integral over phase space:

$$S^{cl}_{\alpha\beta}(\omega) = \int_{-\infty}^{\infty} dt\, \mathrm{e}^{i\omega t} \int dp dq\, \rho(p,q) \left[\partial_\alpha \mathcal{H}(p(t), q(t)) \partial_\beta \mathcal{H}(p,q) - M_\alpha(p,q) M_\beta(p,q)\right], \tag{162}$$

where $p \equiv p(0)$, $q = q(0)$, $M_\alpha(p,q)$ is the generalized force or the infinite time average of $-\partial_\alpha \mathcal{H}(p(t), q(t))$ starting from the initial conditions $q(0), p(0)$. This generalized force is nothing but the Born-Oppenheimer force emerging in the adiabatic approximation (see Sec. V). When doing this integral, one should think of integrating over p and q as integrating over initial conditions weighted by the probability $\rho(p,q)$. For instance, the "Heisenberg" operator $\partial_k \mathcal{H}(p(t), q(t)) = q(t)^2/2$ should be thought of as half the value of q^2 at time t after starting at $t = 0$ from the state (p,q). Let us analyze the example from the previous section and find g_{kk} for the harmonic oscillator in the thermal equilibrium. Time dependence of $q(t)$ for the oscillator is

$$q(t) = q(0)\cos(\Omega t) + \frac{p(0)}{m\Omega}\sin(\Omega t) \equiv q\cos(\Omega t) + \frac{p}{m\Omega}\sin(\Omega t)\ , \tag{163}$$

Therefore the generalized force

$$M_k(p,q) = -\frac{\overline{q^2(t)}}{2} = -\frac{q^2}{4} - \frac{p^2}{4m^2\Omega^2} = -\frac{1}{2m\Omega^2}\mathcal{H}(p,q) = -\frac{\mathcal{H}(p,q)}{2k}, \tag{164}$$

where the overline stands for time averaging. As expected the generalized force $M_k(p,q)$ only depends on the conserved quantity, which is the Hamiltonian. Then the integrand appearing in the spectral function is given by

$$\begin{aligned}\partial_k\mathcal{H}(p(t),q(t))\partial_k\mathcal{H}(p,q) - M_k(q,p)^2 &= \frac{1}{4}q^2\left[q\cos(\Omega t) + \frac{p}{m\Omega}\sin(\Omega t)\right]^2 - \frac{1}{16}\left(q^2 + \frac{p^2}{m^2\Omega^2}\right)^2 \\ &= \frac{1}{16}\left(q^4 - \frac{p^4}{m^4\Omega^4}\right) + \frac{q^2}{8}\left[\left(q^2 - \frac{p^2}{m^2\Omega^2}\right)\cos(2\Omega t) + \frac{qp}{m\Omega}\sin(2\Omega t)\right].\end{aligned} \tag{165}$$

To calculate $S^{cl}_{\alpha\beta}(\omega)$ now according to Eq. (162) we have to average the expression above over the probability distribution and take the time integral. Under the averaging over the equilibrium density matrix the first, time-independent term vanishes because $\langle q^4\rangle = \langle p^4/(m^4\Omega^4)\rangle$. Similarly the last term averages to zero: $\langle q^3 p\rangle = 0$. So the only non-zero contribution to the spectral function comes from the second term proportional to $\cos(2\Omega t)$. Because the integrals are all Gaussian, we may apply Wick's theorem to get

$$\langle q^4\rangle = 3\langle q^2\rangle^2 = \frac{12}{k^2}\left\langle \frac{kq^2}{2}^2\right\rangle = \frac{12}{k^2}\frac{(k_BT)^2}{4} = \frac{3}{k^2}(k_BT)^2, \quad \langle q^2p^2/m^2\Omega^2\rangle = \langle q^2\rangle^2 = (k_BT)^2.$$

Therefore

$$S^{cl}_{kk}(\omega) = \frac{(k_BT)^2}{4k^2}\int_{-\infty}^{\infty} dt\, e^{i\omega t}\cos(2\Omega t) = \frac{(k_BT)^2}{4k^2}\pi\left(\delta(\omega+2\Omega) + \delta(\omega-2\Omega)\right). \tag{166}$$

Then, via the dynamical definition of the geometric tensor (Eq. (124)),

$$\hbar^2 g_{kk} = \int_0^\infty \frac{d\omega}{2\pi}\frac{S_{kk}(\omega) + S_{kk}(-\omega)}{\omega^2} = \frac{(k_BT)^2}{16k^2\Omega^2} = \frac{(k_BT)^2}{16m^2\Omega^6}, \tag{167}$$

which indeed coincides with the classical limit of the quantum geometric tensor (158).

Let us now show how the same result can be reproduced using the language of the adiabatic gauge potentials. According to Eq. (65) the adiabatic gauge potential should satisfy

$$-\partial_k\mathcal{H}(q,p) = M_k(q,p) - \frac{\partial\mathcal{A}^{cl}_k}{\partial q}\frac{\partial\mathcal{H}}{\partial p} + \frac{\partial\mathcal{A}^{cl}_k}{\partial p}\frac{\partial\mathcal{H}}{\partial q}, \tag{168}$$

Using Eq. (164) the equation above reduces to

$$\frac{p^2}{4mk} - \frac{q^2}{4} = -\frac{\partial\mathcal{A}^{cl}_k}{\partial q}\frac{p}{m} + \frac{\partial\mathcal{A}^{cl}_k}{\partial p}kq \tag{169}$$

It is easy to check that the desired adiabatic gauge potential is

$$\mathcal{A}_k^{cl} = -\frac{qp}{4k}, \tag{170}$$

which coincides with the earlier result Eq. (160) in the classical limit and as we already showed reproduces the correct metric tensor.

For simple cases like this, the gauge potentials can be found explicitly and can be much easier to work with than correlation functions of the generalized forces. For more complicated situations such as the Duffing oscillator, one can imagine doing a similar construction numerically or iteratively and/or utilizing the correlation function of the generalized forces. In classical chaotic systems the gauge potentials and hence the geometric tensor will not necessarily converge (Jarzynski, 1995). The issue comes from a divergent low-frequency tail in the spectrum of generic observables due to the presence of diffusive modes. Physically these divergences are always cut off by either coupling to the bath or finite duration of the physical process. But introducing a consistent cutoff is beyond the level of the present discussion and will be a subject of future research.

IV. GEOMETRIC TENSOR AND NON-ADIABATIC RESPONSE.

Key concept: The geometric tensor appears naturally through response coefficients of the system to the rate of change of parameters $\dot{\lambda}_a$. The Berry curvature shows up as a Coriolis-type force while the metric tensor defines broadening of the energy distribution (energy variance). In the classical (high temperature) limit, the metric tensor also defines the leading non-adiabatic correction to the energy through renormalization of the mass.

A. Dynamical Quantum Hall effect

We already noted in the first section that the gauge potentials appear in the Galilean term in the moving Hamiltonian:

$$\tilde{\mathcal{H}}_m = U^\dagger \mathcal{H} U - \dot{\lambda}_\alpha \tilde{\mathcal{A}}_\alpha = \tilde{\mathcal{H}} - \dot{\lambda}_\alpha \tilde{\mathcal{A}}_\alpha. \tag{171}$$

Then we introduced the geometric tensor χ, which we found could be written as the covariance of the gauge potentials. In this section, we connect the dots between these observations by relating the geometric tensor to the dynamical response of physical observables.

We start by noting that the bare Hamiltonian in the moving frame $\tilde{\mathcal{H}}$ is diagonal and thus only produces shifts in the energies but does not couple them, so it is not responsible for the transitions between levels. Conversely the Galilean term generally has off-diagonal elements and thus causes transitions between levels. Near the adiabatic limit the Galilean term is small and thus can be treated as a perturbation. Because the gauge potentials are simultaneously responsible for the non-adiabatic response of the systems and for the geometry we just discussed in the previous section it is thus not very surprising that the response coefficients can be related to the geometric tensor. The goal of this section is precisely to establish such connection.

Let us now consider the setup where the system is initially prepared at equilibrium (for concreteness in the ground state) at some initial value of the coupling $\boldsymbol{\lambda}_0 \equiv \boldsymbol{\lambda}(t=0)$. Then the coupling starts changing in time. To avoid the need of worrying about initial transients, which can be done but makes the derivations more involved, we will assume that the rate of change of the coupling is a smooth function of time. Under this smooth transformation, at leading order in $|\dot{\lambda}|$ the system follows the ground state of the moving Hamiltonian $\mathcal{H}_m$. One can worry whether the adiabatic theorem applies to this Hamiltonian, which is still time-dependent; later we will give a more rigorous derivation of the result using the machinery of adiabatic perturbation theory (see Refs. (Gritsev and Polkovnikov, 2012; Rigolin et al., 2008) for more details). For now let us simply note, as we already did in the very first section, that the adiabatic approximation applied to the moving Hamiltonian encodes the leading non-adiabatic corrections beyond the standard adiabatic approximation, where the system follows the eigenstates of the instantaneous Hamiltonian $\tilde{H}$. Already at this level of approximation we can derive very important results such as emergence of the Coriolis force and the mass renormalization.

Applying first order perturbation theory to the moving frame Hamiltonian $\mathcal{H}_m$, the amplitude to transition to the excited state $|n\rangle$ of the bare Hamiltonian $\tilde{\mathcal{H}}$ due the Galilean term is given by

$$a_n = \dot{\lambda}_\alpha \frac{\langle n|\mathcal{A}_\alpha|0\rangle}{E_n - E_0} \tag{172}$$

One can alternatively understand this result as coming from the instantaneous measurement process viewed as a sudden quench, where the rate $\dot{\lambda}$ is quenched to zero. It is convenient to represent observables as generalized force operators conjugate to some other coupling λ_β:

$$\mathcal{M}_\beta = -\partial_\beta \mathcal{H}. \tag{173}$$

The matrix elements of these objects already appeared in the definition of the geometric tensor so it is convenient to continue dealing with them. Generalized forces defined as expectation values of the generalized force operators, appear quite naturally in many problems. For example, the magnetization is a generalized force conjugate to the magnetic field, current is a generalized force conjugate to the vector potential, nearest neighbor correlation function can be viewed as a generalized force conjugate to the nearest neighbor hopping or interaction, etc. Indeed any observable $\mathcal{O}$ can be represented as some generalized force operator by adding a source term $-\lambda\mathcal{O}$ to the Hamiltonian. Taking the expectation value of $\mathcal{M}_\beta$ and using Eq. (62) for the matrix elements of the gauge potential, we find that

$$\begin{aligned} M_\beta \equiv \langle\psi|\mathcal{M}_\beta|\psi\rangle &= M_\beta^{(0)} - \sum_{n\neq 0}(a_n^*\langle n|\partial_\beta\mathcal{H}|0\rangle + a_n\langle 0|\partial_\beta\mathcal{H}|n\rangle) \\ &\approx M_\beta^{(0)} + i\hbar\dot{\lambda}_\alpha\sum_{n\neq 0}\frac{\langle 0|\partial_\beta\mathcal{H}|n\rangle\langle n|\partial_\alpha\mathcal{H}|0\rangle - \langle 0|\partial_\alpha\mathcal{H}|n\rangle\langle n|\partial_\beta\mathcal{H}|0\rangle}{(E_n-E_0)^2} \\ &= M_\beta^{(0)} + \hbar F_{\beta\alpha}\dot{\lambda}_\alpha, \end{aligned} \tag{174}$$

where $M_\beta^{(0)}$ is the generalized force evaluated in the instantaneous ground state (i.e., in the adiabatic limit). This relation shows that the leading non-adiabatic (Kubo) correction to the generalized force comes from the product of the Berry curvature and the rate of change of the parameter $\boldsymbol{\lambda}$. Using our previous intuition that Berry curvature behaves as a magnetic field in parameter space, we see that this Kubo correction is the Lorentz (or the Coriolis) force in parameter space (Berry, 1989). Because the integral of the Berry curvature over a closed parameter manifold is a quantized first Chern number, this effective Lorentz force leads to a quantized response, which one can term the dynamical quantum Hall effect (Gritsev and Polkovnikov, 2012).

Let us first illustrate that this relation reproduces the standard integer quantum Hall effect (QHE). We will make only two generic assumptions: (i) the ground state of the system is not-degenerate (although degeneracies can lead interesting phenomena like the fractional QHE) and (ii) the Hamiltonian of the system can be represented in the form

$$\mathcal{H} = \sum_{j=1}^{N}\frac{\left(\mathbf{p}_j - e\mathbf{\Lambda}_j\right)^2}{2m_j} + V(\mathbf{r}_1,\mathbf{r}_2,\ldots\mathbf{r}_N), \tag{175}$$

where V is an arbitrary momentum independent potential energy which can include both interactions between particles and an external potential. As before, we use the $\mathbf{\Lambda}_j \equiv \mathbf{\Lambda}(\mathbf{r}_j)$ notation for the vector potential to avoid confusion with the gauge potential. Let us assume that the vector potential consists of some static part (not necessarily uniform) representing a static magnetic field and an extra dynamic part representing the electric field in the system, where throughout this section we work in the Coulomb gauge, $\boldsymbol{\mathcal{E}} = \partial_t\mathbf{\Lambda}$. We will choose the components of the time-dependent vector potential as our parameters, i.e.

$$\lambda_x = \Lambda_x,\ \lambda_y = \Lambda_y. \tag{176}$$

The generalized force with respect to λ_y is

$$\mathcal{M}_y = -\partial_{\lambda_y}\mathcal{H} = \sum_j \frac{e}{m_j}\left(p_j^{(y)} - e\Lambda_j^{(y)}\right) = \mathcal{J}_y, \tag{177}$$

which is the current operator along the y-direction. In the absence of the electric field there is no average current, $\langle 0|\mathcal{J}_y|0\rangle = 0$ so the dynamical Hall relation reads

$$J_y = \hbar F_{\lambda_y\lambda_x}\dot{\lambda}_x = \hbar F_{\lambda_y\lambda_x}\mathcal{E}_x, \tag{178}$$

To find the Hall conductivity we note that the total current J is related to the two-dimensional current density j via

$$J_y = L_x L_y j_y, \tag{179}$$

where L_x and L_y are the dimensions of the sample. Therefore the Hall conductivity $\sigma_{xy} = j_y/\mathcal{E}_x$ is related to the Berry curvature via

$$\sigma_{xy} = \frac{\hbar F_{\lambda_x\lambda_y}}{L_x L_y}. \tag{180}$$

If we now focus on bulk response by considering a system with periodic boundary conditions (eliminating the edges), the parameter λ_x can be gauged away once it reaches $\lambda_x^0 = 2\pi\hbar/eL_x$, and similarly for λ_y. This corresponds to threading a flux quantum through the torus (Laughlin, 1981). Since the ground state returns to itself upon insertion of a flux quantum along either direction, this defines a closed manifold in λ space on which we can define a Chern number. Furthermore, as $\lambda_{x,y}^0$ are very small and generally immeasurable in the thermodynamic limit, we can average over them to get the averaged conductance

$$\sigma_{xy} \approx \frac{\hbar\overline{F_{\lambda_x\lambda_y}}}{L_x L_y} = \frac{\hbar}{L_x L_y}\frac{\int_0^{\lambda_x^0} d\lambda_x \int_0^{\lambda_y^0} d\lambda_y F_{\lambda_x\lambda_y}}{\lambda_x^0\lambda_y^0} \tag{181}$$

$$= \frac{\hbar}{L_x L_y}\frac{2\pi C_1}{(2\pi\hbar/eL_x)(2\pi\hbar/eL_y)} \tag{182}$$

$$= C_1\frac{e^2}{h}\ . \tag{183}$$

Thus the quantization of the conductance in the quantum Hall effect can be thought of as the topological response to insertion of flux quanta along the two directions in the system.

Exercise IV.1. Show that for a system of free fermions in the thermodynamic limit with a gap between filled and unfilled bands, the many-body Berry curvature (and its Chern number) with respect to gauge potentials reduce to the sum of band Chern numbers defined in Exercise III.5:

$$F_{\lambda_x \lambda_y} = \frac{1}{\lambda_x^0 \lambda_y^0} \sum_\alpha \int_{FBZ} F^\alpha_{k_x k_y} dk_x dk_y \ , \tag{184}$$

where the integral is over the first Brillouin zone and the sum is over filled bands α.

The second example we discuss is our old friend, the spin-1/2 in a time-dependent magnetic field. Because this is a purely quantum system we will again set $\hbar = 1$. Suppose that the spin is prepared in the ground state along a magnetic field whose angle then starts to change with time along, e.g., the θ-direction. The generalized force along the orthogonal ϕ-direction is just the ϕ-component of the magnetization. In the adiabatic limit it is clearly zero since in this case the magnetization simply follows the magnetic field. The leading non-adiabatic correction is then given by the Berry curvature:

$$M_\phi = \langle \mathcal{M}_\phi \rangle \approx F_{\phi\theta} \dot{\theta} \ , \tag{185}$$

where $F_{\phi\theta} = \sin\theta/2$ (see Sec. I). Similarly, if we again ramp the magnetic field in the $x - z$ plane ($\phi = 0$), but now with a time dependent x-component and a time independent z-component, we have

$$M_y = F_{yx} \dot{h}_x. \tag{186}$$

Then by a standard transformation from spherical to Cartesian coordinates, we find

$$F_{yx} = \frac{F_{\phi\theta}}{h^2 \tan\theta} = \frac{\cos\theta}{2h^2} \ . \tag{187}$$

In Fig. 14 we show numerically computed dependence of the transverse y-magnetization on the rate of change of the magnetic field v for a particular protocol

$$\mathcal{H} = -\sigma_z - h_x(t)\sigma_x, \tag{188}$$

where $h_x(t) = 0.5 + vt$. The transverse magnetization is computed at time $t = 0$ and the initial condition corresponds to the ground state at large negative time $t = -100/v$. As is evident from the figure, at slow rates the dependence of the transverse magnetization on the rate is linear and the slope is exactly given by the Berry curvature.

Integrating the measured Berry curvature over the angles of the field, one can measure the Chern number, which we found to be $C_1 = 1$ for this example in Sec. III.B.2. Interesting, even within such a simple system, one can already observe a topological transition where the Chern

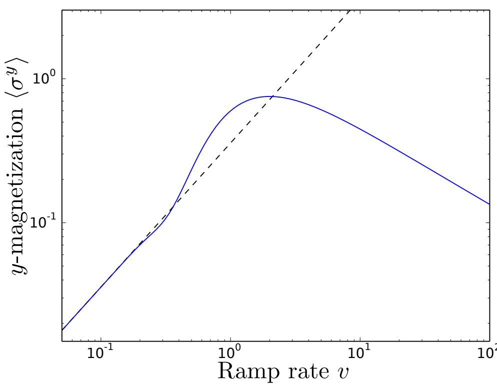

FIG. 14 Dependence of the transverse magnetization on the rate of change of the magnetic field along the x-direction (see text for details). The dashed line shows the expected low-velocity asymptote from the dynamical Hall effect, Eq. (186). Adopted from Ref. (Gritsev and Polkovnikov, 2012)

number changes from 1 to 0. For this we can consider a slight modification into the Hamiltonian by adding a constant static magnetic field along the z direction.

$$\mathcal{H} = -\frac{1}{2}\left[h_0\sigma_z + h_1\cos(\theta)\sigma^z + h_1\sin(\theta)\cos(\phi)\sigma^x + h_1\sin(\theta)\sin(\phi)\sigma^y\right]. \tag{189}$$

Then as one changes the magnetic field $\mathbf{h_1}$ along the sphere of constant radius at fixed h_0 we can have two different scenarios. First, $h_0 < h_1$ still corresponds to the total magnetic field encircling the origin $h = 0$ and thus produces a Chern number equal to one. The second scenario is realized when $h_0 > h_1$. Then the total magnetic field does not enclose the origin and the Chern number is zero. The easiest way to see this is to take the limit $h_1 \to 0$ and recall that the Chern number can not change unless the surface crosses a gapless crossing point. This phase transition was recently observed in experiments on superconducting qubits (Schroer et al., 2014). Recall that the Chern number tells the magnetic monopole charge enclosed by our surface in parameter space. For the spin-1/2 we saw that the only monopole resided at $\mathbf{h} = 0$ and carries charge 1. Therefore, one can interpret this topological transition as simply a shift of the surface in parameter space such that, for large h_0, it does not enclose the degeneracy at the origin. Interestingly this phase transition maps exactly to the phase transition in the Haldane model discussed in Exercise III.5 if one identifies angles of the magnetic field with the Bloch momenta. In this mapping the offset magnetic field h_0 plays the same role as the sublattice symmetry breaking parameter Min the band model.

We have used a simple single-particle problem to illustrate the topological response of spins to a magnetic field. The situation becomes much more interesting if we consider interacting systems. In particular, following Ref. 20 we quote the numerical results for the Chern number computed through the non-adiabatic response for a disordered spin chain:

$$\mathcal{H} = -\mathbf{h} \cdot \sum_{j=1}^{N} \zeta_j \boldsymbol{\sigma}_j - J \sum_{j=1}^{N-1} \eta_j \boldsymbol{\sigma}_j \cdot \boldsymbol{\sigma}_{j+1}, \tag{190}$$

where ζ_j and η_j are drawn from a uniform distribution in the interval $[0.75, 1.25]$. We fix the $|\mathbf{h}| = 1$ and look into the Berry curvature associated with angles of the magnetic field θ and ϕ as a function of J (see Fig. 15). Because of the $SU(2)$ invariance of the system, as for a single spin the Chern number and the Berry curvature are simply different by a factor of 2. At large negative

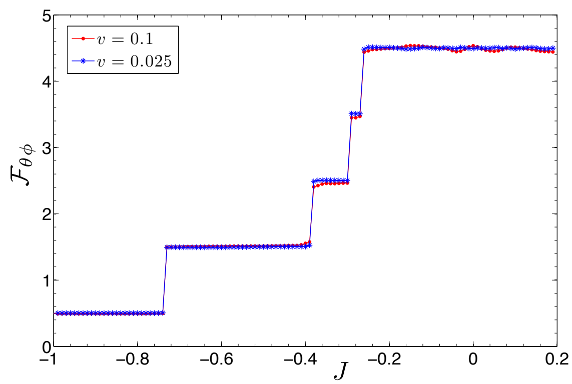

FIG. 15 Berry curvature at the equatorial plain $\theta = \pi/2$ for a disordered spin chain as a function of the coupling J for 9 spins. At large negative J the system minimizes the total spin to $S = 1/2$. The Berry curvature is also 1/2, corresponding to Chern number equal to one. At small J the system becomes polarized and the Chern number is 9.

J the system minimizes the total spin to $S = 1/2$ the Berry curvature is also $1/2$, corresponding to Chern number equal to one. At small J the system becomes polarized and the Chern number is L for a chain of length L. In between the Berry curvature and thus the Chern number changes in steps. If one breaks the $SU(2)$ invariance by considering, e.g., anisotropic interactions, the quantization of the Berry curvature disappears while the Chern number remains quantized. The minimal model for observing this is a two-spin system, which was recently realized experimentally also using superconducting qubits (Roushan et al., 2014).

Exercise IV.2. Using two superconducting qubits, in Ref. 41, the authors are able to create Hamiltonian of the form

$$\mathcal{H} = -B_r \hat{n}(\theta, \phi) \cdot \big(\boldsymbol{\sigma}_1 + \boldsymbol{\sigma}_2\big) + B_0 \sigma_1^z + g\big(\sigma_1^x \sigma_2^x + \sigma_1^x \sigma_2^x\big) \ , \tag{191}$$

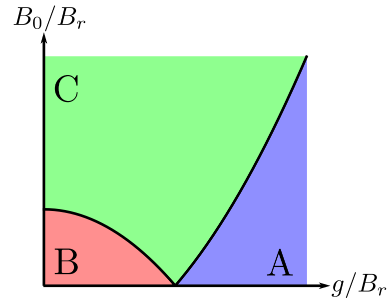

FIG. 16 Topological phase diagram of the two-qubit model in Eq. (191).

where $\hat{n}$ is a unit vector. For fixed magnitudes B_r, B_0, and g, they consider the Chern number with respect to the angles θ and ϕ as they encompass a sphere in parameter space. Here you will derive the theory behind some of the experimental results in the paper.

- Assume the system begins in its ground state at $\theta = 0$, after which the angle θ is ramped slowly with time at fixed $\phi = 0$. Use the dynamical quantum Hall effect to find an expression for the Berry curvature $F_{\theta\phi}$. Assuming the experimentalists are able to measure $\langle \boldsymbol{\sigma} \rangle$ for each qubit separately, what should they measure to find $F_{\theta\phi}$?

- The Chern number is given by $C_1 = (2\pi)^{-1} \int d\theta d\phi F_{\theta\phi}$. For the given Hamiltonian, why is it sufficient to measure at $\phi = 0$ instead of integrating over ϕ?

- The topological phase diagram of this model is depicted in Fig. 16. Let's begin by imagining that there are no interactions between the qubits ($g = 0$). Using the solution of the single qubit above, what are the values of the Chern number in regions A and B?

- Now turn off the "pinning field" $B_0 = 0$ and turn on very strong interaction, $g \gg B_r$. Argue that in this limit, deep in region C, the Chern number vanishes. Note that we have now found the Chern number in various limits of the phase diagram. Away from these limits, the math is much less trivial. Nevertheless, the Chern number remains perfectly quantized until a topological transition is reached, in which the gap above the ground state closes.

- Bonus: Find an analytical solution to the phase transition lines in Fig. 16. Hint: degeneracies are generally protected by a symmetry, so look along lines of high symmetry.

Exercise IV.3. Let's consider another unusual situation where topology emerges. A quintessential model of topology in condensed matter systems is the Harper-Hofstadter model, where a magnetic flux is placed through each plaquette of a square lattice to create a lattice realization of the quantum

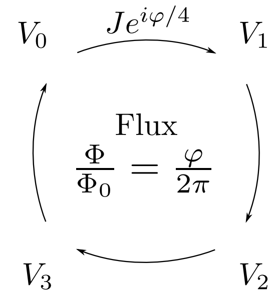

FIG. 17 Illustration of a single plaquette with flux, similar to what is realized in Ref. 1.

Hall effect. Here we will show that topology manifests at the level of a single plaquette in such a model (Fig. 17). Consider a single particle living on such a plaquette with flux $\Phi = \varphi\Phi_0/2\pi$ through it, such that the particle picks up phase $\varphi/4$ ($-\varphi/4$) each time it hops clockwise (counter-clockwise). Furthermore, put potentials V_j on the four sites, setting $V_0 = 0$ without loss of generality. We will see that there is a non-zero Chern number with respect to the effective three-dimensional manifold defined by $x = \varphi - \pi$, $y = V_1 - V_3$, and $z = V_2$.

- In order to get a non-zero Chern number, we must first identify singularities that can act as sources of Berry curvature. Begin with $V_j = 0$ for all j. Show that a degeneracy appears at $\varphi = \pi$. Then show that this degeneracy extends into a line of degeneracies for $V_1 = V_3$.

- Let's pick one point on this line of degeneracies by fixing $V_1 = -V_3$. Then show that setting any of the above perturbations x, y, or z to a small non-zero value breaks the degeneracy. Therefore, there exists an isolated degeneracy (a Berry monopole) at $x = y = z = 0$.

- Finally, consider a small sphere of radius r in this parameter space, i.e., let $x = r\sin\theta\cos\phi$, $y = r\sin\theta\sin\phi$, $z = r\cos\theta$. Argue that the first Chern number with respect to the angles θ and ϕ is non-zero for small but non-zero r. Show numerically that its value can be measured using the dynamical Hall effect.

B. Metric tensor as the dynamical response.

Originally Provost and Vallee thought that the metric tensor was a nice but unmeasurable mathematical object. On the other hand, it was very soon understood that the Berry curvature, i.e. its imaginary part, is responsible for many different physical phenomena such as the Aharonov-Bohm effect and the quantum Hall effect. In Sec. III.A we already discussed that the ground state metric tensor can be expressed through the measurable imaginary part of the Kubo susceptibility (see Eq. (127)). In Appendix B we extended this relation to finite temperature density matrices. Here let us show that the metric tensor like the Berry curvature has a direct physical meaning of the non-adiabatic response coefficient.

Let us again use the result of the adiabatic perturbation theory for transition amplitudes (172) and compute the energy variance due to the ramp rate:

$$\Delta E^2 = \langle \mathcal{H}^2 \rangle - \langle \mathcal{H} \rangle^2 = \sum_n |a_n|^2 E_n^2 - \left(\sum_n E_n |a_n|^2 \right)^2$$
$$= \sum_{\alpha\beta} \dot{\lambda}_\alpha \dot{\lambda}_\beta \left[\sum_{n \neq 0} (E_n - E_0)^2 \frac{\langle 0|\partial_\alpha \mathcal{H}|n\rangle \langle n|\partial_\beta \mathcal{H}|0\rangle}{(E_n - E_0)^4} \right] + O(|\dot{\boldsymbol{\lambda}}|^2) = \hbar^2 \sum_{\alpha\beta} \dot{\lambda}_\alpha g_{\alpha\beta} \dot{\lambda}_\beta + O(|\dot{\boldsymbol{\lambda}}|^2). \quad (192)$$

So the metric tensor defines the leading non-adiabatic correction to the energy variance, which, by energy conservation, is equal to the variance of work done on the system during the ramp δw^2. It is easy to see that this result is not tied to the ground state and applies to any other initial eigenstate. For mixed states with non-zero initial fluctuations metric tensor describes the increase in energy fluctuations due to the ramp, i.e.

$$\Delta E^2 = \Delta E_{\rm ad}^2 + \hbar^2 \sum_{\alpha\beta} \dot{\lambda}_\alpha g_{\alpha\beta} \dot{\lambda}_\beta + O(|\dot{\boldsymbol{\lambda}}|^2), \quad (193)$$

where $\Delta E_{\rm ad}$ is the width of the energy distribution for the adiabatic ramp with $|\dot{\boldsymbol{\lambda}}|^2 \to 0$.

In the high-temperature limit the average work and work fluctuations are not independent. The satisfy Einstein's relations, which are in turn derived from fluctuation theorems (see Refs. (Bunin et al., 2011; D'Alessio et al., 2015): $\delta w^2 \approx 2k_B T w$. Therefore in this classical or high-temperature case the metric tensor gives the leading non-adiabatic contribution to the energy:

$$E \approx E_{ad} + \frac{\hbar^2}{2k_B T} \sum_{\alpha\beta} \dot{\lambda}_\alpha g_{\alpha\beta} \dot{\lambda}_\beta + O(|\dot{\boldsymbol{\lambda}}|^2) \quad (194)$$

This non-adiabatic contribution to the energy is clearly proportional to the square of the velocity $\dot{\boldsymbol{\lambda}}$ and thus describes a correction to the kinetic energy associated with the parameter $\boldsymbol{\lambda}$. Therefore $\hbar^2 g_{\alpha\beta}/(k_B T)$ plays the role of the mass renormalization of this parameter. We will derive this result more carefully in the next section.

Exercise IV.4. Using the leading order adiabatic perturbation theory like we did in Eq. (192) prove Eq. (194) in the high-temperature limit assuming that the adiabatic (equilibrium) density matrix of the system is described by the Gibbs distribution: $\rho_n \approx 1/Z \exp[-E_n/(k_B T)]$. Hint: you can use the relation

$$\frac{\rho_n - \rho_m}{E_m - E_n} \approx \frac{1}{k_B T}\rho_n, \quad \text{if} \quad k_B T \gg |E_n - E_m|.$$

On passing we note that one can relate the metric tensor to the probability of doing zero work during an infinitesimal double quench (Kolodrubetz et al., 2013), which is connected to the well-known Loschmidt echo (Silva, 2008). These energy/work distributions are in principle measurable for a wide variety of systems, and in particular there has been a recent upswelling of progress in the field spurred by non-equilibrium fluctuation relations that also make reference to the work distribution (Jarzynski, 1997).

V. NON-ADIABATIC RESPONSE AND EMERGENT NEWTONIAN DYNAMICS.

Key concept: For slow macroscopic degrees of freedom $\boldsymbol{\lambda}$ coupled to fast degrees of freedom, Newtonian equations of motion emerge from leading non-adiabatic corrections to the Born-Oppenheimer approximation. In the classical or high-temperature limit, the emergent mass tensor is proportional to the metric tensor, while in the quantum low-temperature limit it is described by a related susceptibility expressed through the gauge potentials.

A. Adiabatic perturbation theory.

In the previous section, we argued that the leading non-adiabatic correction in $\dot{\boldsymbol{\lambda}}$ to the wave function of the system can be found from an assumption that the system follows the instantaneous ground state of the moving Hamiltonian $\tilde{\mathcal{H}}_m = \tilde{\mathcal{H}} - \dot{\lambda}_\alpha \tilde{\mathcal{A}}_\alpha$. From this we saw how leading non-adiabatic corrections to generalized forces and the energy broadening connect the geometric tensor to response coefficients. In this section, we extend the previous analysis to a more general class of systems, which are not necessarily in a ground state and which might have gapless excitations. This chapter closely follows Ref. 19. Our starting point will be the von Neumann equation for time evolution of the density matrix in the moving frame

$$i\frac{d\rho}{dt} = \left[\mathcal{H} - \dot{\lambda}_\alpha \mathcal{A}_\alpha, \rho\right],$$

where we remember that $\mathcal{H}$ is the diagonal Hamiltonian in the instantaneous basis. We again temporarily in this section set $\hbar = 1$ in all intermediate formulas to simplify notations. Also for simplicity we drop the tilde signs in this section over the Hamiltonian, gauge potentials and other observables. As expressions for all resulting expectation values are gauge invariant (independent of the choice of frame) so the tilde signs in the final expressions can be dropped anyway. As before, we will use standard perturbation theory (Kubo formalism), where the Galilean term plays the role of the perturbation, but now considering the full time dependent Hamiltonian. We will go to the interaction picture (i.e., the Heisenberg representation with respect to $\mathcal{H}$) via the time-dependent (diagonal) unitary $V(t) = e^{-i\int^t \mathcal{H}(t')dt'}$:

$$\rho = \mathrm{e}^{-i\int^t \mathcal{H}(t')dt'} \rho_H \mathrm{e}^{i\int^t \mathcal{H}(t')dt'} = V\rho_H V^\dagger,\ \mathcal{A}_\alpha = V A_{H,\alpha} V^\dagger\ . \tag{195}$$

Note that because the Hamiltonian $\mathcal{H}$ is diagonal by construction and thus commutes with itself at different times it remains unchanged in the interaction picture $\mathcal{H}_H = \mathcal{H}$ as in the conventional case where $\mathcal{H}$ is time-independent. For the same reason we do not need to worry about time-ordering in Eq. (195), which illustrates the difference between the "interaction" picture above and the Heisenberg representation: in the latter one has to use the full time-dependent Hamiltonian (not its instantaneous diagonal part) and thus the time-ordered integral.

In this interaction picture, the von Neumann equation becomes

$$i\,\frac{d\rho_H}{dt} = -\dot{\lambda}_\alpha\left[\mathcal{A}_{H,\alpha}(t), \rho_H(t)\right], \tag{196}$$

which is equivalent to the integral equation

$$\rho_H(t) = \rho_H(0) + i\int_0^t dt'\dot{\lambda}_\alpha(t')\left[\mathcal{A}_{H,\alpha}(t'), \rho_H(t')\right] \tag{197}$$

Next we are going to utilize the standard linear response Kubo formalism to perturbatively solve this integral equation (Mahan, 2000). As the Hamiltonian $\mathcal{H}$ is generally time-dependent its spectrum explicitly depends on $\boldsymbol{\lambda}(t)$. However, this dependence is trivial because it only amounts to using phase factors $\phi_n = \int_0^t E_n(t')dt'$ instead of $\phi_n = E_n t$. To simplify derivations we will assume a $\boldsymbol{\lambda}$-independent spectrum for the remainder of this section and only comment in the end how one should modify the final expressions if this is not the case (see Ref. (D′Alessio and Polkovnikov, 2014) for a more detailed derivation).

We assume that the system is initially prepared in a stationary state of the Hamiltonian $\mathcal{H}(\boldsymbol{\lambda}(0))$, after which one slowly turns on the ramping protocol. In the leading order in perturbation theory we can substitute the stationary density matrix into the R.H.S. of the integral equation (Eq. (197)):

$$\rho_H(t) = \rho_0 + i\int_0^t dt'\dot{\lambda}_\alpha(t')\left[\mathcal{A}_{H,\alpha}(t'), \rho_0\right] + O(\dot{\lambda}^2), \tag{198}$$

where we used that $\rho_{H,0} = \rho_0$ because ρ_0 is stationary and hence commutes with $\mathcal{H}$. From this we can find the linear response correction to the generalized forces:

$$\langle \mathcal{M}_\alpha(t) \rangle \approx M_\alpha^{(0)} + i \int_0^t dt' \, \dot{\lambda}_\beta(t') \langle [\mathcal{M}_{H,\alpha}(t), \mathcal{A}_{H,\beta}(t')] \rangle_0, \tag{199}$$

where $M_\alpha^{(0)} \equiv \langle \mathcal{M}_\alpha \rangle_0$ is the instantaneous generalized force. Evaluating the expectation value of the commutator in the co-moving basis and using Eq. (62) for the matrix elements of the gauge potential, we find

$$\begin{aligned}
\langle [\mathcal{M}_{H,\alpha}(t), \mathcal{A}_{H,\beta}(t')] \rangle_0 &= \sum_n \rho_n^0 \langle n | \mathcal{M}_{H,\alpha}(t) \mathcal{A}_{H,\beta}(t') | n \rangle - h.c. \\
&= \sum_{m \neq n} \rho_n^0 \langle n | e^{i\mathcal{H}t} \mathcal{M}_\alpha(t) e^{-i\mathcal{H}t} | m \rangle \langle m | e^{i\mathcal{H}t'} \mathcal{A}_\beta(t') e^{-i\mathcal{H}t'} | n \rangle - h.c. \\
&= \sum_{m \neq n} \rho_n^0 e^{i(E_n - E_m)(t-t')} \langle n | \mathcal{M}_\alpha(t) | m \rangle \left(\frac{\langle m | \mathcal{M}_\beta(t') | n \rangle}{i(E_n - E_m)} \right) - h.c. \\
&= i \sum_{m \neq n} \frac{\rho_n^0 - \rho_m^0}{E_m - E_n} e^{i(E_n - E_m)(t-t')} \langle n | \mathcal{M}_\alpha(t) | m \rangle \langle m | \mathcal{M}_\beta(t') | n \rangle \ , \qquad (200)
\end{aligned}$$

The time-dependence on the observables is reminder that we are working in the instantaneous frame, which changes in time together with $\boldsymbol{\lambda}$. Substituting this expression back into Eq. (199) and switching to integration variable $t'' = t - t'$, we find a general expression for the microscopic force:

$$\langle \mathcal{M}_\alpha(t) \rangle = M_\alpha^{(0)} - \int_0^t dt'' \dot{\lambda}_\beta(t-t'') \sum_{n \neq m} \frac{\rho_n^0 - \rho_m^0}{E_m - E_n} e^{i(E_m - E_n)t''} \langle m | \mathcal{M}_\alpha(t) | n \rangle \langle n | \mathcal{M}_\beta(t-t'') | m \rangle + O(\dot{\boldsymbol{\lambda}}^2) \, . \tag{201}$$

This expression will generally hold for arbitrary systems as long as $|\dot{\boldsymbol{\lambda}}|$ is sufficiently small that the $\dot{\boldsymbol{\lambda}}^2$ term can be neglected. We can simplify this expression further by using the time scale separation. Recall that by the assumption $\boldsymbol{\lambda}$ represents slow variables in the system. Mathematically this statement implies that the non-equal time correlation function of the generalized forces $\langle \mathcal{M}_{H,\alpha}(t'') \mathcal{M}_{H,\beta}(0) \rangle_{0,c}$ decays much faster than the characteristic time scale of changing $\boldsymbol{\lambda}(t)$. Because we are interested in long time dynamics of the system, we expect therefore that the system will forget its long-time history: $\langle \mathcal{M}_{H,\alpha}(t) \mathcal{M}_{H,\beta}(t - t'') \rangle_{0,c} \to 0$ as $t'' \gg \tau$, where τ is the characteristic relaxation time scale of fast degrees of freedom. Thus unless we are interested in short time transient dynamics $t \lesssim \tau$ we can extend the upper integration limit in Eq. (201) to ∞. It is then natural to expand $\dot{\lambda}_\mu(t - t'')$ into a Taylor series near $t'' = 0$: $\dot{\lambda}_\beta(t - t'') \approx \dot{\lambda}_\beta(t) - t'' \ddot{\lambda}_\beta(t) + \dots$. As we will see shortly, it is important to keep the first two terms in this expansion and all other terms, in most cases, describe unessential subleading corrections.[15] Similarly we can approximate $\mathcal{M}_\beta(t-t'') \approx \mathcal{M}_\beta(t)$ as the next order correction $\partial_\alpha \mathcal{M}_\beta(t)\dot{\lambda}_\alpha(t)$ will result in quadratic correction in $\dot{\boldsymbol{\lambda}}$ in Eq. (201). Then by grouping terms, we find

$$\langle \mathcal{M}_\alpha(t)\rangle = M_\alpha^{(0)} - \dot{\lambda}_\beta(\eta_{\alpha\beta} - F_{\alpha\beta}) - \ddot{\lambda}_\beta(\kappa_{\alpha\beta} + F'_{\alpha\beta}) + O(\dddot{\boldsymbol{\lambda}}, \dot{\boldsymbol{\lambda}}^2) \,, \tag{202}$$

where we split the coefficients in front of $\dot{\lambda}_\beta$ and $\ddot{\lambda}_\beta$ into symmetric ($\eta_{\alpha\beta}$ and $\kappa_{\alpha\beta}$) and anti-symmetric ($F_{\alpha\beta}$ and $F'_{\alpha\beta}$) components. For instance,

$$\begin{aligned} \eta_{\alpha\beta} &= \frac{1}{2}\int_0^\infty dt'' \sum_{n\neq m} \frac{\rho_n^0 - \rho_m^0}{E_m - E_n} e^{i(E_m - E_n)t''} \left[\langle m|\mathcal{M}_\alpha|n\rangle\langle n|\mathcal{M}_\beta|m\rangle + \alpha \leftrightarrow \beta\right], \\ F_{\alpha\beta} &= -\frac{1}{2}\int_0^\infty dt'' \sum_{n\neq m} \frac{\rho_n^0 - \rho_m^0}{E_m - E_n} e^{i(E_m - E_n)t''} \left[\langle m|\mathcal{M}_\alpha|n\rangle\langle n|\mathcal{M}_\beta|m\rangle - \alpha \leftrightarrow \beta\right], \end{aligned} \tag{203}$$

where all matrix elements (and in general energies) as well as the eigenstates correspond to the instantaneous parameter value $\boldsymbol{\lambda}(t)$.

It is now straightforward to evaluate the remaining integrals over t''. As usually one can regularize them by inserting small decaying exponential $\exp[-\delta t'']$ with infinitesimal positive δ. For instance, in Eq. (203), one uses

$$\int_0^\infty \exp[i(E_m - E_n)t'' - \delta t'']dt'' = \frac{1}{\delta - i(E_m - E_n)} \xrightarrow{\delta\to 0} iP\left(\frac{1}{E_m - E_n}\right) + \pi\delta(E_n - E_m), \tag{204}$$

where P stands for the principal value. Note that the first term is antisymmetric under the permutation of indexes n and m, while the second is symmetric. Because, as is evident from Eq. (202), the permutation of n and m is equivalent to the permutation of α and β, we see that the principal value determines the antisymmetric coefficient $F_{\alpha\beta}$ and the second, symmetric term determines $\eta_{\alpha\beta}$. Therefore

$$\begin{aligned} F_{\alpha\beta}(\lambda) &= -i\sum_{n\neq m} \frac{\rho_n^0 - \rho_m^0}{(E_m - E_n)^2}\langle m|\mathcal{M}_\alpha|n\rangle\langle n|\mathcal{M}_\beta|m\rangle \\ &= i\sum_{n\neq m} \rho_n^0 \frac{\langle n|\mathcal{M}_\alpha|m\rangle\langle m|\mathcal{M}_\beta|n\rangle - \langle n|\mathcal{M}_\beta|m\rangle\langle m|\mathcal{M}_\alpha|n\rangle}{(E_n - E_m)^2} \,, \end{aligned} \tag{205}$$

where all energies and matrix elements are evaluated at λ. If we compare this expression with Eq. (121) and use that $F_{\alpha\beta} = i(\chi_{\alpha\beta} - \chi_{\beta\alpha})$ (c.f. Eq. (103)), we will recognize $F_{\alpha\beta}$ is just the average of the Berry curvature over the adiabatic density matrix ρ^0.

[15] An important exception is a motion of a charged object in a vacuum, where the friction force is proportional to the third derivative of the coordinate. In this case one has to keep the next term to this expansion.

Similarly for a thermal density matrix ρ^0 the symmetric part of the response coefficient is given by

$$\eta_{\alpha\beta} = \frac{\pi}{k_B T} \sum_{n\neq m} \rho^0_m \langle m|\mathcal{M}_\alpha|n\rangle\langle n|\mathcal{M}_\beta|m\rangle \delta(E_n - E_m),$$

where we used that for a thermal ensemble with $\rho^0_n \propto e^{-E_n/k_B T}$,

$$\frac{\rho^0_n - \rho^0_m}{E_m - E_n} \to \frac{1}{k_B T}\rho^0_n \tag{206}$$

when $E_m \to E_n$. As we will see shortly, $\eta_{\alpha\beta}$ represents the friction force on the system. It is non-zero only if the system has gapless excitations. Therefore, at zero temperature or for a system with a discrete energy spectrum the friction coefficient is always zero unless the system is gapless or quantum critical, because one cannot satisfy the δ function constraint. Because throughout these notes we assume this is the case we set $\eta_{\alpha\beta} \to 0$.

In a similar spirit one can derive the other two coefficients. Let us use that

$$\begin{aligned} -\int_0^\infty t' \exp[i(E_m - E_n)t' - \delta t']dt' &= \partial_\delta \int_0^\infty \exp[i(E_m - E_n)t' - \delta t']dt' \\ &= -\frac{1}{(\delta - i(E_n - E_m))^2} \xrightarrow{\delta\to 0} \frac{1}{(E_n - E_m)^2} - i\pi\delta'(E_n - E_m), \end{aligned} \tag{207}$$

Plugging this result into Eq. (201) we see that now the off-shell term is symmetric, while the on-shell term is antisymmetric. The first (off-shell) term defines the coefficient $\kappa_{\alpha\beta}$, which as we will see shortly determines the mass renormalization

$$\kappa_{\alpha\beta} = \sum_{n\neq m} \frac{\rho^0_n - \rho^0_m}{(E_m - E_n)^3} \langle m|\mathcal{M}_\alpha|n\rangle\langle n|\mathcal{M}_\beta|m\rangle = \sum_{n\neq m} \frac{\rho^0_n - \rho^0_m}{E_m - E_n} \langle m|\mathcal{A}_\alpha|n\rangle\langle n|\mathcal{A}_\beta|m\rangle \tag{208}$$

At low temperatures $k_B T \to 0$ and hence $\rho^0_n \to \delta_{n0}$ this expression reduces to

$$\kappa_{\alpha\beta} \approx \hbar \sum_{m\neq 0} \frac{\langle 0|\mathcal{M}_\alpha|m\rangle\langle m|\mathcal{M}_\beta|0\rangle + \nu \leftrightarrow \mu}{(E_m - E_0)^3}, \tag{209}$$

while at high temperatures (or near the classical limit) we find

$$\kappa_{\alpha\beta} \approx \frac{1}{2k_B T} \sum_n \rho^0_n \left(\langle n|\mathcal{A}_\alpha \mathcal{A}_\beta|n\rangle_c + \alpha \leftrightarrow \beta\right) = \frac{\hbar^2}{k_B T}\, g_{\alpha\beta} \tag{210}$$

where $g_{\alpha\beta}$ is the Fubini-Study metric tensor for the finite temperature ensemble. We reintroduced the factor of $\hbar$ into the expression for the mass tensor to highlight that it has a well defined classical limit. It is straightforward to see that at any temperature the mass tensor $\kappa_{\alpha\beta}$ can be written as the integral of the connected imaginary time correlation function of the gauge potentials $\mathcal{A}_\alpha$ and $\mathcal{A}_\beta$:

$$\kappa_{\alpha\beta} = \frac{1}{2\hbar}\int_0^{\hbar/k_B T} d\tau \langle \mathcal{A}_{H,\alpha}(-i\tau)\mathcal{A}_{H,\beta}(0) + \alpha \leftrightarrow \beta\rangle_{0,c} \ , \tag{211}$$

where

$$\mathcal{A}_{H,\alpha}(-i\tau) = \exp[\tau\mathcal{H}/\hbar]\mathcal{A}_\alpha \exp[-\tau\mathcal{H}/\hbar]$$

is the imaginary time Heisenberg representation of the operator $\mathcal{A}_\alpha$. Then Eq. (211) immediately follows from Eq. (208) if we use the identity

$$\frac{1}{\hbar}\int_0^{\hbar/k_B T} d\tau \ \rho_n^0 \ e^{-(E_m-E_n)\tau/\hbar} = \frac{\rho_n^0 - \rho_m^0}{E_m - E_n} \tag{212}$$

While we did not explain yet why the tensor $\kappa_{\alpha\beta}$ is related to mass, let us point out that its high temperature asymptotic is perfectly consistent with the equipartition theorem if α and β describe macroscopic coordinates, say the position of the center of mass: $\alpha, \beta \in \{x, y, z\}$. In this case as we discussed earlier the gauge potential reduces to the total momentum operator of fast degrees of freedom $\mathcal{A}_\alpha = P_\alpha$ and thus e.g. the xx component of the mass according to Eq. (210) satisfies

$$\kappa_{xx} = \frac{1}{k_B T}\langle P_x^2\rangle_c \quad \Leftrightarrow \quad \frac{\langle P_x^2\rangle_c}{2\kappa_{xx}} = \frac{k_B T}{2}, \tag{213}$$

which is indeed the famous equipartition theorem of the statistical physics. As a corollary to our derivation we point that Eq. (211) generalizes the equipartition theorem to quantum systems and applies at any temperatures. Perhaps a less trivial statement is that Eq. (210) applies to all types of motion. For example, in a scale-invariant Hamiltonian where the slow parameter corresponds to dilations, the additional mass in the classical limit is given by the product of the variance of the dilation operator and the inverse temperature, and similarly for whatever parameters the problem presents.

Finally, the antisymmetric tensor F' is given by

$$F'_{\alpha\beta} = -i\pi \sum_{n\neq m} \frac{\rho_n^0 - \rho_m^0}{E_m - E_n} \langle n|\mathcal{M}_\alpha|m\rangle\langle m|\mathcal{M}_\beta|n\rangle \, \delta'(E_n - E_m) \tag{214}$$

Similar to $\eta_{\alpha\beta}$, this tensor is an on-shell contribution responsible for dissipation, but usually it is subleading to η. Like F, this tensor is always zero if the instantaneous Hamiltonian respects time-reversal symmetry.

B. Born Oppenheimer Approximation

Up to now we were considering the parameter $\boldsymbol{\lambda}$ as an external slow field. This is usually justified when the back action of fast degrees of freedom is negligible. However, there are many instances where such back action can not be neglected despite the time scale separation. For example in atomic, molecular systems, as well as more complex materials the motion of nuclei is much slower than the motion of electrons due to large mass difference but the forces exerted by electrons on nuclei cannot be neglected. In systems with emergent macroscopic collective degrees of freedom like order parameters, dynamics of the latter can be much slower than that of microscopic degrees of freedom but yet it is entirely determined by interactions with these degrees of freedom (e.g. slow magnetization waves often originate from fast motion of electrons with different spin). In thermodynamic heat engines fast degrees of freedom (e.g. atoms) exert a macroscopic force on a macroscopic object (e.g. a piston) causing motion of the latter due to its energy exchange with fast atoms. In all such situations it is natural to assume that fast degrees of freedom nearly adiabatically follow equilibrium corresponding to instantaneous positions of slow degrees of freedom. These ideas were first developed by Born and Oppenheimer in the context of atoms in 1927 and are known now as the Born-Oppenheimer approximation. Let us briefly discuss this approximation since it is the starting point of our further analysis. For simplicity we will assume that the slow degrees of freedom are classical, which is often justified since we are assuming they are macroscopic, while we will treat quantum degrees of freedom fully quantum mechanically.

Let us assume quite generally that the total Hamiltonian describing the degree of freedom $\boldsymbol{\lambda}$ and the rest of the system is

$$\mathcal{H}_{tot}(\boldsymbol{\lambda}) = \mathcal{H}_0(\boldsymbol{\lambda}) + \mathcal{H}(\boldsymbol{\lambda}), \tag{215}$$

where $\mathcal{H}_0(\boldsymbol{\lambda})$ is the Hamiltonian describing the bare motion of $\boldsymbol{\lambda}$. The choice of splitting $\mathcal{H}_{tot}$ between $\mathcal{H}_0$ and $\mathcal{H}$ is somewhat arbitrary and we can well choose $\mathcal{H}_0 = 0$ so that $\mathcal{H}_{tot} = \mathcal{H}$, however, for an intuitive interpretation of the results, it is convenient to assume that $\mathcal{H}_0(\boldsymbol{\lambda})$ represents a massive degree of freedom in some external potential $V(\boldsymbol{\lambda})$:

$$\mathcal{H}_0(\boldsymbol{\lambda}) = \frac{1}{2} p_\alpha m^{-1}_{\alpha\beta} p_\beta + V(\boldsymbol{\lambda}),$$

where $m^{-1}_{\alpha\beta}$ is the inverse mass tensor. In the infinite mass limit ($||m_{\alpha\beta}|| \to \infty$), $\boldsymbol{\lambda}$ represents an external (control) parameter whose dynamics is specified a priori. When $||m_{\alpha\beta}||$ is finite, $\boldsymbol{\lambda}$ is a dynamical variable and its dynamics needs to be determined self-consistently. The whole system can be described by coupled Hamiltonian equations of motion

$$m_{\alpha\beta}\frac{d\lambda_\alpha}{dt}=p_\beta,\quad \frac{dp_\alpha}{dt}=-\frac{\partial V}{\partial\lambda_\alpha}+\mathrm{Tr}[\rho(t)\mathcal{M}_\alpha(\boldsymbol{\lambda}(t))],\quad i\frac{d\rho(t)}{dt}=[\mathcal{H}(\boldsymbol{\lambda}(t)),\rho(t)]. \tag{216}$$

Technically one can derive this equation from the path integral representation of the full quantum-mechanical evolution taking the saddle point with respect to the classical field $\boldsymbol{\lambda}$ and treating other microscopic degrees of freedom fully quantum-mechanically. Alternatively, as was originally suggested by Born and Oppenheimer, one can assume that the quantum density matrix describing the full system factorizes into the product of density matrices for the slow degree $\boldsymbol{\lambda}$ and other degrees of freedom and then taking the classical limit $\boldsymbol{\lambda}$.

The key assumption of the Born-Oppenheimer approximation is that as $\boldsymbol{\lambda}$ is slow one can substitute the full density matrix $\rho(t)$ by its adiabatic limit ρ_0 and use this ρ_0 in the second of the equations (216). Under these conditions the dynamics of $\boldsymbol{\lambda}$ is described by a motion in the modified potential:

$$m_{\alpha\beta}\frac{d\lambda_\alpha}{dt}=p_\beta,\quad \frac{dp_\alpha}{dt}=-\frac{\partial V}{\partial\lambda_\alpha}+M_\alpha^{(0)}(\boldsymbol{\lambda}). \tag{217}$$

Due to the Feynman-Hellman theorem, in equilibrium

$$M_\alpha^{(0)}(\boldsymbol{\lambda})=-\mathrm{Tr}[\rho_0\partial_\alpha\mathcal{H}]=-\partial_\alpha\mathrm{Tr}[\rho_0\,\mathcal{H}]\implies \dot p_\alpha=-\partial_\alpha\big(V+\mathrm{Tr}[\rho_0\mathrm{H}]\big).$$

So the slow degree of freedom effectively moves in the renormalized Born-Oppenheimer potential

$$V'(\boldsymbol{\lambda})=V(\boldsymbol{\lambda})+\mathrm{Tr}[\rho_0\mathcal{H}(\boldsymbol{\lambda})]. \tag{218}$$

C. Emergent Newtonian dynamics.

While the Born-Oppenheimer approximation is very powerful for many systems it completely misses non-adiabatic corrections to the density matrix. We already alluded to the fact that these corrections give rise to the Lorentz force, friction, mass renormalization and other effects, which we will briefly discuss below. To take these corrections into account and thus to go beyond the Born-Oppenheimer approximation we simply need to combine the equations of motion (216) and the non-adiabatic expansion of the generalized force (202)

$$\frac{d}{dt}\left[(m_{\alpha\beta}+\kappa_{\alpha\beta}+F'_{\alpha\beta})\dot\lambda_\beta\right]+(\eta_{\alpha\beta}-\hbar F_{\alpha\beta})\dot\lambda_\beta=-\frac{\partial V}{\partial\lambda_\alpha}+M_\alpha^{(0)} \tag{219}$$

up to terms of order $\dot\lambda^2$. The symmetric tensor in the first term in this equation represents the renormalized mass thus $\kappa_{\alpha\beta}$ indeed represents the mass renormalization. The term $\eta_{\alpha\beta}\dot\lambda_\mu$ is clearly the dissipative force. The Berry curvature defines an analogue of the Coriolis or the Lorentz force and the other antisymmetric on-shell contribution encoded in F' is effectively an antisymmetric friction term. In these notes we are focusing on quantum systems with discrete spectrum. Therefore there are no on-shell contributions and hence we set η and F' to zero for the remainder of these notes. We also point out that within the accuracy of our expansion one can equally write the renormalized mass term as $\kappa_{\alpha\beta}\ddot{\lambda}_\beta$ or as we did as $d_t[\kappa_{\alpha\beta}\dot{\lambda}_\beta]$. Indeed it is easy to see that the difference between these two terms if $d_\gamma\kappa_{\alpha\beta}\dot{\lambda}_\beta\dot{\lambda}_\gamma \sim O(|\dot{\boldsymbol{\lambda}}^2|)$. However, a more careful analysis shows that the mass renormalization terms gives a conservative contribution to the energy of the system, i.e. is given by the full derivative of the renormalized Hamiltonian and therefore writing it as in Eq. (219) is more accurate (D′Alessio and Polkovnikov, 2014).

In the absence of dissipative contributions it is easy to check that the equations of motion (219) come from the Lagrangian:

$$\mathcal{L} = \frac{1}{2}\,\dot{\lambda}_\alpha\,(m+\kappa)_{\alpha\beta}\,\dot{\lambda}_\beta + \dot{\lambda}_\beta\,A_\beta(\boldsymbol{\lambda}) - V'(\boldsymbol{\lambda}), \tag{220}$$

where

$$A_\beta(\boldsymbol{\lambda}) = Tr[\rho_0\mathcal{A}_\beta]$$

is the equilibrium Berry connection and V' is the Born-Oppenheimer potential (218). In the zero temperature case the Berry connection reduces to the ground state Berry connection and the Born-Oppenheimer potential reduces to the sum of the bare potential and the instantaneous ground state energy of the system at given $\boldsymbol{\lambda}$. From the Lagrangian (220) we can define the canonical momenta conjugate to the coordinates λ_ν:

$$p_\alpha \equiv \frac{\partial\mathcal{L}}{\partial\dot{\lambda}_\alpha} = (m_{\alpha\beta}+\kappa_{\alpha\beta})\dot{\lambda}_\beta + A_\alpha(\boldsymbol{\lambda}) \tag{221}$$

and the emergent Hamiltonian:

$$\mathcal{H}_\lambda \equiv \dot{\lambda}_\alpha\,p_\alpha - \mathcal{L} = \frac{1}{2}(p_\alpha - A_\alpha)(m+\kappa)^{-1}_{\alpha\beta}(p_\beta - A_\beta) + V'(\boldsymbol{\lambda}). \tag{222}$$

Clearly the equilibrium Berry connection term plays the role of the vector potential. Thus we see that the formalism of effective Hamiltonian dynamics for arbitrary macroscopic degrees of freedom is actually emergent. Without the mass renormalization this (minimal coupling) Hamiltonian was derived earlier (Berry, 1989). Away from the ground state the dissipative tensors (η and F') are, in general, non-zero and it is not possible to reformulate Eq. (219) via the Hamiltonian or Lagrangian formalism.

Exercise V.1. Verify explicitly that the Lagrangian and the Hamiltonian equations of motion given by the Lagrangian (220) and the Hamiltonian (222) are equivalent to Newtonian equations of motion (219) (assuming that there are no dissipative contributions: $\eta = F' = 0$).

D. Beyond Newtonian dynamics. Snap modulus

Within the developed formalism we can continue the non-adiabatic expansion for the generalized force (201). To simplify the analysis in this section let us assume that the parameter λ is single component and thus all antisymmetric contributions vanish. As was mentioned in an earlier footnote, in this way one can recover the third derivative friction term, which describes dissipation due to radiation in Lorentz-invariant systems. Since we are focusing here on non-dissipative systems with a discrete spectrum this term will be zero. So the next non-zero term will appear if we go to the fourth derivative in λ. Such high-derivative term might look totally irrelevant given our assumption of time scale separation. But it has very important implications defining the leading correction to the Newtonian dynamics and thus showing the regime of its validity. Furthermore, as we will demonstrate later (see discussion below Eq. (224)) this term is closely related to the Unruh effect for accelerated photons confined to the cavity and has interesting observable physical consequences for the dynamics of the cavity.

It is straightforward to see that continuing the Taylor expansion in t'' in Eq. (201) we find up to the fourth order (and in the absence of dissipative odd derivative terms)

$$\langle \mathcal{M}_\alpha \rangle \approx M_\alpha^{(0)} - \kappa \ddot{\lambda} + \zeta \frac{d^4 \lambda}{dt^4}, \tag{223}$$

where

$$\zeta = \sum_{n \neq m} \frac{\rho_n - \rho_m}{(E_m - E_n)^3} |\langle m | \mathcal{A}_\lambda | n \rangle|^2 = \sum_{n \neq m} \frac{\rho_n - \rho_m}{(E_m - E_n)^5} |\langle m | \mathcal{M}_\lambda | n \rangle|^2. \tag{224}$$

Following the definition of the fourth derivative of the position as snap (Visser, 2004) we term the coefficient ζ as the <u>snap modulus</u>.

Exercise V.2. Derive Eq. (224).

Exercise V.3. Derive the microscopic expression for the dissipative contribution entering the generalized force, which is proportional to $\dddot{\lambda}$. Show that if the temperature is positive it can only lead to dissipation of the bare energy of λ, i.e. due to this term $d\mathcal{H}_\lambda/dt \le 0$, where $\mathcal{H}_\lambda$ is given by (222).

Substituting this generalized force into the equations of motion (216) we get

$$M\ddot{\lambda} = -\partial_\lambda V' - \kappa\ddot{\lambda} + \zeta\lambda^{(4)}\ . \tag{225}$$

Multiplying by the velocity $\dot{\lambda}$ and rearranging, this becomes

$$\begin{aligned} 0 &= \dot{\lambda}\partial_\lambda V' + (M+\kappa)\ddot{\lambda}\dot{\lambda} - \zeta\lambda^{(4)}\dot{\lambda} \\ &\approx \frac{d}{dt}\left(V' + \frac{M+\kappa}{2}\dot{\lambda}^2 - \frac{\zeta}{2}\left(2\dot{\lambda}\dddot{\lambda} - \ddot{\lambda}^2\right)\right)\ , \end{aligned}$$

up to terms of order $\dot{\lambda}^3$. Equivalently there is an emergent energy conservation law with

$$\mathcal{E}_\lambda = K + V'(\lambda) = \text{const}, \tag{226}$$

where the kinetic energy in the presence of the snap modulus reads

$$K = \frac{M+\kappa}{2}\dot{\lambda}^2 + \frac{\zeta}{2}\left(\ddot{\lambda}^2 - 2\dot{\lambda}\dddot{\lambda}\right) \tag{227}$$

Completing the square and ignoring the higher order term $\dddot{\lambda}^2$ one can approximately rewrite the kinetic energy as

$$K \approx \frac{M+\kappa}{2}\left(\dot{\lambda} - \frac{\zeta}{\kappa+M}\dddot{\lambda}\right)^2 + \frac{\zeta}{2}\ddot{\lambda}^2 \tag{228}$$

so that the third derivative term plays a role similar to the gauge potential. In this derivation we assumed for simplicity that both κ and ζ are independent of λ. One can check that if this is not the case the correct equations of motion follow from the conservation of the energy $\mathcal{E}_\lambda$. This energy function does not represent a Hamiltonian any longer since it explicitly depends on higher order derivatives. Nevertheless one can define the Lagrangian and get the equations of motion from extremizing the action.

VI. EXAMPLES OF EMERGENT NEWTONIAN DYNAMICS.

A. Particle in a moving box

Let us illustrate this formalism with a few simple examples. In this section we will explicitly insert all factors of $\hbar$ to better see when these effects could be observed in realistic systems. First we consider a massless spring connected to a wall, as illustrated in the left panel of Fig. 18. We imagine that a quantum particle of mass m is initially prepared in the ground state of the confining potential. As in the previous example we will compute how the mass of a classical object (the wall) coupled to a quantum environment (the particle in the well) is renormalized, which in practice could be measured by, for example, a change in the oscillation frequency of the spring.

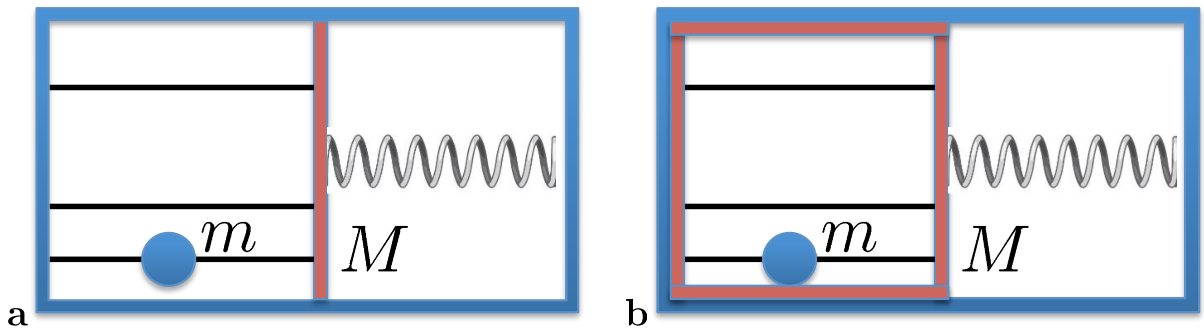

FIG. 18 (Color on-line) Schematic of a quantum piston. a) The spring is connected to a wall of the potential in which a quantum particle of mass m is initially confined into the ground state. b) As in a) but now the spring is connected to the whole potential well which moves rigidly. The horizontal black lines represent the low energy wave functions of the quantum particle in the confining potential.

According to Eq. (209) the mass renormalization is given by

$$\kappa_{RR} = 2\hbar^2 \sum_{n\neq 0} \frac{|\langle n|\mathcal{M}_\lambda|0\rangle|^2}{(E_n - E_0)^3}, \tag{229}$$

where $\lambda = X_R$ is the position of the right potential wall. We approximate the confining potential as a very deep square well potential:

$$\mathcal{H} = \frac{p^2}{2m} + V\big(\Theta(X_L - x) + \Theta(x - X_R)\big)\ . \tag{230}$$

Then $\mathcal{M}_\lambda \equiv -\partial_\lambda \mathcal{H} = V\delta(x - X_R)$ and we find

$$\kappa_{RR} = 2\hbar^2 \sum_{n\neq 0} \frac{V^2|\psi_0(X_R)|^2|\psi_n(X_R)|^2}{(E_n - E_0)^3}. \tag{231}$$

Using the well known result for a deep but finite square well potential

$$|\psi_n(X_R)| = \sqrt{\frac{2}{L}}\sqrt{\frac{E_n}{V}},$$

where the factor of $\sqrt{2/L}$ comes from the normalization of the wave-function in a square potential of length L, we obtain

$$\kappa_{RR} = 2\hbar^2 \left(\frac{2}{L}\right)^2 \sum_{n\neq 0} \frac{E_0 E_n}{(E_n - E_0)^3}. \tag{232}$$

Substituting

$$E_n = \frac{\hbar^2 k_n^2}{2m}, \quad k_n = \frac{n+1}{L}\,\pi, \quad \forall n \geq 0$$

we arrive at

$$\kappa_{RR} = m\,\frac{16}{\pi^2}\sum_{n\geq 1}\frac{(n+1)^2}{[(n+1)^2-1]^3} = m\,\frac{2\pi^2-3}{6\pi^2} \approx 0.28m$$

The result is identical if we connect the piston to the left wall, i.e. $\kappa_{LL} = \kappa_{RR}$.

Exercise VI.1. Derive the result Eq. (VI.A) using the gauge potential. In particular, repeat steps similar to the ones for the harmonic oscillator leading to Eq. (160) to find the gauge potential corresponding to moving X_R. Then using this gauge potential and Eq. (209) compute the mass correction of the piston.

Now let us consider a slightly different setup where the spring connects to the whole box (see Fig. 18b) so that $\lambda = X_+$ now indicates the center of mass of the well. From Galilean invariance we expect $\kappa = m$. In fact, since now both potentials walls are moving, our expression gives

$$\mathcal{M}_+ = -\partial_+\mathcal{H} = V(\delta(x-X_R) - \delta(x-X_L)),$$

where X_L and X_R are the left and right positions of the walls. Thus using Eq. (229) we obtain

$$\kappa_{++} = 2\hbar^2\sum_{n\neq 0}\frac{V^2(\psi_0(X_L)\psi_n(X_L) - \psi_0(X_R)\psi_n(X_R))^2}{(E_n-E_0)^3} \tag{233}$$

Since in a symmetric potential well $\psi_n(X_R) = (-1)^n\psi_n(X_L)$, only the odd terms contribute in the equation above. Following the same line of reasoning as before we arrive at (note the extra factor of 4 with respect to Eq. (232))

$$\kappa_{++} = 2\hbar^2\left(\frac{2}{L}\right)^2 4\sum_{n=odd}\frac{E_0E_n}{(E_n-E_0)^3} = m\frac{64}{\pi^2}\sum_{n=odd}\frac{(n+1)^2}{[(n+1)^2-1]^3} = m \tag{234}$$

So indeed we recover the expected result. This simple calculation illustrates that we can understand the notion of the mass as a result of virtual excitations created due to the acceleration of the external coupling, which in this case is the position of the wall(s).

This result can be found using the language of gauge potentials. As we showed earlier for the global translations $X_L = X_R$ is the momentum operator: $\mathcal{A}_+ = \hat{p}$. So the renormalization can be also found from Eq. (VI.A)

$$\kappa_{++} = 2\sum_{n\neq 0}\frac{|\langle 0|\hat{p}|n\rangle|^2}{E_n - E_0} = m. \tag{235}$$

Exercise VI.2. Verify that Eq. (235) gives the correct expression for the mass (234).

Notice that the expression for the mass (234) is expected to hold not only for a square well but any translationally invariant system non-relativistic system. As we already discussed it can be viewed as a sum rule or a quantum generalization of the equipartition theorem.

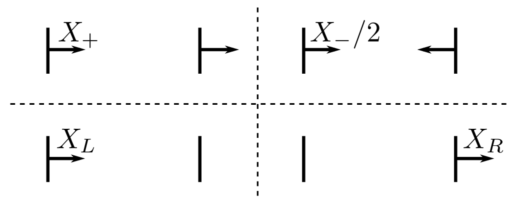

FIG. 19 Four possible modes of motion for the walls of the cavity.

If instead we analyze the setup where the two walls are connected to a spring and move towards each other so that $\lambda = X_-$ is the (instantaneous) change in the length of the potential well (see Fig. 19) we find

$$\begin{aligned}\kappa_{--} &= 2\hbar^2 \sum_{n\neq 0} \frac{V^2(\psi_0(X_L)\psi_n(X_L) + \psi_0(X_R)\psi_n(X_R))^2}{4(E_n - E_0)^3} \\ &= m\frac{16}{\pi^2} \sum_{\substack{n=even \\ n\neq 0}} \frac{(n+1)^2}{[(n+1)^2-1]^3} = m\frac{\pi^2-6}{12\pi^2} \approx 0.033m.\end{aligned} \tag{236}$$

Let us note a peculiar property of the dressed mass. Clearly $\kappa_{LL}+\kappa_{RR} \approx 0.56m \neq \kappa_{++}, \kappa_{--}$, i.e. the mass renormalization of the two walls is not the same as the sum of the mass renormalization of each wall measured separately. This is a result of interference, which is apparent in Eqs. (233) and (236). Note that $(\kappa_{++} + 4\kappa_{--})/2 = \kappa_{LL} + \kappa_{RR}$. Thus the mass behaves similarly to the intensity in the double pass interferometer, where the sum of intensities in the symmetric and antisymmetric channels is conserved. This analogy will become more clear after Exercise (VI.4), where you will compute the full mass renormalization tensor, whose normal modes correspond to κ_{++} and κ_{--}, which interfere to give κ_{LL} and κ_{RR}.

It is straightforward to generalize this calculation for a particle in the box prepared in an excited state $|n\rangle$:

$$\kappa_{++}^n = 2\sum_{n'\neq n} \frac{|\langle n'|p|n\rangle|^2}{E_{n'} - E_n} = m\frac{64}{\pi^2} \sum_{n'=n+\mathrm{odd}} \frac{(n'+1)^2(n+1)^2}{[(n'+1)^2-(n+1)^2]^3} = m\ . \tag{237}$$

Similar expressions hold for κ_{--}^n and κ_{RR}^n, but unlike the Galilean mass κ_{++} the latter two depend on n. In particular (c.f. Exercise VI.1),

$$\kappa_{RR}^n = 2\hbar^2 \sum_{m\neq n} \frac{|\langle m|\partial_{X_R}|n\rangle|^2}{(E_m - E_n)} = 2\sum_{m\neq n} \frac{|\langle m|\mathcal{D}|n\rangle|^2}{E_m - E_n} = \frac{m}{3}\left(1 - \frac{3}{2\pi^2 n^2}\right), \tag{238}$$

where

$$\mathcal{D} = \frac{x\hat{p} + \hat{p}x}{2L}$$

is the dilation operator introduced earlier (c.f. Eq. (161)). In the classical limit the renormalized mass approaches $m/3$. This result can be also easily recovered from the equipartition theorem. Indeed according to Eq. (210) the high temperature asymptotic of the metric tensor is given by the variance of the gauge potential, which is the dilation operator in this case:

$$\kappa_{RR}^n \xrightarrow{n\gg 1} \frac{1}{k_B T}\langle \mathcal{D}\rangle^2 \approx \frac{1}{k_B T}\frac{\langle x^2\rangle\langle p^2\rangle}{L^2} = \frac{m}{3}, \tag{239}$$

where we used that in the classical limit according to the Gibbs statistics probability distributions for the coordinate and the momentum factorize.

Exercise VI.3. Complete missing steps in deriving Eqs. (237) and (238).

The fact that the mass κ_{RR} or in short the dilation mass, since it corresponds to the dilations of the system, is equal to one third of the usual translational mass might look a bit strange. One would naively expect that the effect of interference terms appearing e.g. in Eq. (233) will disappear in the classical limit as usually happens. Indeed it is easy to see that such terms appear with opposite signs depending on whether the parity of the state n is even or odd (for the excited state the equivalent expression will involve double summation over n and n' and the sign of the interference term will depend on the parity difference between n and n'). Because $E_{n'} - E_n$ is a smooth function of n and n' one would expect that these oscillations will cancel each other. However, this is not the case because the mass is always, even in the classical limit $n \gg 1$, is dominated by the nearest excitations $n' = n \pm 1, n \pm 2$ so $E_{n'} - E_n$ can not be considered as a smooth continuous function of $n - n'$.

Instead this mass dressing can be qualitatively understood by noting that upon compression of the box (a.k.a. dilations, the generator of the κ_{--} term), the mass m pushes back against the walls much like a massive spring or a rubber band. Then if we push on the right end of the massive spring to give it a velocity v_R with the other end held clamped at $x = 0$, the velocity of the spring

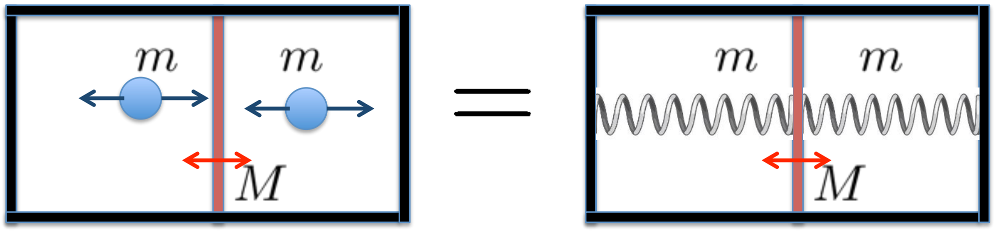

FIG. 20 A figure illustrating equivalence of a piston confined between two cavities with an ideal gas to the piston connected to two springs of mass m, where m is the mass of the gas in each cavity. Note that analogy extends not only to forces (as it is usually discussed) but also to masses.

will be a linear function of the position, $v(x) = v_R x/L$. The kinetic energy of the massive spring in this case is

$$T = \int_0^L \frac{1}{2}\mu v^2(x)dx = \frac{\mu}{2}\int_0^L \frac{x^2 v_R^2}{L^2} = \frac{1}{6}m v_R^2 = \frac{\kappa_{RR}}{2}v_R^2\,, \tag{240}$$

where $\mu = m/L$ is the mass density of the spring. The corollary of this interpretation is that one can extend the analogy of the freely moving piston confined between two ideal gases (see Fig. 20). As is discussed in many textbooks, in this setup near equilibrium the two gases exert effective elastic forces on the piston from effective massless springs and the spring constant is proportional to the pressure. Our result shows that this analogy extends beyond this, at least in the non-interacting limit, giving equivalence of this setup to the piston coupled to two massive springs with the mass of each spring being the same as the mass of the gas on each side of the piston.

Exercise VI.4. Show that for an arbitrary eigenstate n, the mass tensor is diagonal in the X_+, X_- basis, i.e., $\kappa_{+-} = \kappa_{-+} = 0$. Then find the full mass tensor in the X_R, X_L basis by using the Jacobian matrix $J = [\partial X_{+,-}/\partial X_{R,L}]$: $\kappa_{\{R,L\}} = J^T \kappa_{\{+,-\}} J$. Confirm that this gives the correct value of $\kappa_{RR} = \kappa_{LL}$ for the ground state (Eq. (VI.A)).

Exercise VI.5. Derive the gauge potential for the compression w.r.t. X_-. Using the equipartition theorem evaluate the mass κ_{--} in the classical limit (corresponding to the highly excited state of the particle) and prove it is equal to $m/12$. Argue that in the high temperature limit the off-diagonal components of the metric tensor $g_{+-} = 0$ and hence the mass tensor is also diagonal in the $+-$ space.

Exercise VI.6. For the harmonic oscillator presented in Sec. I, translations and dilations correspond to changing x_0 and $k = m\omega^2$ respectively. Find the diagonal components of the mass tensor $\kappa_{x_0 x_0}$ and κ_{kk} for an arbitrary eigenstate $|n\rangle$. Show that these connect to the metric tensor, which was derived for x_0 and k in Exercise (III.3) and Eq. (157), respectively

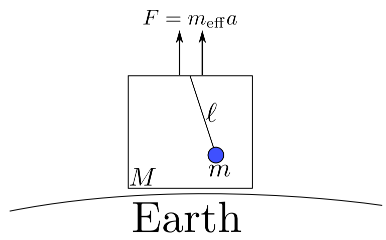

FIG. 21 Illustration of pendulum in a box being pulled away from the earth (see Exercise (VI.7)).

Exercise VI.7. Consider the setup illustrated in Fig. 21 in which a pendulum with mass m attached to a box of mass M is pulled away from the surface of the earth. Using the results of the previous problem, find the effective mass M_{eff} that setup will appear to have when lifted away from the earth as a function of its temperature T. For simplicity, you may assume that T is large enough that the problem may be treated classically.

---

1. Classical derivation of the mass for a particle in a moving box.

The example of the piston shows how the formalism of adiabatic perturbation theory can be used to find both the anticipated translational mass of the box with a particle inside and the less obvious dilation mass. These examples are sufficiently simple that they can be recovered from more elementary methods, although as we will see the actual derivations are more complicated and harder to extend to more complex setups. It is nevertheless instructive to see how the mass renormalization can be found from simple kinematics.

Let us start by computing the translational mass. Namely let us imagine a classical slow box of mass M, initially at rest, with a fast particle of mass m inside it. At time $t = 0$ we start accelerating the box with, for simplicity, constant acceleration a. Let us compute the force exerted on the box by the particle. We will find the force by computing the average momentum transferred to the particle during one cycle and divide by the period. Note that we are interested in the force averaged over the period. One can do the averaging in two equivalent ways: time averaging and space averaging. The second way, i.e. space averaging, is actually somewhat simpler because the wall is accelerating and time averaging should be done with some care. In quantum language this space averaging of the force is equivalent to the averaging of $\mathcal{M}$ over the stationary probability distribution.

Let us imagine that starting at time $t = 0$ the box of length L is pulled with a constant

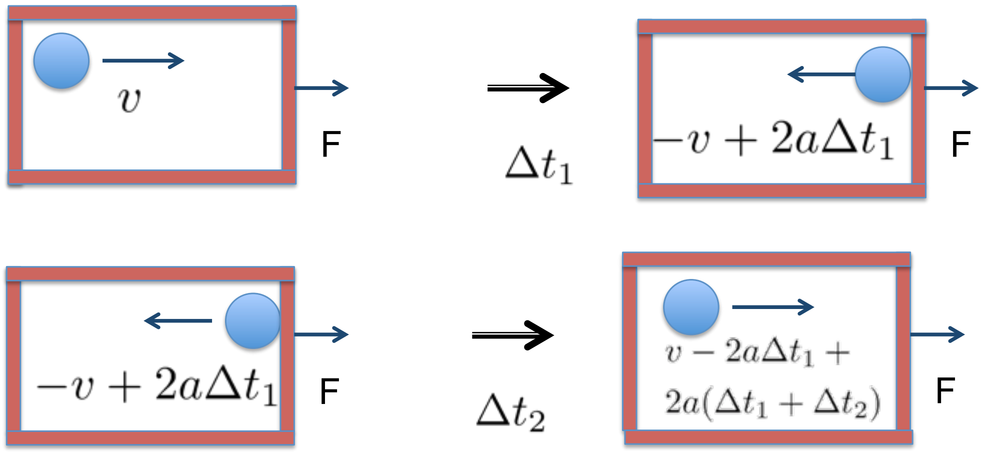

FIG. 22 Figure illustrating an elementary classical calculation of the translational mass. See text for details.

acceleration a by some external force F (see Fig. 22). Let us also assume that the particle starts near the left wall (the position of the particle can be chosen arbitrarily) and moves in positive direction with initial velocity v. After time Δt_1 this particle collides with the right wall. By that time the wall moves distance $\Delta x_1 = L + a\Delta t_1^2/2$ and acquires the velocity $V_1 = a\Delta t_1$. Then it reflects back with velocity

$$v_1 = -v + 2V_1 = -v + 2a\Delta t_1.$$

The total transferred momentum to the particle during this collision is

$$\Delta p_1 = m(v_1 - v) = 2mv + 2ma\Delta t_1.$$

Then the particle moves backwards and collides with the left wall after time Δt_2. By that time the left wall moved by the distance $\Delta x_2 = a(\Delta t_1 + \Delta t_2)^2/2$ and acquired the velocity $v_2 = a(\Delta t_1 + \Delta t_2)$. The particle now reflects with the velocity

$$v_2 = -v_1 + 2a(\Delta t_1 + \Delta t_2) = v + 2a\Delta t_2.$$

Hence the total transferred momentum to the particle is

$$\Delta p_2 = m(v_2 - v_1) = 2mv + 2ma(\Delta t_2 - \Delta t_1).$$

Now we can compute the force exerted by the wall on this particle as

$$f = \frac{\Delta p_1 + \Delta p_2}{\Delta t_1 + \Delta t_2} = \frac{2ma\Delta t_2}{\Delta t_1 + \Delta t_2}. \tag{241}$$

This expression is rather complicated as we yet have to compute Δt_1 and Δt_2, as functions of v, a, L. However, to find the mass we are interested only in the leading non-adiabatic response linear in acceleration. The numerator of Eq. (241) is already linear in a, which means that we can safely compute all time intervals only to zeroth order in a, which is trivial:

$$\Delta t_1 \approx \Delta t_2 \approx L/v.$$

Combining all this together we find

$$f \approx \frac{2ma}{2} = ma \tag{242}$$

as expected. So the total force required to accelerate the box and the particle is thus

$$f_{\rm tot} = (m+M)a, \tag{243}$$

which is precisely Newton's second law with the mass equal to the sum of the two masses. It is of course not surprising that we were able to reproduce this simple and expected result from more elementary methods. However, it is very instructive to see that we again relied in time scale separation and found this result only in the leading order adiabatic expansion with the small parameter $a\Delta t_1/v = aL/v^2$.

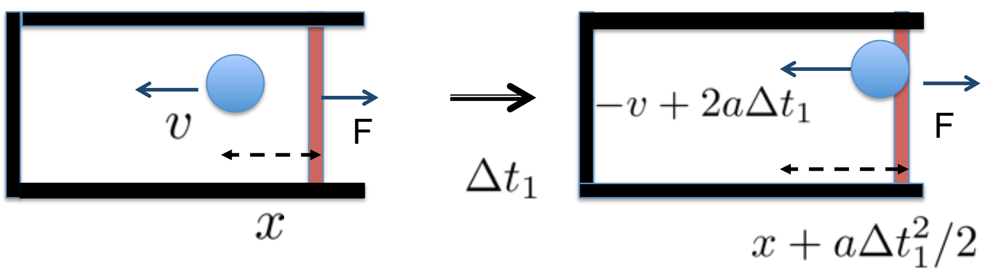

FIG. 23 Figure illustrating an elementary classical calculation of the dilation mass of the piston. See text for details.

Now let us analyze another setup where the force F is only applied to the right wall such that it moves with the acceleration a while the left wall remains static (see Fig. 23) . As we will see, the classical elementary derivation not involving gauge potentials becomes much more delicate as the force now depends on the initial position of the particle x. It is convenient to define x measured from the left static wall in the interval $[-L, L]$ such that the subinterval $[-L, 0]$ corresponds to the particle moving to the left (as shown in the figure) and the subinterval $[0, L]$ corresponding to the particle moving to the right i.e. towards the moving wall. We assume that we start from a stationary probability distribution described by a uniform distribution of x. As in the previous example the particle hits the right wall after the time Δt_1, which can be found from

$$-L + x + v\Delta t_1 = \frac{a\Delta t_1^2}{2}$$

Instead of solving this quadratic equation in general we will only find Δt_1 to the order in acceleration:

$$\Delta t_1 \approx \frac{L-x}{v} + \frac{a}{2}\frac{(L-x)^2}{v^3} \tag{244}$$

The transferred momentum to the particle is thus

$$\Delta p_1 = -2mv + 2ma\Delta t_1$$

The particle will return to the original position (and thus will complete the cycle) after time Δt_2 which can be found from[16]

$$\Delta t_2 = \frac{L + x + a\Delta t_1^2/2}{v - 2a\Delta t_1},$$

where we took into account that (i) the particle has to travel a longer distance because of the displacement of the wall and (ii) that it moves back with a reduced velocity. The force can be found as before by computing the ratio of the total momentum transfer over the period. To the leading linear order in acceleration it is

$$f(x) = \frac{\Delta p_1}{\Delta t_1 + \Delta t_2} \approx -\frac{mv^2}{L} + ma\left[\frac{5}{2} - \frac{2x}{L} - \frac{x^2}{2L^2}\right]. \tag{245}$$

The first term is nothing but the usual generalized force proportional to pressure (which resists compression of the piston). The second term is proportional to the acceleration and thus should define the mass. Unlike the previous case of the translationally invariant motion, this term explicitly depends on the initial coordinate of the particle. Taking the average over these coordinates, which is equivalent to the average over the density matrix in the quantum case, we find the average force

$$\overline{f} = \frac{1}{2L}\int_{-L}^{L} f(x)dx = -\frac{mv^2}{L} + 2ma + \frac{ma}{3} \approx -\frac{m(v - aL/v)^2}{L} + \frac{ma}{3} \tag{246}$$

The first term here is now the standard force due to the pressure averaged over the cycle, with $\overline{v} = v - aL/v$ being the average velocity of the particles. The second term is the nonadiabatic correction due to the acceleration, which gives the correct result from Eq. (239). As we see even in this simple example "elementary" classical derivation of the dilation mass is very delicate. It requires careful analysis of several contributions to the force of the same order and the correct identification of different terms.

[16] More accurately the cycle is complete when the particle returns to a slightly shifted dilated position x'. However, it is easy to see that this effect is canceled in the linear order in a as this shift has opposite effects on particles with opposite initial values of x.

B. Mass of a massless relativistic scalar field in a cavity.

For a massive particle in a box, we have seen that the box acquires an extra mass due to translations or dilations that derives from the bare mass of the particle. We now ask what happens for massless particles in a box, such as a phonon, photon or some other excitation with a linear dispersion. For example one can imagine a vibrating string confined between two clamps (see Fig. 24). The effective mass of photons in a cavity has been investigated since the early days of relativity, and the current theoretical understanding is that they appear to have a mass E/c^2 proportional to their energy (cf. Refs. (Kolbenstvedt, 1995) and (Wilhelm and Dwivedi, 2015) for a recent discussion). Here we will compute the renormalization of the mass of the cavity containing particles with relativistic dispersion inside as before through the non-adiabatic correction to the generalized force. This will allow us to identify both the classical (thermal) and quantum (zero point) contributions to the photon mass.

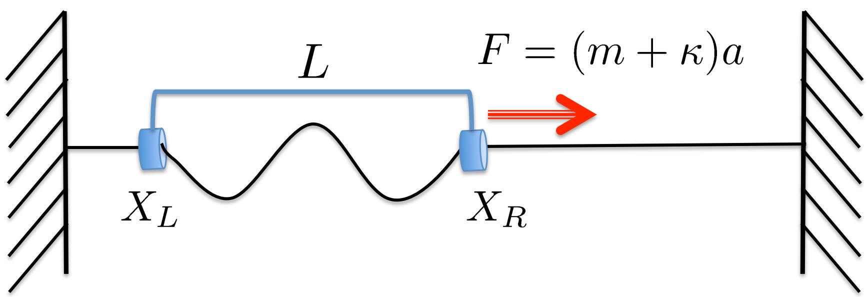

FIG. 24 Example of a system with a linear dispersion (guitar string) confined between two clamps. It is intuitively clear that moving the clamps is harder in the presence of vibrations as they should be dragged together with the clamps. This amounts to dressing the mass of the clamps analyzed here.

A simple example realizing such a setup would be a vibrating string confined between two clamps (see Fig. 24). Instead of the string one can imagine a Luttinger liquid confined between two impurities or a phonon (photon) gas confined between two reflecting mirrors. In our analysis we will ignore potential retardation effects on the confining potential. Specifically as before we will assume that $X_L(t)$ and $X_R(t)$ are given functions of time and e.g. for the symmetric mode $X_R(t) - X_L(t) = \text{const}(t)$ in the lab reference frame. This is perfectly justified in the case of a non-relativistic guitar string but might play an effect in the case of photons. For example, if we pull the right clamp with some force, there will be some delay before the left clamp starts moving. This implies that the bouncing photon will feel slightly different accelerations from the two walls and this may have some effect on the mass renormalization.

We will consider the following model Hamiltonian describing a massless scalar harmonic field confined to the cavity:

$$\mathcal{H} = \frac{1}{2}\int_{X_L}^{X_R} dx \left[\Pi(x)^2 + c^2\left(\frac{\partial\Phi}{\partial x}\right)^2\right] , \tag{247}$$

where Φ is the field (describing displacement of atoms from equilibrium positions in the case of the string) and Π is the momentum canonically conjugate to Φ. In the case of photons Φ represents the vector potential Λ. Then the momentum $\Pi(x)$ and the gradient of $\Phi(x)$ appearing in the Hamiltonian represent the electric field $E = \partial_t\Lambda \propto \Pi$ and magnetic field $B \propto \partial_x\Lambda$ respectively. For computing the translational mass we will assume that the cavity of length L extends from $X_L = -L/2 + X_+$ to $X_R = L/2 + X_+$. We consider a simple choice of vanishing Dirichlet boundary conditions: $\Phi(X_L) = \Phi(X_R) = 0$. For the string this implies that vibrations vanish at the boundary. For electromagnetic waves such boundary conditions can be realized by using a superconducting cavity such that the photons acquire a mass μ outside the cavity due to the Anderson-Higgs mechanism (Anderson, 1963). In the context of Klein-Gordon theory, this is represented by the Hamiltonian.

$$\mathcal{H} = \frac{1}{2}\int_{-\infty}^{\infty} dx \left[\Pi(x)^2 + c^2\left(\frac{\partial\Phi}{\partial x}\right)^2 + \mu^2\left(\Theta(X_R - x) + \Theta(x - X_L)\right)\Phi^2(x)\right] . \tag{248}$$

The two Hamiltonians (247) and (248) are equivalent to each other in the limit $\mu \to \infty$. They can be used for two equivalent derivations of the mass renormalization as we show below: the first one is based on gauge potentials and the second one is based on generalized forces.

The Hamiltonian (247) (and similarly (248)) is harmonic and thus can be diagonalized expanding the fields $\Phi(x)$ and $\Pi(x)$ in normal modes

$$\Phi(x) = \sum_j f_j(x) Q_j \ , \ \Pi(x) = \sum_j f_j(x) P_j \ , \tag{249}$$

where the (real-valued) mode functions f_j satisfy the usual orthonormality and completeness relations

$$\int_{-\infty}^{\infty} f_j(x) f_k(x) dx = \delta_{jk}, \quad \sum_j f_j(x) f_j(x') = \delta(x - x'). \tag{250}$$

The completeness relation ensures that the mode operators Q_j and P_j are canonically conjugate:

$$[Q_j, P_k] = i\hbar\delta_{jk} \ . \tag{251}$$

The mode functions, diagonalizing the Hamiltonian (248) must satisfy the wave equation:

$$-c^2\partial_x^2 f_j = \omega_j^2 f_j \tag{252}$$

with vanishing boundary conditions for the Hamiltonian (247) and the Klein-Gordon equation with spatially dependent mass for the Hamiltonian (248):

$$- c^2\partial_x^2 f_j + \mu^2 \left(\Theta(X_R - x) + \Theta(x - X_L)\right) f_j = \omega_j^2 f_j \ . \tag{253}$$

It is straightforward to verify that in the limit $\mu \to \infty$ the mode functions are identical:

$$f_j(x) = \sqrt{\frac{2}{L}} \sin\left(k_j(x - X_L)\right), \tag{254}$$

where $k_j = \pi j/L$, $j = 1, 2, \ldots$ and the mode frequencies are $\omega_j = k_j c$. Then the Hamiltonian can be diagonalized in terms of usual ladder operators

$$a_j \equiv \sqrt{\frac{\omega_j}{2\hbar}} Q_j + i\sqrt{\frac{1}{2\hbar\omega_j}} P_j, \quad a_j^\dagger \equiv \sqrt{\frac{\omega_j}{2\hbar}} Q_j - i\sqrt{\frac{1}{2\hbar\omega_j}} P_j$$

to give

$$\mathcal{H} = \hbar \sum_j \omega_j (a_j^\dagger a_j + 1/2) \ . \tag{255}$$

The eigenstates of this Hamiltonian are clearly harmonic oscillator eigenstates $|n\rangle = |n_1, n_2, \ldots\rangle$, where $n_j = 0, 1, 2, \ldots$ denotes the number of photons in the mode j.

For this system it is possible to explicitly find the gauge potentials by writing the eigenstates of the Hamiltonian in the first quantized notation extending the derivation of Eq. (159) to multiple modes. Each normal mode the wave function is given by the single-particle eigenstates of the harmonic oscillator:

$$\phi_{n_j}(Q_j) = \sqrt{\frac{1}{\ell_j}}\, \psi_{n_j}(Q_j/\ell_j), \tag{256}$$

where $\ell_j = \sqrt{\hbar/2\omega_j}$ and ψ_{n_j} is expressed through the Hermite polynomials (Landau and Lifshitz, 1981). As will become clear shortly we will not need to explicitly know this function. The full photon many-body wave-function is just the properly normalized symmetrized product of the single-mode wave function:

$$\Psi_{n_1, n_2 \ldots}(Q_1, Q_2, \ldots) = C \sum_{\{\sigma\}} \prod_j \phi_{n_j}(Q_{\sigma_j}), \tag{257}$$

where $\{\sigma\}$ denotes all possible permutations of the mode indexes and C is the normalization constant. Using that the normal coordinates Q_j and the oscillator lengths ℓ_j can depend on λ through the mode functions and the mode frequencies we can write

$$\partial_\lambda \Psi = \sum_j \left[\frac{\partial Q_j}{\partial\lambda}\frac{\partial \Psi}{\partial Q_j} + \frac{\partial \ell_j}{\partial\lambda}\frac{\partial \Psi}{\partial \ell_j}\right]. \tag{258}$$

Let us observe that

$$\frac{\partial Q_j}{\partial \lambda} = \int_{X_L}^{X_R} dx\, \partial_\lambda f_j(x)\, \Phi(x) + \frac{\partial X_R}{\partial \lambda} f_j(X_R)\Phi(X_R) - \frac{\partial X_L}{\partial \lambda} f_j(X_L)\Phi(X_L).$$

For the vanishing boundary conditions that we are considering, the last two terms are equal to zero. In the first term we can re-express $\Phi(x)$ back through the mode functions (c.f. Eq. (249)). Then we find

$$\frac{\partial Q_j}{\partial \lambda} = \int_{X_L}^{X_R} dx\, \partial_\lambda f_j(x) \sum_i f_i(x') Q_i = \sum_i \zeta^\lambda_{ji} Q_i,$$

where

$$\zeta^\lambda_{ji} = \int_{X_L}^{X_R} dx\, f_i(x) \partial_\lambda f_j(x).$$

From differentiating the orthonormality relation of the mode functions (250) with respect to λ, we see that $\zeta^\lambda_{ij} = -\zeta^\lambda_{ji}$ and thus $\zeta^\lambda_{jj} = 0$. As in Eq. (159) for the harmonic oscillator we find

$$\frac{\partial \phi_n(Q)}{\partial \ell} = -i \frac{PQ + QP}{2\hbar\ell} \phi_n$$

The last identity we need is

$$\frac{\partial \ell_j}{\partial \lambda} = \frac{\partial \ell_j}{\partial \omega_j} \frac{\partial \omega_j}{\partial \lambda} = -\frac{1}{2} \frac{\ell_j}{\omega_j} \frac{\partial \omega_j}{\partial \lambda}.$$

Combining all these results together we find

$$i\hbar \partial_\lambda \Psi \equiv \mathcal{A}_\lambda \Psi = \left[\sum_{i \neq j} Q_i \zeta^\lambda_{ij} P_j - \frac{1}{2} \sum_j \frac{1}{\omega_j} \frac{\partial \omega_j}{\partial \lambda} \frac{P_j Q_j + Q_j P_j}{2} \right] \Psi. \tag{259}$$

Therefore the gauge potential is

$$\mathcal{A}_\lambda = \sum_{i \neq j} Q_i \zeta^\lambda_{ij} P_j - \frac{1}{2} \sum_j \frac{\partial \log \omega_j}{\partial \lambda} \frac{P_j Q_j + Q_j P_j}{2}. \tag{260}$$

It is convenient to rewrite this gauge potential in terms of the ladder operators:

$$\mathcal{A}_\lambda = \frac{i\hbar}{4} \sum_{i \neq j} \zeta^\lambda_{ij} \left(\left[\sqrt{\frac{\omega_j}{\omega_i}} - \sqrt{\frac{\omega_i}{\omega_j}} \right] (a_i^\dagger a_j^\dagger - a_i a_j) + \left[\sqrt{\frac{\omega_j}{\omega_i}} + \sqrt{\frac{\omega_i}{\omega_j}} \right] (a_j^\dagger a_i - a_i^\dagger a_j) \right) - \frac{i\hbar}{4} \sum_j \frac{\partial \log \omega_j}{\partial \lambda} (a_j^\dagger a_j^\dagger - a_j a_j) \tag{261}$$

It is clear that the only nonzero matrix elements of the gauge potential correspond either to scattering one particle or simultaneous creation or annihilation of two-particles. In particular,

$$
\begin{aligned}
\langle \dots n_i - 1 \dots n_j + 1 \dots | \mathcal{A}_\lambda | \dots n_i \dots n_j \dots \rangle &= i\hbar \sqrt{n_i(n_j+1)} \frac{\omega_i + \omega_j}{2\sqrt{\omega_i \omega_j}} \zeta_{ij}^\lambda; \\
\langle \dots n_i + 1 \dots n_j + 1 \dots | \mathcal{A}_\lambda | \dots n_i \dots n_j \dots \rangle &= -i\hbar \sqrt{(n_i+1)(n_j+1)} \frac{\omega_i - \omega_j}{2\sqrt{\omega_i \omega_j}} \zeta_{ij}^\lambda; \\
\langle \dots n_j + 2 \dots | \mathcal{A}_\lambda | \dots n_j \dots \rangle &= -\frac{i\hbar}{4} \frac{\partial \log \omega_j}{\partial \lambda} \sqrt{(n_j+1)(n_j+2)}; \qquad (262) \\
\langle \dots n_i - 1 \dots n_j - 1, \dots | \mathcal{A}_\lambda | \dots n_i \dots n_j \dots \rangle &= i\hbar \sqrt{n_i n_j} \frac{\omega_i - \omega_j}{2\sqrt{\omega_i \omega_j}} \zeta_{ij}^\lambda; \\
\langle \dots n_j - 2 \dots | \mathcal{A}_\lambda | \dots n_j \dots \rangle &= \frac{i\hbar}{4} \frac{\partial \log \omega_j}{\partial \lambda} \sqrt{n_j(n_j-1)}.
\end{aligned}
$$

Substituting these gauge potentials into the general expression for the mass (208) and noting that the energy differences between the connected states are $\pm(\omega_i - \omega_j)$ for the scattering terms conserving the number of particles or $\pm(\omega_i + \omega_j)$ for non-conserving terms we find

$$
\kappa_\lambda = \frac{\hbar}{4} \sum_{i \neq j} \left[\frac{n_i - n_j}{\omega_j - \omega_i} \frac{(\omega_i + \omega_j)^2}{\omega_i \omega_j} + \frac{n_i + n_j + 1}{\omega_i + \omega_j} \frac{(\omega_i - \omega_j)^2}{\omega_i \omega_j} \right] (\zeta_{ij}^\lambda)^2 + \frac{\hbar}{8} \sum_j \frac{2n_j + 1}{\omega_j} \left(\frac{\partial \log \omega_j}{\partial \lambda} \right)^2 \qquad (263)
$$

Clearly this expression splits into the two parts $\kappa_\lambda^{\text{ph}}$ linear in the occupation numbers and $\kappa_\lambda^{\text{vac}}$, which is the vacuum contribution:

$$
\begin{aligned}
\kappa_\lambda^{\text{ph}} &= \hbar \sum_{i \neq j} n_j \frac{\omega_i^2 + 3\omega_j^2}{\omega_j(\omega_i^2 - \omega_j^2)} (\zeta_{ij}^\lambda)^2 + \frac{\hbar}{4} \sum_j n_j \frac{(\partial_\lambda \omega_j)^2}{\omega_j^3} \\
\kappa_\lambda^{\text{vac}} &= \frac{\hbar}{4} \sum_{i \neq j} \frac{(\omega_i - \omega_j)^2}{(\omega_i + \omega_j)\omega_i \omega_j} (\zeta_{ij}^\lambda)^2 + \frac{\hbar}{8} \sum_j \frac{(\partial_\lambda \omega_j)^2}{\omega_j^3} \qquad (264)
\end{aligned}
$$

The expression above applies to any choice of the parameter λ. Moreover in this derivation we never used any specific dispersion relation so it applies both to massive and massless harmonic systems. In particular, it will apply to the massive Klein-Gordon theory confined to a cavity. And finally we never explicitly used the fact that the cavity is one dimensional. So if we extend the integrals defining the mode function overlaps ζ_{ij}^λ to d-dimensions, Eq. (264) will describe the mass renormalization of an arbitrary d-dimensional cavity with vanishing boundary conditions.

As with the single-particle case we focus on two possible motions: translations and dilations. For the translational motion $\lambda = X_+$ such that $\partial_+ X_R = \partial_+ X_L = 1$ obviously $\partial_+ \omega_j = 0$ and for the overlaps using the explicit expressions for the mode functions (254) we find

$$
\zeta_{ij}^+ = \frac{1}{L} \frac{2ij}{i^2 - j^2} (1 - (-1)^{i-j}). \qquad (265)
$$

For the dilations $\lambda = X_R$ and hence $\partial_\lambda X_R = 1,\ \partial_\lambda X_L = 0$ we can find

$$\zeta_{ij}^R = \frac{1}{L}\frac{2ij}{i^2 - j^2}(1 - \delta_{ij}). \tag{266}$$

In addition

$$\frac{d\log\omega_j}{dX_R} = -\frac{1}{L}.$$

Before proceeding with further analysis of the mass for translations and dilations of the cavity let us briefly show an alternative derivation of the same result based on generalized forces and Eq. (248). While the result will be equivalent, this derivation has its own advantages as it allows one to overcome the additional step of finding gauge potentials, which might prove difficult in more complicated setups, and therefore can be more amenable to numerical methods. Differentiating the Hamiltonian (248) with respect to λ we find the generalized force operator:

$$\mathcal{M}_\lambda \equiv -\partial_\lambda \mathcal{H} = -\mu^2 \left(\frac{\partial X_R}{\partial \lambda}\Phi^2(X_R) - \frac{\partial X_L}{\partial \lambda}\Phi^2(X_L) \right). \tag{267}$$

Substituting the mode expansion of the fields and taking the large μ limit one finds

$$\Phi^2(X_L) = \sum_{ij} f_i(X_L) f_j(X_L) Q_i Q_j = \frac{2c^2}{\mu^2 L}\sum_{ij} k_i k_j Q_i Q_j, \quad \Phi^2(X_R) = \frac{2c^2}{\mu^2 L}\sum_{ij}(-1)^{i+j} k_i k_j Q_i Q_j \tag{268}$$

Exercise VI.8. Prove that using the generalized forces (267) and the general expression for the mass (208) you can reproduce the identical expression for the mass as using the language of gauge potentials in Eq. (263).

Translations. Let us now analyze in detail the translational motion of the cavity. Substituting the expression for the overlap (265) into Eq. (264) we find

$$\kappa_+^{\rm ph} = \frac{16}{L^2}\sum_{i-j\ \rm odd} \hbar\omega_j n_j \frac{\omega_i^2(\omega_i^2 + 3\omega_j^2)}{(\omega_i^2 - \omega_j^2)^3} = \frac{2}{c^2}\sum_j \hbar n_j \omega_j = \frac{2E}{c^2}, \tag{269}$$

where $E = \sum_j \hbar n_j \omega_j$ is the total thermal energy of the photon gas inside the cavity. It is interesting that the result is completely universal, i.e. it does not depend on the energy distribution among the modes. Except for the prefactor of 2 this result is fully consistent with expectations from the special relativity. The possible origin for the discrepancy is that we assumed that the walls move with identical velocities in the lab frame, i.e. that we ignored any potential effects of retardation of the interaction keeping the walls of the cavity together. While this assumption might not be justified for real photons or other particles propagating with the speed of light, it is perfectly justified for slower excitations like phonons as in the setup shown in Fig. 24.

Next let us evaluate the vacuum contribution to the mass:

$$\kappa_+^{\text{vac}} = \frac{4\hbar}{L^2} \sum_{i+j \text{ odd}} \frac{\omega_i \omega_j}{(\omega_i + \omega_j)^3} = \frac{4\hbar}{\pi L c} \sum_{i+j \text{ odd}} \frac{ij}{(i+j)^3}. \tag{270}$$

This sum is formally divergent. The reason for this divergence comes from the assumption that the cavity is perfectly reflecting at all wavelengths. In reality this is never the case. For instance, if we are considering photons reflected from a metal, then the cutoff will be given by the plasma frequency, beyond which the metal becomes transparent. For the situation of the string shown in Fig. 24 the short distance cutoff would be given by the clamp radius: waves with very short wavelength would freely pass through the clamps, while longer wavelengths will be stopped. In the Klein-Gordon theory with a variable mass (248) the cutoff is formally given by μ. The easiest way to introduce cutoff to the problem is to add smooth cutoff function (e.g. a Gaussian) to the sum:

$$\kappa_+^{\text{vac}} \to \frac{4\hbar}{\pi L c} \sum_{i+j \text{ odd}} \frac{ij}{(i+j)^3} \mathrm{e}^{-(\omega_i+\omega_j)^2/\omega_\Lambda^2} = \frac{4\hbar}{\pi L c} \sum_{i+j \text{ odd}} \frac{ij}{(i+j)^3} \mathrm{e}^{-\epsilon^2 (i+j)^2}, \tag{271}$$

where $\epsilon = \pi c/(L\omega_\Lambda)$ and ω_Λ is the cutoff frequency. We can evaluate this sum in two steps. First let us make the substitution $i + j = m$ and $i - j = n$ where m and n are integers: $m = 3, 5, \dots$ and $n = -m+2, -m+4, \dots m-2$. Then it is straightforward to evaluate the sum over n:

$$\kappa_+^{\text{vac}} = \frac{2\hbar}{3\pi L c} \sum_{m=3,5,\dots} \frac{m^2-1}{m^2} \exp[-\epsilon^2 m^2] = C\frac{\hbar\omega_\Lambda}{c^2} - \frac{\pi\hbar}{12Lc} = C\frac{\hbar\omega_\Lambda}{c^2} + \frac{2E_c}{c^2}, \tag{272}$$

where C is a non-universal constant depending on the cutoff details and

$$E_c = -\frac{\pi\hbar c}{24L} \tag{273}$$

is the Casimir energy of the one-dimensional cavity (Bordag et al., 2001), i.e. the universal (cutoff independent) contribution of the zero point fluctuations to the ground state energy of the cavity. It is interesting that as with the thermal energy there is an additional factor of two in the Casimir energy contribution to the cavity mass. The first, cutoff-dependent, correction to the mass does not depend on L and thus can be interpreted as the renormalization of the mass of the cavity walls and thus absorbed into the definition of M. Apart from this correction we see that

$$\kappa_+ = 2\frac{E + E_c(L)}{c^2} \tag{274}$$

In a similar manner we can compute the snap modulus ζ representing the leading correction to Newtonian equations of motion (see Sec. V.D). Using Eq. (224) and repeating the same steps as deriving the mass we find

$$\zeta_+ = \zeta_+^{\rm ph} + \zeta_+^{\rm vac}, \tag{275}$$

where

$$\zeta_+^{\rm ph} = \frac{16L^2}{\pi^4 c^4} \sum_{i+j \text{ odd}} \hbar\omega_j n_j \frac{i^2(i^4 + 10 i^2 j^2 + 5 j^4)}{(i^2 - j^2)^5} = \frac{L^2}{\pi^4 c^4}\frac{\pi^4}{6} \sum_i \hbar\omega_j n_j = \frac{EL^2}{6c^4}, \tag{276}$$

$$\zeta_+^{\rm vac} = \frac{4\hbar L}{\pi^3 c^3} \sum_{i+j \text{ odd}} \frac{ij}{(i+j)^5} = \frac{12-\pi^2}{144\pi}\frac{\hbar L}{c^3}. \tag{277}$$

Interestingly the first "thermal" contribution to the snap modulus also depends only on the total energy of the system. It gives a small correction to the Newtonian dynamics of the cavity as long as the round trip time of the photon L/c is short compared to the characteristic time scales characterizing the motion of the cavity, e.g., the period of its oscillation. The second vacuum term has a very interesting interpretation too related to the Unruh effect (Crispino et al., 2008). Indeed this term is responsible for the energy correction proportional to the acceleration squared. On the other hand according to the Unruh effect an accelerated cavity acquires temperature proportional to the acceleration: $k_B T \sim \hbar \ddot{\lambda}/c$ and as a result the thermal energy $E_U \sim (k_B T)^2 L/(\hbar c) \sim \hbar L/c^2 \ddot{\lambda}^2$. So we see that

$$\frac{\zeta \ddot{\lambda}^2}{2} \sim \frac{E_U}{c^2}.$$

This contribution to the energy of the cavity, which goes beyond the standard paradigm of the Hamiltonian dynamics, can be interpreted as the result of vacuum heating by acceleration. We note that this interpretation is not precise as in order for the adiabatic perturbation theory to be valid the acceleration should be small such that the Unruh temperature should be smaller than the photon mode splitting. The Unruh effect is usually discussed in the continuum limit, when the cavity modes are not quantized. Nevertheless such an interpretation is very appealing and requires deeper investigation.

Exercise VI.9. Derive the expressions for the snap modulus (276) and (277).

Exercise VI.10. Assume that the cavity with photons inside is connected to a spring and undergoes small oscillations. Using the perturbation theory analyze the leading effect of the snap modulus on the motion of the cavity. You can assume that at time $t = 0$ the cavity is suddenly displaced by distance λ_0 from the equilibrium position and then released.

Dilations. Now let us analyze the second setup corresponding to dilations, where the left wall of the cavity is fixed and the right is free to move, i.e. $\lambda = X_R$. The derivations are very similar to the case of translations, so we will only quote the final results. As before it is convenient to split the mass into the thermal and vacuum contributions

$$\kappa_R = \kappa_R^{\mathrm{ph}} + \kappa_R^{\mathrm{vac}}, \tag{278}$$

where

$$\kappa_R^{\mathrm{ph}} = \frac{\hbar}{L^2}\sum_{i\neq j}\frac{n_i - n_j}{\omega_j - \omega_i}\frac{ij}{(i-j)^2} + \frac{\hbar}{L^2}\sum_{i,j}\frac{n_i + n_j}{\omega_i + \omega_j}\frac{ij}{(i+j)^2} = \frac{2E}{3c^2} \tag{279}$$

and

$$\begin{aligned}\kappa_R^{\mathrm{vac}} &= \frac{\hbar}{\pi L c}\sum_{ij}\frac{ij}{(i+j)^3}\mathrm{e}^{-\epsilon^2(i+j)^2} = \frac{\hbar}{6\pi L c}\sum_{m=2,3,\ldots}\frac{m^2-1}{m^2}\mathrm{e}^{-\epsilon^2 m^2}\\ &= C'\frac{\hbar\omega_\Lambda}{c^2} - \frac{\hbar}{12\pi L c}\left(\frac{\pi^2}{3}+1\right) = C'\frac{\hbar\omega_\Lambda}{c^2} + \frac{2E_c}{3c^2}\left(1+\frac{3}{\pi^2}\right).\end{aligned} \tag{280}$$

The thermal contribution to the dilation mass is again, as in the single-particle case, one third of the thermal translational mass. Therefore the equivalence of the gas to the massive spring (c.f. Fig. 20) extends to the relativistic gas. On the other hand, the quantum contribution to the dilation mass, as in the non-relativistic case (cf. Eq. (238)), contains an additional correction.

Exercise VI.11. Consider the massive Klein-Gordon Hamiltonian with vanishing boundary conditions:

$$\mathcal{H} = \frac{1}{2}\int_{-X_L}^{X_R} dx \left[\Pi(x)^2 + c^2\left(\frac{\partial\Phi}{\partial x}\right)^2 + \mu_0^2\Phi^2(x)\right], \tag{281}$$

where μ_0 is finite now.

- By repeating the arguments above prove that mass is still given by Eq. (264) with same overlaps ζ_{ij} as in the massless case and the massive dispersion: $\omega_j = \sqrt{\mu_0^2 + k_j^2}$, $k_j = \pi j/L$.

- Evaluate the thermal contribution to the translational mass. In particular, prove that

$$\kappa_+^{\mathrm{ph}} = \sum_j \hbar\omega_j n_j \left(1 + \frac{c^2 k_j^2}{\omega_j^2}\right). \tag{282}$$

  From this expression recover the non-relativistic limit as μ_0 becomes large.

- Show that for the dilation mass

$$\kappa_R^{\rm ph} = \frac{\kappa_+^{\rm ph}}{3}$$

irrespective of μ_0.

- Analyze the Casimir vacuum contribution for the translational mass. Show that it vanishes as μ_0 becomes large.

Exercise VI.12. Argue that, as was the case for the massive particle in a box, the photon mass tensor is diagonal in the $\{X_+, X_-\}$ basis, i.e., $\kappa_{+-} = 0$. Using this compute the mass $\kappa_{--} \equiv \kappa_-$ from κ_+ and κ_R.

Exercise VI.13. Consider a three-dimensional rectangular cavity with the Hamiltonian described by

$$\mathcal{H} = \frac{1}{2}\int d^3r \left[\Pi(r)^2 + c^2 \left(\nabla\Phi\right)^2\right] , \tag{283}$$

where the integration goes over the interval $x \in [-X_L, X_R]$, $y \in [-L_x/2, L_x/2]$, $z \in [-L_z/2, L_z/2]$ with vanishing boundary conditions. Find the thermal contributions to the translational and dilation mass along the x-direction. For this observe that the y and z components of the momentum are conserved and therefore $c^2(k_y^2 + k_z^2)$ plays the role of the mass μ_0 analyzed in the previous problem. Use the results of the previous problem to show that

$$\kappa_{+,x}^{\rm ph} = \sum_{\mathbf{j}} \hbar\omega_{\mathbf{j}} n_{\mathbf{j}} \left(1 + \frac{k_{x_j}^2}{\mathbf{k}_{\mathbf{j}}^2}\right). \tag{284}$$

Using this result prove that

$$\overline{\kappa}_+ \equiv \frac{\kappa_{+,x} + \kappa_{+,y} + \kappa_{+,z}}{3} = \frac{4}{3}\frac{E}{c^2}. \tag{285}$$

Classical derivation of the mass renormalization.

Similar to the example of a massive particle in a box discussed in Sec. VI.A.1, we consider taking a semi-classical limit for the photon problem. First we note that the dominant contribution to the mass in Eq. (263) in the semi-classical limit ($k_B T \gg \hbar c/L$) is given by the first term in the sum, which corresponds to number conserving processes. This e.g. follows from observing that the first term is dominated by neighboring modes $|\omega_i - \omega_j| \sim c/L$ as it is singular when $|\omega_i - \omega_j| \to 0$ while the second term is regular. This immediately translates to the suppression of the second contribution by a dimensionless factor $\hbar c/(Lk_BT)$, which vanishes in the semi-classical limit. Therefore, instead of photons it suffices to consider classical number-conserving particles with relativistic dispersion confined to a box, as illustrated in Fig. 25a. Consider for simplicity the one-dimensional case in which we start with a microcanonical ensemble with particles with energy E_0 uniformly distributed within the box. We then gradually begin to accelerate the box until the final velocity v is reached. During and after the acceleration, when the particle hits a wall moving away from it with velocity v, it is red-shifted from original frequency E_0 to the new energy $E_1 = E_0(1 - 2v/c + v^2/c^2)/\sqrt{1 - v^2/c^2}$ (this energy shift is equivalent to the frequency shift for photons). It simply follows from the energy and momentum conservation. A similar blue shift occurs upon hitting a wall moving towards the particle. The combination of these processes causes particles to equilibrate in the lab frame such that forward-moving particles are blue shifted compared to the backwards moving particles (Fig. 25). Numerically calculating the total energy of particles in the box, we can verify that the total energy after slowly accelerating to velocity v, averaged over initial conditions, is $E_{\rm tot} \approx E_0(1 + v^2/c^2) = E_0 + \kappa v^2/2$. Thus, as in the quantum case, we find that $\kappa = 2E/c^2$ in these semi-classical simulations. Similar simulations can be done for the case of massive relativistic particles or three-dimensional photons, all of which confirm the quantum predictions of Eq. (284) (Fig. 25c).

Le us comment that this mass renormalization $\kappa \sim E/c^2$ is typically tiny for real photons but can be observable for other types of systems. For example, in the guitar string setup illustrated in Fig. 24 one can easily show that $\kappa \propto \mu A_{\rm osc}^2/L$, where μ is the mass density of the string and $A_{\rm osc}$ is the amplitude of the oscillations, so by either using a heavier string or plucking it more strongly, one can readily enhance this effect to the point that it might be observable.

Exercise VI.14. Confirm that the photon contribution to the dilation mass of the three-dimensional case satisfies $\kappa_{--}^{\rm 3d-ph}(\mathbf{p}) = \frac{1}{12}\kappa_{++}^{\rm 3d-ph}(\mathbf{p})$, where $\kappa_{++}^{\rm 3d-ph}(\mathbf{p}) = 2[1-(p_y^2+p_z^2)/2p^2]E_{\mathbf{p}}/c^2$ (see Eq. (284)).

C. Classical central spin (rigid rotor) problem

As another example let us consider a macroscopic rotor interacting with a bath of N independent spin-1/2 particles (Fig. 26a). This discussion closely follows that of Ref. (D′Alessio and Polkovnikov, 2014). We consider an interaction where the rotor with orientation $\hat{n} = (\sin\theta\cos\phi, \sin\theta\sin\phi, \cos\theta)$ produces a magnetic field parallel to $\hat{n}$ that interacts with the magnetic

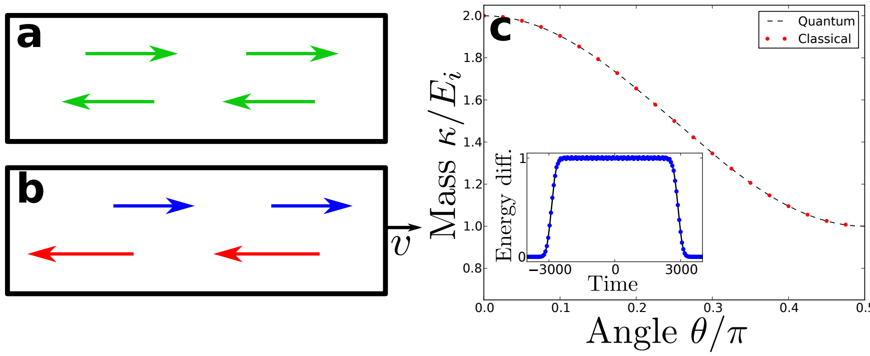

FIG. 25 (Semi)classical mass of relativistic particles. (a) Initial setup. Particles are prepared at initial energy E_0 and uniform probability distribution in space. (b) Cavity is slowly accelerated to velocity $v \ll c$. Doppler shifts of the particles upon hitting the cavity walls yield an equilibrium distribution in which forward-moving particles are blue-shifted and backward-moving particles are red-shifted. (c) The results of the simulation in a 3D cavity show that the semi-classical mass matches the quantum prediction (284). Here $\theta = \tan^{-1}\left(k_\perp/k_x\right)$ parameterizes the initial direction of the particle in the cavity. The inset shows excess particle energy $(E - E_0)/v_0^2$ (blue dots) and v^2/v_0^2 during a slow ramp from velocity 0 to v_0 with $\theta = 0$. The particles first heat as the box accelerates and then cool back down as the box decelerates, indicating that the dynamics is reversible as the mass correction should be.

moments in the spin bath via Zeeman coupling of random magnitude. If instead of the rotor we use the quantum spin operator, this model is known as the central spin model.

The Hamiltonian describing the system of the form in Eq. (215) is

$$\mathcal{H}_0 = \frac{\mathbf{L}^2}{2I} + V(\mathbf{n}), \quad \mathcal{H} = -\mathbf{n} \cdot \sum_{i=1}^{N} \Delta_i \boldsymbol{\sigma}_i, \tag{286}$$

where I is the momentum of inertia, which for simplicity we take to be isotropic, $V(\mathbf{n})$ is a time-dependent external potential, and $\mathbf{L}$ is the angular momentum of the rotor. This example is similar to the one considered earlier except that the effective magnetic field is no longer confined to the xz plane and we no longer assume that it is given by an external protocol. Rather, the time evolution of this system needs to be found self-consistently. Each spin evolves according to the von Neumann equation with the time-dependent Hamiltonian $\mathcal{H}(\mathbf{n}(t))$:

$$i\hbar \frac{d\rho}{dt} = [\mathcal{H}(\mathbf{n}(t)), \rho] \ . \tag{287}$$

The rotor evolves according to the Hamilton equations of motion

$$I\dot{\mathbf{n}} = \mathbf{L} \times \mathbf{n}, \quad \dot{\mathbf{L}} = \mathbf{n} \times \left(\mathbf{M}_{ext} + \left\langle -\frac{\partial \mathcal{H}}{\partial \mathbf{n}} \right\rangle\right) = \mathbf{n} \times \left(\mathbf{M}_{ext} + \sum_i \Delta_i \langle \boldsymbol{\sigma}_i \rangle\right) \tag{288}$$

where $\mathbf{M}_{ext} = -\frac{\partial V(\mathbf{n})}{\partial \mathbf{n}}$ is the external force on the rotor, such as the torque generated by an external magnetic field, and $\langle \ldots \rangle$ indicates the quantum average over the density matrix $\rho(t)$. We assume that initially $\mathbf{n}_0 = (0,0,1)$ and the spins are in thermal equilibrium with respect the Hamiltonian $\mathcal{H}(\mathbf{n}_0)$, giving $\langle\sigma_i^x\rangle_0 = \langle\sigma_i^y\rangle_0 = 0$ and $\langle\sigma_i^z\rangle_0 = \tanh(\beta\Delta_i)$.

For the toy model proposed here, these coupled equations can be easily solved numerically. In fact, according to the Ehrenfest theorem, the evolution of the expectation values follow the classical equation of motion and Eq. (287) can be replaced with the much simpler equation $\hbar\dot{\mathbf{m}}_i = 2\Delta_i\,\mathbf{m}_i\times\mathbf{n}$ where $\mathbf{m_i} = \langle\boldsymbol{\sigma}_i\rangle$. Therefore the exact dynamics of the system consists of the vectors $(\mathbf{L},\mathbf{n},\{\mathbf{m}_i\})$ precessing around each other.

We now compare the exact dynamics with the emergent Newtonian dynamics. First, we note that the form of Eqs (288) immediately implies

$$\begin{aligned} &\dot{\mathbf{n}}\cdot\mathbf{L} = 0,\ \mathbf{n}\cdot\dot{\mathbf{L}} = 0 \implies \mathbf{n}\cdot\mathbf{L} = \text{const} \\ &|\mathbf{n}|^2 = \text{const} \implies \dot{\mathbf{n}}\cdot\mathbf{n} = 0 \implies \ddot{\mathbf{n}}\cdot\mathbf{n} = -|\dot{\mathbf{n}}|^2 \end{aligned} \tag{289}$$

We wish to compute the approximate generalized force $\langle\boldsymbol{\mathcal{M}}\rangle = -\langle\partial_{\mathbf{n}}\mathcal{H}\rangle$ in terms of the tensors κ and F. The dissipative terms η and F' are zero since there are no gapless excitations. Therefore Eq. (202) reduces to:

$$\langle\boldsymbol{\mathcal{M}}\rangle \approx \mathbf{M}_0 + \hbar F_{\nu\mu}\dot{n}_\mu - \kappa_{\nu\mu}\ddot{n}_\mu$$

where $\nu,\mu\in\{x,y,z\}$. Using the expression for the spin-1/2 ground and excited states from earlier (Eq. (2)), it follows that

$$\begin{aligned} \mathbf{M}_0 &\equiv \langle\boldsymbol{\mathcal{M}}\rangle_0 = \hat{n}\sum_i \Delta_i\tanh(\beta\Delta_i) \\ F_{\mu\nu} &= F_0\begin{pmatrix} 0 & -n_z & n_y \\ n_z & 0 & -n_x \\ -n_y & n_x & 0 \end{pmatrix}, \\ \kappa_{\mu\nu} &= \kappa_0\begin{pmatrix} 1-n_x^2 & -n_xn_y & -n_xn_z \\ -n_yn_x & 1-n_y^2 & -n_yn_z \\ -n_zn_x & -n_zn_y & 1-n_z^2 \end{pmatrix}. \end{aligned}$$

where $F_0 \equiv \frac{1}{2}\sum_i \tanh(\beta\Delta_i)$ and $\kappa_0 \equiv \hbar^2\sum_i \frac{\tanh(\beta\Delta_i)}{4\Delta_i}$. Substituting these expressions in Eq. (288) we find

$$I\dot{\mathbf{n}} = \mathbf{L}\times\mathbf{n},\ \dot{\mathbf{L}} = \mathbf{n}\times\mathbf{M}_{ext} - \hbar F_0\,\dot{\mathbf{n}} - \kappa_0\,(\mathbf{n}\times\ddot{\mathbf{n}})\ .$$

To compute $I\ddot{\mathbf{n}} = \dot{\mathbf{L}}_\perp\times\mathbf{n} + \mathbf{L}_\perp\times\dot{\mathbf{n}}$, it is now useful to split up $\mathbf{L}$ as $\mathbf{L} = \mathbf{L}_\perp + \hat{n}L_\parallel$, where $L_\parallel = \hat{n}\cdot\mathbf{L}$ is a constant of motion (see Eq. (289)). Then, using Eq. (289) and the fact that $\mathbf{L}_\perp = I\,(\mathbf{n}\times\dot{\mathbf{n}})$

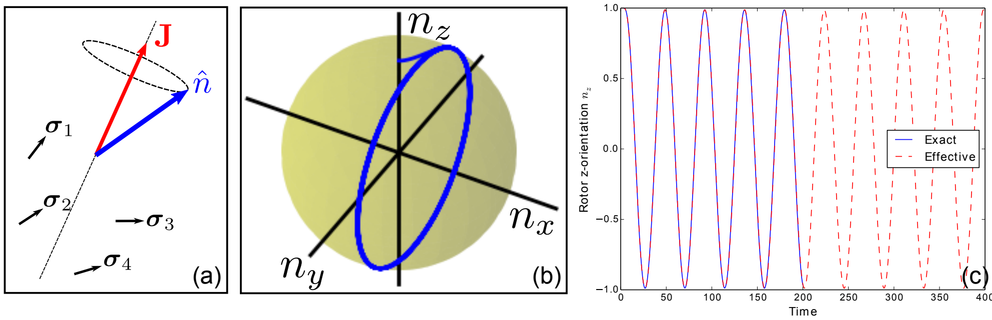

FIG. 26 Dynamics of the rigid rotor coupled to $N = 20$ spins-1/2. (a) Illustration of the setup described in detail in the text. (b, c) Solution of the exact dynamics (blue line) and effective dynamics (dashed red line) to the model with $\beta = 0.1$, $I = 1$, and Δ_i randomly distributed in $(1, 2)$. The initial conditions are $\mathbf{n}_0 = (0, 0, 1)$ and $\mathbf{L}_0 = (0, 0, 0)$ and initially the spins are in thermal equilibrium (see main text). The external force is ramped from its initial value of zero to final value $M^* = 0.1$ in time $t_c = 10$ according to the protocol $\mathbf{M}_{ext}(t) = M^* \sin^2\left(\frac{\pi t}{2t_c}\right) \hat{x}$ for $0 \le t \le t_c$, after which it is held fixed at $\mathbf{M}_{ext}(t > t_c) = M^* \hat{x}$.

we arrive at:

$$I_{eff}\ddot{\mathbf{n}} = (\mathbf{n} \times \mathbf{M}_{ext}) \times \mathbf{n} - L_{eff}^{\|}(\dot{\mathbf{n}} \times \mathbf{n}) - I_{eff}|\dot{\mathbf{n}}|^2\mathbf{n} \,, \tag{290}$$

where the renormalized moment of inertia is $I_{eff} = I + \kappa_0$ and the renormalized angular momentum is $L_{eff}^{\|} = L_{\|} + \hbar F_0$.

From this equation we see that the motion of the rotor is strongly renormalized by the interaction with the spin-$\frac{1}{2}$ particles. Moreover we see that, even when the external force is absent ($\mathbf{M}_{ext} = 0$) and $L_{\|} = 0$, the Berry curvature (F_0) causes a Coriolis-type force that tilts the rotation plane of the rotor. Indeed if we start with uniform rotations of the rotor in the xz plane, i.e. $\mathbf{n}$, $\dot{\mathbf{n}}$ lie in the xz plane, we immediately see that the Berry curvature causes acceleration orthogonal to the rotation plane. The physics behind the Coriolis force is intuitively simple. At any finite angular velocity of the rotor, the spins will not be able to follow adiabatically the rotor and thus will be somewhat behind. As a result there will be a finite angle between the instantaneous direction of the spins and the rotor so the spins will start precessing around the rotor, and the rotor will in turn start precessing around the spins. Fig. 26c shows an example where this Coriolis-induced precession can be observed.

D. Quenched BCS superconductor

In the previous sections, we have coupled the internal dynamics of our systems to external parameters such as the position of a box. A natural question that arises is whether these effective

Newtonian dynamics can occur in situations where the classical dynamical degree of freedom is emergent, such as a macroscopic order parameter. We will now show that this possible in the case of a quenched BCS superfluid, which has been studied extensively since its realization in ultracold fermionic gases (Andreev et al., 2004; Barankov and Levitov, 2006; Barankov et al., 2004; Yuzbashyan and Dzero, 2006). It has been shown that the resulting equations of motion are integrable, but generally involve keeping track of every mode in the BCS theory. We will see how adiabatic perturbation theory gives new insight into this problem, allowing us to reduce the coupled equations of motion of the different momentum modes to a single integral equation in which the emergent slow mode – the superconducting gap Δ – is treated with the preceding formalism.In such a setup the equations of motion entirely emerge from the interactions with microscopic degrees of freedom and e.g. the mass is entirely determined by these interactions.

The system that we consider is a BCS superconductor with short-range interactions in which the interaction strength g can be tuned as a function of time. This is a natural situation in, for example, ultracold atoms, where the interaction strength can be tuned by a Feshbach resonance (Chin et al., 2010). We start from the pairing Hamiltonian in d dimensions

$$\mathcal{H} = \sum_{\mathbf{k}\sigma} \epsilon_{\mathbf{k}} c^\dagger_{\mathbf{k}\sigma} c_{\mathbf{k}\sigma} - g \sum_{\mathbf{k},\mathbf{q}} c^\dagger_{\mathbf{k}\uparrow} c^\dagger_{-\mathbf{k}\downarrow} c_{\mathbf{q}\uparrow} c_{-\mathbf{q}\downarrow} \ , \tag{291}$$

which is exactly solvable within mean field theory. Here the single-particle energy of mode $\mathbf{k}$ is $E_{\mathbf{k}}$, from which the chemical potential is subtracted to get $\epsilon_{\mathbf{k}} = E_{\mathbf{k}} - \mu$. The mean-field decoupling consists of defining a gap $\Delta = g \sum_{\mathbf{k}} \langle c_{\mathbf{k}\uparrow} c_{-\mathbf{k}\downarrow} \rangle$, where the expectation value is taken over an arbitrary time-dependent wave function $|\psi(t)\rangle$ self-consistently. Making this replacement and switching to Anderson pseudospin notation σ, where $\sigma^z_{\mathbf{k}} = 1$ (-1) corresponds to an unfilled (filled) pair, we get

$$\mathcal{H} = -\sum_{\epsilon} \left(\epsilon \sigma^z_\epsilon + \Delta \sigma^x_\epsilon \right) + \frac{\Delta^2}{g} \equiv \sum_\epsilon \mathcal{H}_\epsilon \ , \tag{292}$$

where without loss of generality we assumed that the gap starts real and remains real due to particle-hole symmetry. Note that we have switch from summing over the mode momentum $\mathbf{k}$ to their energies $\epsilon(\mathbf{k})$. The last term in Eq. (292) is often neglected, as it has no effect on the dynamics of the pseudospins. However, since we are interested in the dynamics of Δ, it is convenient to write the Hamiltonian in this expressly energy-conserving form.

To better connect with our previous discussion let us introduce the momentum conjugate to the gap: P_Δ and the bare mass m_0, which we later send to zero. This gives the Hamiltonian (292) an additional term:

$$\mathcal{H} \to \mathcal{H} + \frac{P_\Delta^2}{2m_0} \ , \tag{293}$$

such that the equations of motion for the gap read:

$$m_0\ddot{\Delta} = \langle -\partial_\Delta \mathcal{H}\rangle = -\frac{2\Delta}{g} + \sum_\epsilon \langle \sigma^x_\epsilon\rangle \tag{294}$$

In the limit of zero bare mass $m_0 \to 0$ this equation simply reduces to the self-consistency equation:

$$\Delta = \frac{g}{2}\sum_\epsilon \langle \sigma^x_\epsilon\rangle \ , \tag{295}$$

Note that the average is taken over the non-equilibrium density matrix, which is the solution of the von Neumann's equation:

$$i\frac{d\rho}{dt} = [\mathcal{H}(\Delta(t)), \rho]. \tag{296}$$

Starting in the ground state at some interaction strength g_i, we can ramp the interactions through some arbitrary protocol $g(t)$. For slow enough changes, we expect that the pseudospins σ will be weakly excited above their ground state yielding leading Newtonian correction $\langle \mathcal{M}_\Delta\rangle \approx \langle \mathcal{M}_\Delta\rangle_0 - \kappa\ddot{\Delta}$, where

$$\langle \mathcal{M}_\Delta\rangle_0 = -\frac{2\Delta}{g} + \sum_\epsilon \langle \sigma^x_\epsilon\rangle_0 = -\frac{2\Delta}{g} + \sum_\epsilon \frac{\Delta}{\sqrt{\Delta^2+\epsilon^2}} \ . \tag{297}$$

Similarly, using Eq. (209), the effective mass in the ground state will be

$$\kappa = 2\sum_\epsilon \frac{|\langle e|\sigma_x|g\rangle|^2}{(E_e-E_g)^3} = \frac{1}{4}\sum_\epsilon \frac{\epsilon^2}{(\epsilon^2+\Delta^2)^{5/2}} \ . \tag{298}$$

We can easily simulate both the exact and approximate equations of motion for this theory. More explicitly, we adopt the conventions of Ref. 4 and expand near the Fermi surface by considering a uniform density of states ν extending in a band from $\epsilon = -W/2$ to $W/2$, with $W \gg \Delta$ playing the role of the UV cutoff. This band is then broken up into $N = \nu W$ discrete modes and the physical limit is achieved by taking $W, N \to \infty$. The ramp is specified in a UV-independent way as a function $\Delta_{\mathrm{eq}}(t)$, where from the gap equation in equilibrium (the ground state),

$$\begin{aligned} \Delta_{\mathrm{eq}}(t) &= \frac{g(t)}{2}\sum_\epsilon \frac{\Delta_{\mathrm{eq}}(t)}{\sqrt{\Delta_{\mathrm{eq}}(t)^2+\epsilon^2}} \\ \implies g(t)^{-1} &= \frac{1}{2}\sum_\epsilon \frac{1}{\sqrt{\Delta_{\mathrm{eq}}(t)^2+\epsilon^2}} \approx \frac{\nu}{2}\int_{-W/2}^{W/2} d\epsilon \frac{1}{\sqrt{\Delta_{\mathrm{eq}}(t)^2+\epsilon^2}} = \nu \ln\left(\frac{W}{\Delta_{\mathrm{eq}}(t)}\right) \ . \end{aligned} \tag{299}$$

Note that microscopic parameters such as g can explicitly depend on the cutoff, while emergent objects such as the mass and the generalized force do not:

$$\begin{aligned} \kappa &\approx \frac{\nu}{4}\int_{-W/2}^{W/2} d\epsilon \frac{\epsilon^2}{(\epsilon^2+\Delta^2)^{5/2}} \xrightarrow{W\to\infty} \frac{\nu}{6\Delta^2} \ . \\ \langle \mathcal{M}_\Delta\rangle_0 &= 2\nu\Delta \ln\left(\frac{\Delta_{\mathrm{eq}}}{\Delta}\right) \ . \end{aligned} \tag{300}$$

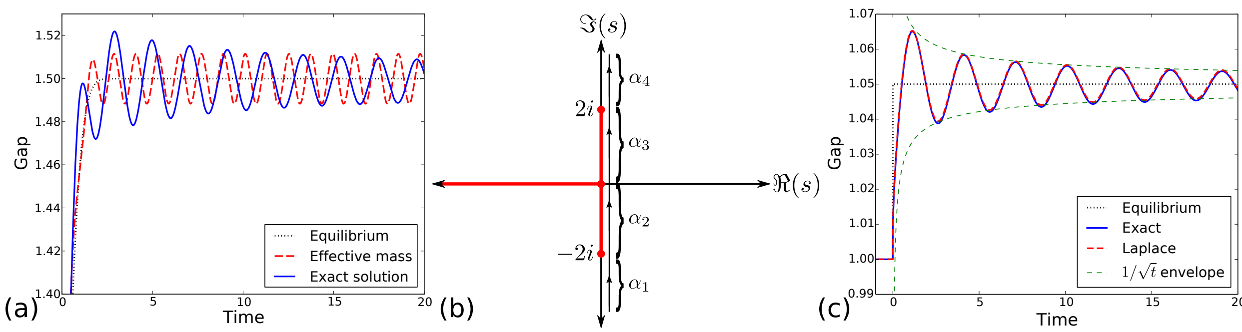

FIG. 27 Dynamics of the gap in a quenched BCS superfluid. (a) Gap vs. time for a ramp from $\Delta_i = 1$ to $\Delta_f = 1.5$ in time $T = 1$. The exact solution (blue) is compared to the dynamics within the effective mass approximation (dashed red). This approximation is clearly insufficient, so we must instead solve the full integral equation, e.g. via Laplace transform. (b) The branch cut structure of $\tilde{\alpha}$, the Laplace transform of $\alpha \propto \Delta - \Delta_f$ (see Eq. (306)). (c) Dynamics of the gap after a small instantaneous quench from $\Delta_i = 1$ to $\Delta_f = 1.05$. The exact dynamics agree well with the solution of the integral equation. The dashed lines shows that $1/\sqrt{t}$ envelope that is analytically found at late times.

Note also that both the mass and the generalized force are proportional to the density of states, i.e., they are extensive.

The simulations described above are plotted in Fig. 27a for a particular protocol in which $\Delta_{\rm eq}$ is slowly ramped from Δ_i to Δ_f: $\Delta_{\rm eq}(t) = \Delta_i + (\Delta_f - \Delta_i)\mathrm{erf}(t/T)$. Quite surprisingly, the effective mass does not accurately described the dynamics of the ramped or quenched BCS superconductor. Other simulations confirm that this is true independent of the initial and final values of the gap or the time scale T of the ramp. A particularly noticeable difference is that the simulations of the full model show damping of the oscillation, while the effective model with mass κ undergoes infinitely long-lived oscillations about the minimum of the potential at $\Delta = \Delta_f$.

To see where this comes from, let us consider small oscillations about the point at the end of the ramp. Linearizing about the final point, there is only one energy/time scale in the system, so the frequency of oscillations must scale as $\omega \sim \Delta_f$. We have seen that the effective mass gives a contribution to the generalized force $\kappa\ddot{\Delta} \sim \kappa A\omega^2 \sim \nu A$, where A is the amplitude of the oscillations. The next correction, which is non-Newtonian, is given by $\zeta\Delta^{(4)}$, where $\Delta^{(n)}$ denotes the nth time derivative. From the expansion that gave us the effective Newtonian dynamics, the coefficient ζ for the ground state is given by

$$\zeta = 2\sum_{n\neq 0}\frac{|\langle n|\partial_\Delta\mathcal{H}|0\rangle|^2}{(E_n - E_0)^5} = \frac{1}{16}\sum_{\epsilon}\frac{\epsilon^2}{(\epsilon^2+\Delta^2)^{7/2}} = \frac{\nu}{60\Delta^4}\ . \tag{301}$$

So the correction is $\zeta\Delta^{(4)} \sim (\nu\Delta^{-4})(A\Delta^4) \sim \nu A$, i.e., it scales exactly the same way as the effective mass contribution. Indeed, if we consider an arbitrary term in the series $\chi_n \Delta^{(n)}$ for arbitrary positive even integer n, we will again find that its contribution scales as νA. Therefore, it is not okay to truncate at second order by considering just the effective mass - indeed, there is no limit where it will be fully correct to truncate at any finite order. This statement that we need to know not just Δ and its acceleration, but rather all of its higher-order (even) derivatives, is tantamount to saying that the local-in-time expansion about the time t is not correct. Therefore, to solve this problem correctly, we must resort to the full integral equation from first order adiabatic perturbation theory (Eq. (201)):

$$\begin{aligned}\langle \mathcal{M}_\Delta \rangle_0 &= 2\int_{t_0}^{t} dt' \dot{\Delta}(t') \sum_{m\neq n} \frac{\rho_n^0 \langle m|\mathcal{M}(t)|n\rangle\langle n|\mathcal{M}(t')|m\rangle}{E_m(t') - E_n(t')} e^{i\int_{t'}^{t} d\tau (E_m(\tau)-E_n(\tau))} + O(\dot{\Delta}^2) \\ &= \int_{t_0}^{t} dt' \dot{\Delta}(t') \sum_{\epsilon} \frac{\epsilon^2}{(\epsilon^2+\Delta(t')^2)\sqrt{\epsilon^2+\Delta(t)^2}} \cos\left(2\int_{t'}^{t} d\tau \sqrt{\epsilon^2+\Delta(\tau)^2}\right) , \end{aligned} \tag{302}$$

where we have taken the real part of the exponential because all the matrix elements are real. With a bit more effort, this integral equation can be solved numerically, and for slow ramps or small quenches, the integral equation agrees with the exact numerics (cf. Fig. 27(c)).

We can gain a bit more understanding of the integral equation by consider the case of a small quench or equivalently the late-time behavior of a slow ramp. Assuming that the deviation $\alpha = (\Delta - \Delta_f)/\Delta_f$ of the gap from equilibrium is small, we can expand the integral equation about $\alpha = 0$. The first order contribution is then

$$-2\nu\Delta_f \alpha(t) = \int_{t_0}^{t} \dot{\alpha}(t') \sum_{\epsilon} \frac{\epsilon^2}{(\epsilon^2+\Delta_f^2)^{3/2}} \cos\left(2\sqrt{\epsilon^2+\Delta_f^2}(t-t')\right) . \tag{303}$$

This restores some degree of locality - the integral equation now only depends on the history of $\dot{\alpha}$ and not directly on $\alpha(t')$. Eq. (303) can be Lorentz transformed to get

$$-2\nu\Delta_f \tilde{\alpha}(s) = (s\tilde{\alpha} - \alpha_0) \sum_{\epsilon} \frac{\epsilon^2}{(\epsilon^2+\Delta_f^2)^{3/2}} \frac{s}{s^2+4(\epsilon^2+\Delta_f^2)} , \tag{304}$$

where $\tilde{\alpha}(s) = \int_0^\infty e^{-st}\alpha(t)$ is the Lorentz transform of α and $\alpha_0 = (\Delta_i - \Delta_f)/\Delta_f$ is the initial condition. The equilibrium correlation function of the pseudospins σ is encoded in the ϵ-dependent terms, so the fermions can be integrated out to give

$$\sum_{\epsilon} \frac{\epsilon^2}{(\epsilon^2+\Delta_f^2)^{3/2}} \frac{s}{s^2+4(\epsilon^2+\Delta_f^2)} = \frac{2\nu}{s}\left[-1 + \frac{\sqrt{4\Delta_f^2+s^2}}{s}\cosh^{-1}\left(\frac{\sqrt{4+s^2/\Delta_f^2}}{2}\right)\right] . \tag{305}$$

Substituting this into Eq. (304) and rearranging, we find that

$$\tilde{\alpha}(s) = \alpha_0 \frac{-s + \sqrt{\Delta_f^2 + s^2}\cosh^{-1}\left(\frac{\sqrt{4+s^2/\Delta_f^2}}{2}\right)}{s\sqrt{\Delta_f^2 + s^2}\cosh^{-1}\left(\frac{\sqrt{4+s^2/\Delta_f^2}}{2}\right)} . \tag{306}$$

Note that, as expected, the only time scale in the problem is set by Δ and α scales linearly with α_0. Therefore, rescaling $\alpha \to \alpha/\alpha_0$, $t \to t\Delta$, and $s \to s/\Delta$, we can attempt to invert the Lorentz transform and solve for $\alpha(t)$.

These small quenches of the order parameter were studied in Ref. 49. Using very different methods, they nevertheless arrived at an equation of motion for the order parameters quite similar to Eq. (306). The inverse Laplace transform is given by

$$\alpha(t) = \frac{1}{2\pi i}\int_{\gamma - i\infty}^{\gamma + i\infty} e^{st}\tilde{\alpha}(s)ds \tag{307}$$

for any $\gamma > 0$. $\tilde{\alpha}$ has branch cuts associated with the square roots at $s = \pm 2i$. We make the the branch cut shown in Fig. 27(b), which does not cross the contour for any $\gamma > 0$. The inverse hyperbolic cosine also has a branch cut on the negative real axis, which again does not affect us. We simply make the obvious branch choice such that $\sqrt{4+s^2}$ and $\cosh^{-1}\left(\sqrt{4+s^2}/2\right)$ are positive and real on the positive real axis, which uniquely defines the function on the chosen contour. Then taking the limit $\gamma \to 0^+$, we split the contour into four pieces, as shown in Fig. 27(b). Taking first α_3, for which $s = ir$ with $0 < r < 2$, the branch choices gives $\sqrt{4+s^2} = \sqrt{4-r^2}$ and $\cosh^{-1}\left(\sqrt{4+s^2}/2\right) = i\cos^{-1}\left(\sqrt{4-r^2}/2\right)$. Thus

$$\begin{aligned}
\alpha_3(t) &= \Re\left[\frac{1}{2\pi i}\int_0^2 idre^{irt}\frac{-ir + \sqrt{4-r^2}\left(i\cos^{-1}\left(\frac{\sqrt{4-r^2}}{2}\right)\right)}{ir\sqrt{4-r^2}\left(i\cos^{-1}\left(\frac{\sqrt{4-r^2}}{2}\right)\right)}\right] \\
&= \frac{1}{2\pi}\int_0^2 dr\sin(rt)\frac{-r + \sqrt{4-r^2}\cos^{-1}\left(\frac{\sqrt{4-r^2}}{2}\right)}{r\sqrt{4-r^2}\cos^{-1}\left(\frac{\sqrt{4-r^2}}{2}\right)} .
\end{aligned} \tag{308}$$

Similarly for the integral α_4 ($s = ir$ for $r > 2$), the branch choices are $\sqrt{4+s^2} = i\sqrt{r^2-4}$ and

$\cosh^{-1}\left(\sqrt{4+s^2}/2\right) = i\pi/2 + \ln\left((\sqrt{r^2-4}+r)/2\right)$. So

$$\begin{aligned}
\alpha_4(t) &= \Re\left[\frac{1}{2\pi i}\int_2^\infty idr e^{irt}\frac{-ir+i\sqrt{r^2-4}\left(\frac{i\pi}{2}+\ln\left(\frac{r+\sqrt{r^2-4}}{2}\right)\right)}{ir(i\sqrt{r^2-4})\left(\frac{i\pi}{2}+\ln\left(\frac{r+\sqrt{r^2-4}}{2}\right)\right)}\right] \\
&= \frac{1}{2\pi}\int_2^\infty \frac{dr}{r\sqrt{r^2-4}\left(\frac{\pi^2}{4}+\ln\left(\frac{r+\sqrt{r^2-4}}{2}\right)^2\right)}\left[\cos(rt)\left(\frac{\pi r}{2}\right)+\right. \\
&\qquad \left.\sin(rt)\left(r\ln\left(\frac{r+\sqrt{r^2-4}}{2}\right)-\sqrt{r^2-4}\left(\frac{\pi^2}{4}+\ln\left(\frac{r+\sqrt{r^2-4}}{2}\right)^2\right)\right)\right]. \quad (309)
\end{aligned}$$

One can easily show that $\alpha_1 = \alpha_4$ and $\alpha_2 = \alpha_3$, so $\alpha(t) = 2(\alpha_1(t)+\alpha_2(t))$. These integrals can be evaluated numerically, the results of which are plotted in Fig. 27c. Clearly they match well with the exact dynamics.

We can also quickly analyze the late time limit of these equations. In this limit, the cosines and sines yield fast-oscillatory integrals, which are then dominated by the stationary points of their integrands. Both α_3 and α_4 have a singularity at $r = 2$ ($s = 2i$). Therefore, the integrals are dominated by this point and we can simply expand the remainder of the integrand about $r = 2$. Thus,

$$\begin{aligned}
\alpha_3(t \gg 1/\Delta_f) &\approx \frac{1}{2\pi}\int_0^2 \frac{-\sin rt}{\pi\sqrt{2-r}}dr \approx -\frac{1}{2\pi^2}\int_{-\infty}^2 \frac{\sin rt}{\sqrt{2-r}}dr = (2\pi^3)^{-1/2}\frac{\cos 2t-\sin 2t}{\sqrt{t}}. \\
\alpha_4(t \gg 1/\Delta_f) &\approx \frac{1}{2\pi^2}\int_2^\infty \frac{\cos rt}{\sqrt{r-2}}dr = (2\pi^3)^{-1/2}\frac{\cos 2t-\sin 2t}{\sqrt{t}}. \quad (310)
\end{aligned}$$

Thus, as seen in Ref. 49, the late time behavior of the gap is described by power law relaxation $\Delta \sim \cos(2\Delta_f t+\varphi)/\sqrt{t}$, unlike the exponential relaxation expected in non-integrable (thermalizing) systems. This behavior can be traced back to the fact that the underlying BCS dynamics is integrable and has been termed collisionless relaxation (Volkov and Kogan, 1974).

It is interesting to extend these results to the finite temperature case. Unlike the previous case where Δ was the only energy scale in the problem, the temperature now introduces a new energy scale that we might expect to cut off the correlation functions such that locality in time is restored. However, a quick calculation similar to that above (not shown) demonstrates that starting from a finite temperature ensemble yields qualitatively similar dynamics as those starting from the ground state. The reason for this is simple: as an integrable model, the adiabatically transported state from the thermal ensemble at Δ_i to the final value Δ_f is not thermal. Such a non-thermal ensemble is referred to as a generalized Gibbs ensemble (Rigol et al., 2007) and has been well-understood to occur in generic integrable systems. Here it manifests as an absence of thermalization that yields similar dynamics at finite energy density as those in the ground state. It is worth pointing out that previous works have shown that large quenches (Barankov and Levitov, 2006) and/or non-trivial initial states (Yuzbashyan and Dzero, 2006) can result in long-lived oscillations that do not relax. Whether or not such dynamics can be captured within the effective Newtonian framework is a fascinating open question which is beyond the scope of these lectures.

VII. SUMMARY AND OUTLOOK.

Over the course of these lectures, we have introduced the concept of gauge potentials and seen how they are connected to a wide variety of ideas from geometry and topology of quantum systems to the emergence of Newtonian dynamics. An important aspect of this perspective is its generality, allowing the derivation of effective dynamics in systems as different as photons in a cavity and quenched BCS superconductors. These ideas are therefore quite amenable to being used in many important experimental systems as a method for understanding the dynamics of slow variables. With numerical methods, these can even be used to understand dynamics in complicated interacting many-body systems using only equilibrium simulations, and therefore have the potential to solve dynamics in complicated systems above one dimension, where exact well-behaved numerical methods are scarce.

An interesting open topic is how these ideas can be utilized in ever more complicated systems, particularly towards understanding the gauge potentials for non-equilibrium systems. For instance, for excited states the gauge potentials are ill-defined if the system is ergodic due to the problem of small denominators. Physically this problem originates from an absence of an adiabatic limit for many-body states essentially described by the random matrix theory (D'Alessio et al., 2015). In classical chaotic systems the situation is similar and these gauge potentials are divergent due to the lack of closed trajectories (Jarzynski, 1995). Nevertheless, adiabatic dynamics certainly exists in ergodic systems and therefore leading corrections to adiabaticity should be addressable in a similar context to what we have done in this review. A fascinating class of non-equilibrium Hamiltonians is periodically-driven systems, where one must differentiate between the effect of the parameters on the slow motion that can be written in terms of an effective time-independent Hamiltonian and the fast micromotion that it periodic with the same period as the drive (Bukov et al., 2015; Shirley, 1965). Finally, all these questions become even more interesting the presence of coupling to an environment, which is usually the situation we are given in realistic experimental systems. These are all fascinating questions, and understanding them will prove very valuable in solving the dynamics of complicated quantum and classical systems.

Acknowledgments

These notes were partially based on works done jointly with L. D'Alessio, V. Gritsev, and Y. Kafri, with whom we acknowledge many useful discussions. We also acknowledge useful discussions with E. Mueller and E. Katz. We thank S. Davidson for preparing the solution manual for the problems. This manual is available upon request. Work of A. P. was supported by AFOSR FA9550-13-1-0039, NSF DMR-1506340 and ARO W911NF1410540. M. K. was supported by Laboratory Directed Research and Development (LDRD) funding from Berkeley Lab, provided by the Director, Office of Science, of the U.S. Department of Energy under Contract No. DE-AC02-05CH11231.

Appendix A: Using gauge transformations for mapping between driven and undriven harmonic systems

In this section we will demonstrate how one can use transformations to the moving frame to map a massive harmonic system with a time dependent mass to a massive or a massless harmonic theory with the time-independent mass. Namely let us consider the system described by the following Hamiltonian:

$$\mathcal{H} = \int d^d x [\Pi^2 + (\nabla\Phi)^2 + m^2(t)\Phi^2], \tag{A1}$$

where d is the spatial dimensionality and Π and Φ are canonically conjugate fields satisfying standard commutation relation: $[\Pi(x), \Phi(x')] = -i\delta(x - x')$ (we set $\hbar = 1$ in this example) if the fields are quantum and $\{\Pi(x), \Phi(x')\} = -\delta(x - x')$ if the fields are classical. Because the Hamiltonian is harmonic, the analysis of quantum and classical systems is identical. Therefore here we focus only on the classical case. We will achieve our goal by doing a series of canonical transformations. Now as we are not assuming that $m(t)$ is a slow function we will not rely on adiabatic gauge potentials. Also for simplicity we completely ignore the issue of the ultra-violet cutoff required to regularize the theory and focus only on the low energy modes. First we perform a dilation transformation

$$\phi(x) = \lambda(t)\Phi(x),\ \pi(x) = \Pi(x)/\lambda(t)$$

and simultaneously rescale the space and time[17]

$$x = \xi/\lambda^2(t),\ dt = d\tau/\lambda^2(t). \tag{A2}$$

The corresponding gauge potential for this transformations, which is a straightforward generalization of the result derived in Exercise II.2, is

$$\mathcal{A}_\lambda = -\frac{1}{\lambda(t)}\int d^d x \pi(x)\phi(x). \tag{A3}$$

Using the general expression for the moving frame Hamiltonian (71) we find

$$\mathcal{H}_m = \int d^d\xi \left[\pi^2 + (\nabla_\xi \phi)^2 + \frac{m^2(\tau)}{\lambda^4}\phi^2 + \frac{d\ln(\lambda)}{d\tau}\pi\phi\right]. \tag{A4}$$

Completing the square and shifting the momentum

$$\tilde{\pi} = \pi + \frac{1}{2}\frac{d\ln(\lambda)}{d\tau}\phi,$$

we make a second gauge transformation (see Exercise (II.10)) for which the second moving Hamiltonian is

$$\mathcal{H}'_m = \int d^d\xi[\tilde{\pi}^2 + (\nabla_\xi\phi)^2 + \kappa^2(\tau)\phi^2], \tag{A5}$$

where the new time dependent mass $\kappa(t)$ and the scaling parameter $\lambda(t)$ are related by the following differential equation:

$$\lambda\frac{d^2\lambda}{d\tau^2} - 4\frac{m^2(\tau)}{\lambda^2} + 4\kappa^2(\tau)\lambda^2 = 0 \tag{A6}$$

One can view this equation as defining $\kappa(\tau)$ in terms of the scaling parameter $\lambda(t)$ or as an implicit time dependence of $\lambda(t)$ required to obtain the desired $\kappa(\tau)$.

Demanding that $\kappa(\tau) = \text{const}$ we can map the original dynamical systems to a static massless theory. Using the relation between the scaled and the original time (A2) we can rewrite this equation in terms of t:

$$\frac{1}{\lambda}\frac{d}{dt}\left(\frac{1}{\lambda^2}\frac{d\lambda}{dt}\right) - 4\frac{m^2(t)}{\lambda^2} + 4\lambda^2\kappa^2 = 0. \tag{A7}$$

This equation simplifies under the reparameterization $\mu = 1/\lambda$:

$$\mu\frac{d^2\mu}{dt^2} - 4\frac{\kappa^2}{\mu^2} + 4m^2(t)\mu^2 = 0. \tag{A8}$$

[17] Note that rescaling of space leads to rescaling of the Poisson bracket $\{\Pi(\xi), \Phi(\xi')\} = -\lambda^2\delta(\xi - \xi'')$. But this is precisely compensated by time rescaling so that the equations of motion $\dot{q} = \{q, \mathcal{H}\}$ remain invariant.

Clearly there is a duality between Eqs. (A6) and (A8) under $\lambda \leftrightarrow \mu$, $t \leftrightarrow \tau$, and $\kappa \leftrightarrow m$. This duality extends to arbitrary time dependent masses $m(t)$ and $\kappa(t)$.

If $m(t)$ is suddenly quenched to a constant value Eq. (A6) can be integrated. It is convenient to require that the scaling field satisfies the initial conditions $\lambda(0) = 1$ and $\dot{\lambda}(0) = 0$ such that the initial state is the same in terms of original fields $\Phi(x)$ and $\Pi(x)$ and the rescaled fields $\tilde{\pi}(\xi)$ and $\phi(\xi)$. Then we find

$$\left(\frac{d\lambda}{d\tau}\right)^2 = 4\kappa^2(1-\lambda^2) + 4m^2\left(1 - \frac{1}{\lambda^2}\right). \tag{A9}$$

Since the solution of this equation qualitatively depends on the relative magnitude between m and κ we discuss these two cases separately. Due to the duality between Eqs. (A6) and (A8) it is sufficient to discuss the solutions only in the τ frame. We will start from the extreme cases where one of the masses is zero.

<u>Mapping from massive to massless theory.</u> Let us consider first the setup where we take the massive setup with $m > 0$ and map it to the massless theory $\kappa(\tau) = 0$. Then integrating Eq. (A9) we find

$$2m\tau = \sqrt{\lambda^2 - 1} \Rightarrow \lambda(\tau) = \sqrt{1 + 4m^2\tau^2} \tag{A10}$$

It is interesting that this problem has a horizon in terms of the original lab time t. Indeed it is easy to check that the relation between t and τ reads:

$$\tau(t) = \frac{1}{2m}\tan(2mt),\ \lambda(t) = \frac{1}{\cos(2mt)} \tag{A11}$$

thus the system reaches the infinite time in the moving frame τ at a finite lab time $t^* = \pi/(4m)$.

<u>Mapping from massless to massive theory.</u> Now consider and opposite scenario, where we take the massless limit with $m = 0$ and map it to the massive setup with $\kappa > 0$. Then clearly the solution of Eq. (A6) is

$$\lambda(\tau) = \cos(2\kappa\tau),\ \tau(t) = \frac{1}{2\kappa}\arctan(2\kappa t),\ \lambda(t) = \frac{1}{\sqrt{1 + 4\kappa^2 t^2}}. \tag{A12}$$

Now the picture is opposite: infinite time in the lab frame maps to a finite time interval in the moving frame. This situation is similar to crossing a black hole horizon in general relativity.

<u>Mapping between two massive theories</u> In general if both κ and m are finite then the scale parameter λ is bounded oscillating between two turning points

$$\lambda_1 = 1,\ \text{and}\ \lambda_2 = \frac{m}{\kappa} \tag{A13}$$

and the period of these oscillations is

$$T_\tau = \frac{\pi}{2\kappa},\ T_t = \frac{\pi}{2m} \tag{A14}$$

While this is outside the scope of our notes, we note that these transformations can be extended to the space-dependent mass as well using the space-time dependent scaling field $\lambda(x,t)$ and rescaling the time and coordinates according to

$$dx = d\xi/\lambda^2(x,\tau),\ dt = d\tau/\lambda^2(x,\tau). \tag{A15}$$

It is easy to check that these are also canonical transformations with the generating function

$$\mathcal{A}_\lambda = -\int d^dx \frac{1}{\lambda(x,t)}\pi(x)\phi(x). \tag{A16}$$

Using the same manipulations as in the translationally invariant case we can map theory with arbitrary space-time mass dependence $m(x,t)$ to a theory with a different mass $\kappa(\xi,\tau)$ solving the partial differential equation for the scaling field

$$\lambda\frac{d^2\lambda}{d\tau^2} - 4\lambda\nabla_\xi^2\lambda - 4\frac{m^2(\tau)}{\lambda^2} + 4\kappa^2(\tau)\lambda^2 = 0. \tag{A17}$$

We derived this mapping for a simple harmonic model. One can, however, extend it to more complex interacting systems. While it might be hard to find the exact gauge transformation, which completely eliminates time dependence of the coupling constants, one can achieve mapping between various models, find conditions under which time-dependent systems effectively behave as time independent, find which gauge transformations lead to asymptotically free theories, where interaction couplings flow to zero with time in the new frame and so on. These are potentially interesting applications of transformations to the moving frame, but they lie outside the scope of our notes.

Appendix B: Metric tensor from Kubo response at finite temperature

Consider a generic Hamiltonian $\mathcal{H}$ with eigenstates $|n\rangle$. We define the metric tensor w.r.t. single parameter λ, alternatively known as the fidelity susceptibility at finite temperature by

$$g_{\lambda\lambda}(T) = \sum_n \rho_n \sum_{m\neq n} \frac{|M_{nm}|^2}{(E_n - E_m)^2}\ , \tag{B1}$$

where $\rho_n = e^{-\beta E_n}/Z$ and $M_{nm} = \langle n|\partial_\lambda \mathcal{H}|m\rangle$. Define the (non-symmetrized) spectral function as

$$S(\omega) = 2\pi \sum_n \rho_n \sum_{m\neq n} |M_{nm}|^2 \delta(E_n - E_m + \omega)\ . \tag{B2}$$

Then it is clear that

$$g = \int_{-\infty}^{\infty} \frac{d\omega}{2\pi} \frac{S(\omega)}{\omega^2} = \int_0^{\infty} \frac{d\omega}{2\pi} \frac{S(\omega) + S(-\omega)}{\omega^2} \ . \tag{B3}$$

We will now see that this expression can be connected to the out-of-phase susceptibility, which is measurable via linear response.

From standard Kubo response, the response function $\epsilon(\omega)$ of the magnetization M to a small periodic perturbation of $\lambda = \lambda_0 e^{-i\omega t}$ is given by (Mahan, 2000)

$$\epsilon(\omega) = i \int_0^{\infty} dt\, e^{i\omega t - \delta t} \langle [M(t), M(0)] \rangle \ , \tag{B4}$$

where δ is an infinitesimal positive number added for convergence, $M(\omega) = \epsilon(\omega)\lambda(\omega)$ and the expectation value is over the thermal density matrix $\hat{\rho} = e^{-\beta\mathcal{H}}/Z$. Note that, unlike the two-time correlation function used in defining the metric, the correlation function in Eq. (B4) need not be connected; this is because the commutator makes $\langle [A, B] \rangle = \langle [A, B] \rangle_c$. Let us next use the Lehmann representation:

$$\begin{aligned}
\epsilon(\omega) &= i \int_0^{\infty} dt\, e^{i\omega t - \delta t} \sum_n \rho_n \big(\langle n | e^{i\mathcal{H}t} M e^{-i\mathcal{H}t} M | n \rangle - h.c. \big) \\
&= i \int_0^{\infty} dt\, e^{i\omega t - \delta t} \sum_n \rho_n \sum_m \big(\langle n | e^{i\mathcal{H}t} M | m \rangle \langle m | e^{-i\mathcal{H}t} M | n \rangle - h.c. \big) \\
&= i \int_0^{\infty} dt\, e^{i\omega t - \delta t} \sum_n \rho_n \sum_m \big(\langle n | e^{iE_n t} M | m \rangle \langle m | e^{-iE_m t} M | n \rangle - h.c. \big) \\
&= i \int_0^{\infty} dt\, e^{i\omega t - \delta t} \sum_n \rho_n \sum_m \big(e^{i(E_n - E_m)t} - e^{i(E_m - E_n)t} \big) \big| M_{nm} \big|^2 \\
&= i \sum_n \rho_n \sum_{m \neq n} \big| M_{nm} \big|^2 \left(\frac{1}{\delta - i(E_n - E_m + \omega)} - \frac{1}{\delta - i(E_m - E_n + \omega)} \right) .
\end{aligned}$$

The imaginary part of the susceptibility $\epsilon''(\omega) = \mathrm{Im}[\epsilon(\omega)]$ is thus

$$\begin{aligned}
\epsilon''(\omega) &= \sum_n \rho_n \sum_{m \neq n} \big| M_{nm} \big|^2 \left(\frac{\delta}{\delta^2 + (E_n - E_m + \omega)^2} - \frac{\delta}{\delta^2 + (E_m - E_n + \omega)^2} \right) \\
&= \pi \sum_n \rho_n \sum_{m \neq n} \big| M_{nm} \big|^2 \big[\delta(E_n - E_m + \omega) - \delta(E_m - E_n + \omega) \big] = \frac{S(\omega) - S(-\omega)}{2}, \ .
\end{aligned} \tag{B5}$$

where we used the identity

$$\lim_{\delta \to 0} \frac{\delta}{\delta^2 + x^2} = \pi \delta(x)$$

and Eq. (B2) to get the last equality. In thermal equilibrium $S(\omega)$ and $S(-\omega)$ satisfy the fluctuation dissipation relation (Mahan, 2000), which we derive for completeness from Eq. (B2):

$$S(-\omega) = 2\pi \sum_{m\neq n} \frac{1}{Z} \mathrm{e}^{-\beta E_n} |M_{nm}|^2 \delta(E_m - E_n + \omega) = 2\pi \sum_{m\neq n} \frac{1}{Z} \mathrm{e}^{-\beta E_m} |M_{nm}|^2 \delta(E_n - E_m + \omega)$$
$$= 2\pi \mathrm{e}^{-\beta\omega} \sum_{m\neq n} \frac{1}{Z} \mathrm{e}^{-\beta E_n} |M_{nm}|^2 \delta(E_n - E_m + \omega) = \mathrm{e}^{-\beta\omega} S(\omega), \quad \text{(B6)}$$

where in the first equality we changed summation indexes $n \leftrightarrow m$ and in the second equality used that $E_m = E_n - \omega$. Therefore

$$\epsilon''(\omega) = \frac{1}{2} S(\omega) \left(1 - \mathrm{e}^{-\beta\omega}\right) \; \Leftrightarrow \; S(\omega) = \frac{2\epsilon''(\omega)}{1 - \exp[-\beta\omega]}.$$

and

$$g = \int_0^\infty \frac{d\omega}{2\pi} \frac{S(\omega) + S(-\omega)}{\omega^2} = \int_0^\infty \frac{d\omega}{\pi} \frac{\epsilon''(\omega)}{\omega^2} \frac{\exp[\beta\omega] + 1}{\exp[\beta\omega] - 1} = \int_0^\infty \frac{d\omega}{\pi} \frac{\epsilon''(\omega)}{\omega^2} \coth(\beta\omega/2). \quad \text{(B7)}$$

References

Aidelsburger, M., M. Atala, M. Lohse, J. T. Barreiro, B. Paredes, and I. Bloch, 2013, Phys. Rev. Lett. **111**, 185301.

Anderson, P. W., 1963, Phys. Rev. **130**, 439.

Andreev, A. V., V. Gurarie, and L. Radzihovsky, 2004, Phys. Rev. Lett. **93**, 130402.

Barankov, R. A., and L. S. Levitov, 2006, Phys. Rev. Lett. **96**, 230403.

Barankov, R. A., L. S. Levitov, and B. Z. Spivak, 2004, Phys. Rev. Lett. **93**, 160401.

Berry, M., 1989, in Geometric Phases In Physics, edited by A. Shapere and F. Wilczek (World Scientific, Singapore), pp. 7–28.

Berry, M. V., 1984, Proc. Roy. Soc. A **392**, 45.

Bordag, M., U. Mohideen, and V. Mostepanenko, 2001, Phys.Rept. **353**, 1.

Bukov, M., L. D'Alessio, and A. Polkovnikov, 2015, Adv. in Phys. **64**.

Bunin, G., L. D'Alessio, Y. Kafri, and A. Polkovnikov, 2011, Nature Phys. **7**, 913.

Campos Venuti, L., and P. Zanardi, 2007, Phys. Rev. Lett. **99**, 095701.

Chin, C., R. Grimm, P. Julienne, and E. Tiesinga, 2010, Rev. Mod. Phys. **82**, 1225.

Crispino, L. C. B., A. Higuchi, and G. E. A. Matsas, 2008, Rev. Mod. Phys. **80**, 787.

D'Alessio, L., Y. Kafri, A. Polkovnikov, and M. Rigol, 2015, arXiv:1509.06411 .

Damle, K., and S. Sachdev, 1996, Phys. Rev. Lett. **76**, 4412.

De Grandi, C., and A. Polkovnikov, 2010, Quantum Quenching, Annealing and Computation, volume 802 (Springer).

Deffner, S., C. Jarzynski, and A. del Campo, 2014, Phys. Rev. X **4**, 021013.

Dirac, P., 1931, Proc. Roy. Soc. A **133**, 60.

D′Alessio, L., and A. Polkovnikov, 2014, Annals of Physics **345**, 141, ISSN 0003-4916.

Gritsev, V., and A. Polkovnikov, 2012, Proceedings of the National Academy of Sciences **109**, 6457.

Hauke, P., M. Heyl, L. Tagliacozzo, and P. Zoller, 2015, arXiv:1509.01739 .

Jackson, J. D., 1999, Classical Electrodynamics (John Wiley & Sons, Inc., Hoboken), 3 edition.

Jarzynski, C., 1995, Phys. Rev. Lett. **74**, 1264.

Jarzynski, C., 1997, Phys. Rev. Lett. **78**, 2690.

Jensen, J., and A. Mackintosh, 1991, Rare earth magnetism: Structures and excitations clarendon.

Kallen, G., 1952, Helvetica Physica Acta (Switzerland) **25**.

Koch, J., T. M. Yu, J. Gambetta, A. A. Houck, D. I. Schuster, J. Majer, A. Blais, M. H. Devoret, S. M. Girvin, and R. J. Schoelkopf, 2007, Phys. Rev. A **76**, 042319.

Kolbenstvedt, H., 1995, American Journal of Physics **63**, 44, ISSN 0002-9505.

Kolodrubetz, M., V. Gritsev, and A. Polkovnikov, 2013, Phys. Rev. B **88**, 064304.

Landau, L., and E. Lifshitz, 1981, Quantum Mechanics: Course of Theoretical Physics Vol. 3 (Butterworth-Heinemann).

Landau, L., and E. Lifshitz, 1982, Mechanics: Course of Theoretical Physics Vol. 1 (Butterworth-Heinemann).

Laughlin, R. B., 1981, Phys. Rev. B **23**, 5632.

Lehmann, H., 1954, Il Nuovo Cimento **11**, 342.

Mahan, G. D., 2000, Many-Particle Physics (Kluwer Academic / Plenum, New York).

Moore, J. E., and L. Balents, 2007, Phys. Rev. B **75**, 121306.

Neupert, T., L. Santos, C. Chamon, and C. Mudry, 2011, Fractional quantum hall states at zero magnetic field.

Provost, J. P., and G. Vallee, 1980, Communications in Mathematical Physics **76**, 289, ISSN 0010-3616.

Qi, X.-L., and S.-C. Zhang, 2010, Physics Today **63**, 33.

Rigol, M., V. Dunjko, V. Yurovsky, and M. Olshanii, 2007, Phys. Rev. Lett. **98**, 050405.

Rigolin, G., G. Ortiz, and V. H. Ponce, 2008, Phys. Rev. A , 052508.

Roushan, P., C. Neill, Y. Chen, M. Kolodrubetz, C. Quintana, N. Leung, M. Fang, R. Barends, B. Campbell, Z. Chen, B. Chiaro, A. Dunsworth, et al., 2014, Nature **515**(7526), 241, ISSN 0028-0836.

Sachdev, S., 1999, Quantum Phase Transitions (Cambridge University Press).

Schroer, M. D., M. H. Kolodrubetz, W. F. Kindel, M. Sandberg, J. Gao, M. R. Vissers, D. P. Pappas, A. Polkovnikov, and K. W. Lehnert, 2014, Phys. Rev. Lett. **113**(5), 050402, URL `http://link.aps.org/doi/10.1103/PhysRevLett.113.050402`.

Shirley, J. H., 1965, Physical Review **138**, B979.

Silva, A., 2008, Phys. Rev. Lett. **101**, 120603.

Thouless, D. J., 1994, Journal of Mathematical Physics **35**, 5362.

Thouless, D. J., M. Kohmoto, M. P. Nightingale, and M. den Nijs, 1982, Phys. Rev. Lett. **49**, 405.

Visser, M., 2004, Class. Quantum Grav. **21**, 2603.

Volkov, A. F., and S. M. Kogan, 1974, Sov. Phys. JETP **38**, 1018.

Wilhelm, K., and B. N. Dwivedi, 2015, New Astronomy **34**, 211, ISSN 1384-1076.

Yuzbashyan, E. A., and M. Dzero, 2006, Phys. Rev. Lett. **96**, 230404.

Zanardi, P., L. Campos Venuti, and P. Giorda, 2007a, Phys. Rev. A **76**, 062318.

Zanardi, P., P. Giorda, and M. Cozzini, 2007b, Phys. Rev. Lett. **99**, 100603.